

# Appendix I

## Meteorological Model Performance



## TABLE OF CONTENTS

1 INTRODUCTION .....	1
2 12 KM MM5 PERFORMANCE IN NORTH CAROLINA.....	1
3 MM5 MODEL PERFORMANCE AT GREENSBORO, NC .....	6
4 UPPER AIR MODEL PERFORMANCE .....	9
5 SUMMARY.....	12

## LIST OF FIGURES

Figure 2-1 Monthly plots of modeled 1.5 meter temperature, bias and absolute error.....	1
Figure 2-2 Monthly plots of modeled 1.5 meter mixing ratio, bias and absolute error. ....	2
Figure 2-3 Monthly plots of modeled 1.5 meter relative humidity, bias and absolute error .....	3
Figure 2-4 Monthly plots of modeled cloud coverage, bias and absolute error. ....	3
Figure 2-5 Monthly plots of modeled wind direction, bias and absolute error.....	4
Figure 2-6 Monthly plots of modeled wind speed, bias and absolute error.....	5
Figure 2-7 Monthly plots of modeled wind speed with calm observations omitted, bias and absolute error. ....	5
Figure 2-8 Monthly plots of modeled wind speed with modeled wind speed below 1.5 m/s omitted, bias and absolute error. ....	6
Figure 3-1 Modeled data compared to surface observations at the Greensboro, NC ASOS site (KGSO) for two weeks typical of winter conditions. ....	7
Figure 3-2 Modeled data compared to surface observations at the Greensboro, NC ASOS site (KGSO) for two weeks typical of summer conditions.....	8
Figure 4-1 The Charlotte, NC (CHANC) profiler winds are co-plotted with the 12-km MM5 winds for (a) 12-23 UTC on January 17, 2002, (b) 00-11 UTC on January 19, 2002, and 00-11 UTC on January 20, 2002. ....	10
Figure 4-2 The Charlotte, NC (CHANC) profiler winds are co-plotted with the 12-km MM5 winds for (a) 00-11 UTC on November 10, 2002, and (b) 12-23 UTC on November 17, 2002.....	11





# 1 INTRODUCTION

The attainment demonstration for the Charlotte-Gastonia-Rock Hill, NC-SC 8-hour ozone nonattainment area (referred to as the Metrolina area) used the meteorological modeling from the Visibility Improvement State and Tribal Association of the Southeast (VISTAS) regional haze modeling. VISTAS is run by the ten Southeast states: Alabama, Florida, Georgia, Kentucky, Mississippi, North Carolina, South Carolina, Tennessee, Virginia and West Virginia. The meteorological model used for this project was the Pennsylvania State University/National Center for Atmospheric Research Mesoscale Meteorological Model (MM5).

The sections that follow summarize the meteorological model performance for North Carolina on the 12 kilometer (km) grid domain. The overall VISTAS meteorological model development and model performance was documented by the VISTAS contractor Baron Advanced Meteorological Systems, LLC and is attached to this Appendix.

## 2 12 KM MM5 PERFORMANCE IN NORTH CAROLINA

In general, the MM5 performance for North Carolina was very similar to the performance for the entire VISTAS modeling domain. The temperature bias was near zero in May, June, and August. July had a slight negative bias near  $-0.25$  Kelvin (K), and September had a negative bias of  $-0.1$  K. The absolute temperature error hovered around 1.5 K from May-September. Figure 2-1 displays the overall temperature, temperature bias and absolute error for North Carolina and the VISTAS modeling domain.

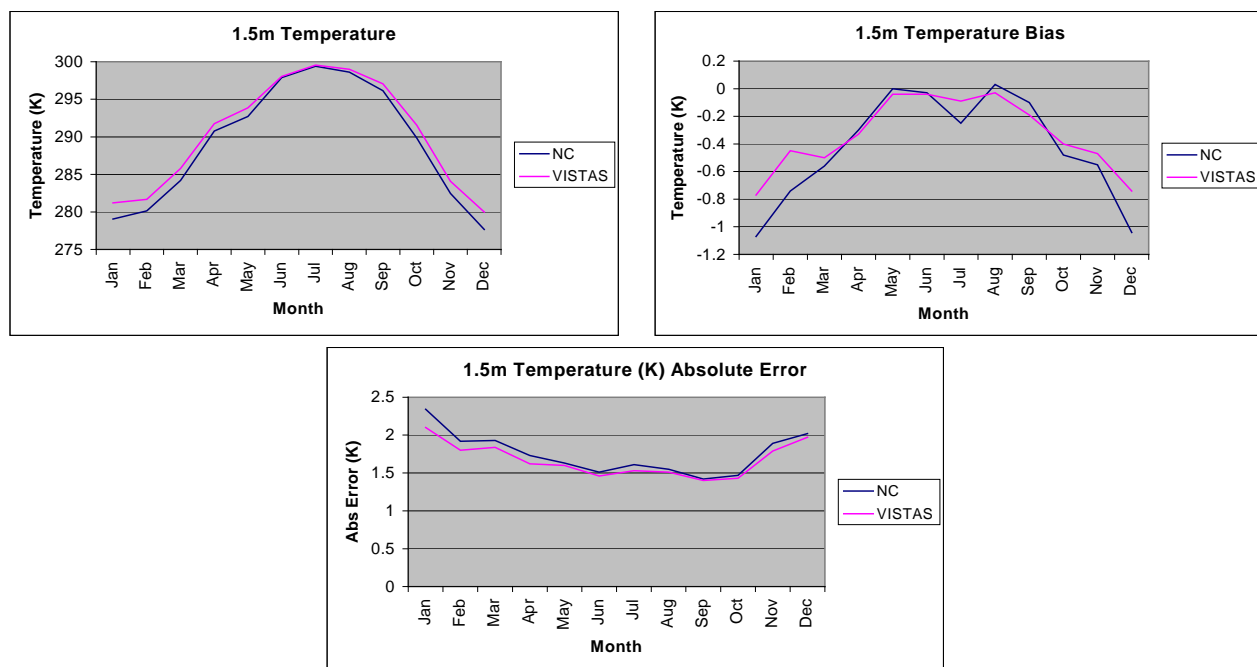


**Figure 2-1 Monthly plots of modeled 1.5 meter temperature, bias and absolute error.**

The mixing ratio bias in North Carolina was closer to neutral as compared to the entire VISTAS domain. The mixing ratio bias in North Carolina was near 0 gram/kilogram (g/kg) in May through July, then fell to -0.2 g/kg in August and to -0.6 in September. The absolute error was only slightly higher in North Carolina than the entire VISTAS domain, peaking at 1.8 g/kg in July. Figure 2-2 displays the overall mixing ratio, mixing ratio bias and absolute error for North Carolina and the VISTAS modeling domain.

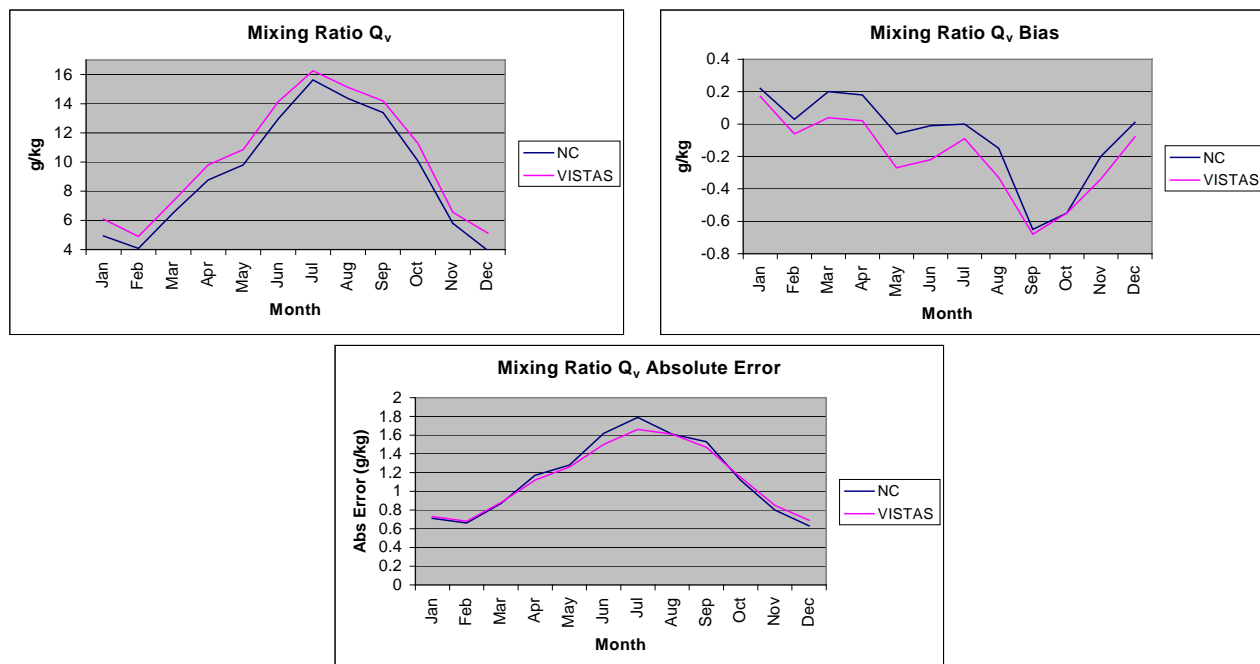


**Figure 2-2 Monthly plots of modeled 1.5 meter mixing ratio, bias and absolute error.**

The relative humidity bias in North Carolina was about 0.5% higher when compared to the entire VISTAS domain. The relative humidity bias in North Carolina generally hovered around  $\pm 3\%$ . The absolute error was slightly higher in North Carolina than the entire VISTAS domain, holding steady around 10% during the ozone season. Figure 2-3 displays the overall relative humidity, relative humidity bias and absolute error for North Carolina and the VISTAS modeling domain.

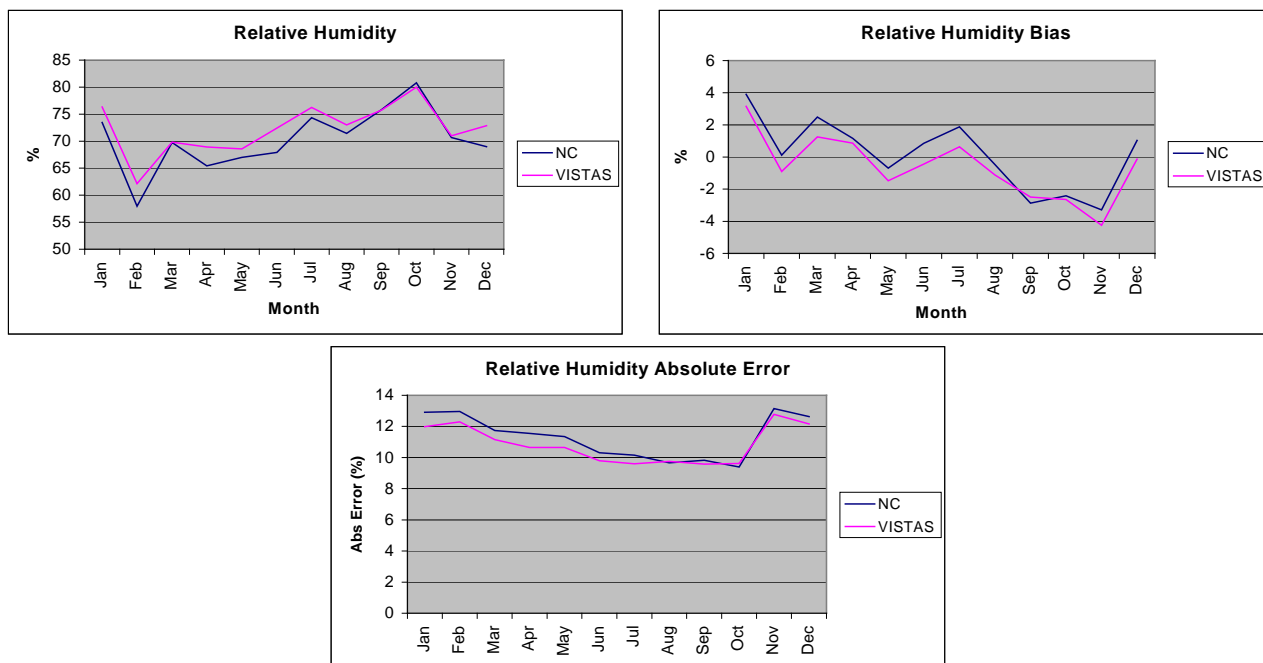


**Figure 2-3 Monthly plots of modeled 1.5 meter relative humidity, bias and absolute error**

The cloud coverage bias in North Carolina was 2 – 3% higher compared to the entire VISTAS domain. The cloud coverage bias peaked near 10% in July, with all other months with a bias less than 5%. The absolute error was generally 1 – 2% lower than the entire VISTAS domain, peaking at 31% in September. Figure 2-4 displays the overall cloud coverage, cloud coverage bias and absolute error for North Carolina and the VISTAS modeling domain.

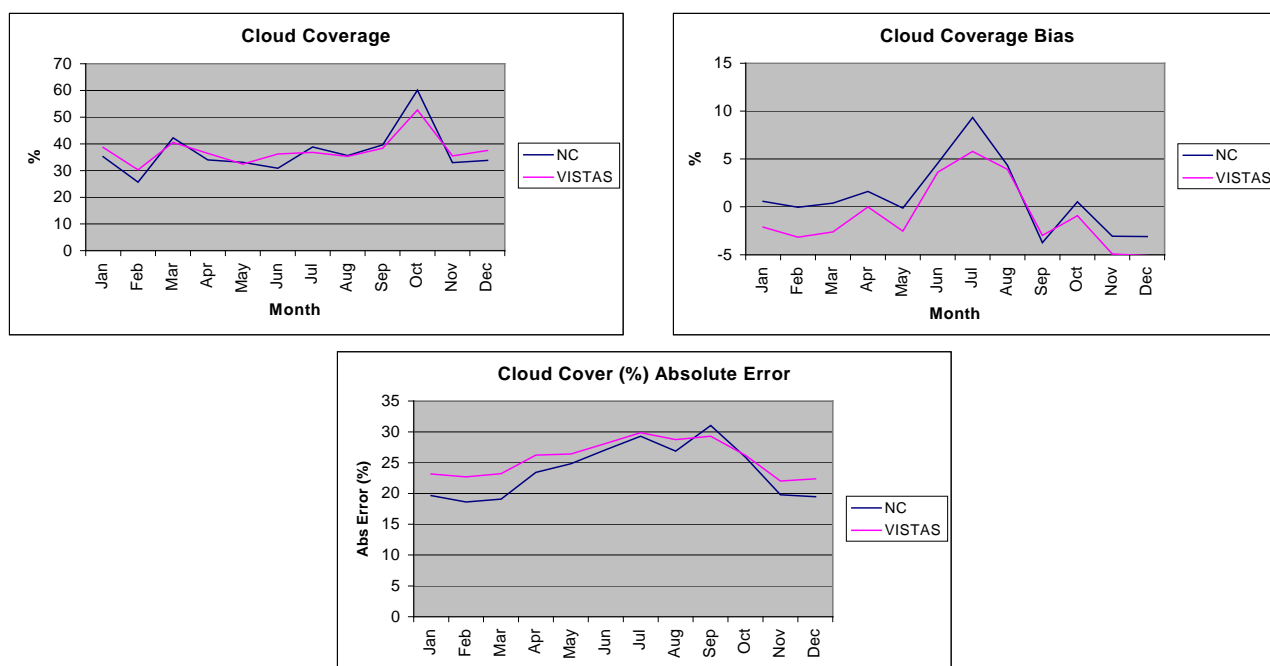


**Figure 2-4 Monthly plots of modeled cloud coverage, bias and absolute error.**

Wind direction was the most erratic of the measurements. The direction bias in North Carolina was more pronounced, being more negative May through July, and more positive in August and September. The absolute error was close to the entire VISTAS domain, peaking at 35 degrees in July when the lightest winds are experienced. Figure 2-5 displays the overall wind direction, wind direction bias and absolute error for North Carolina and the VISTAS modeling domain.

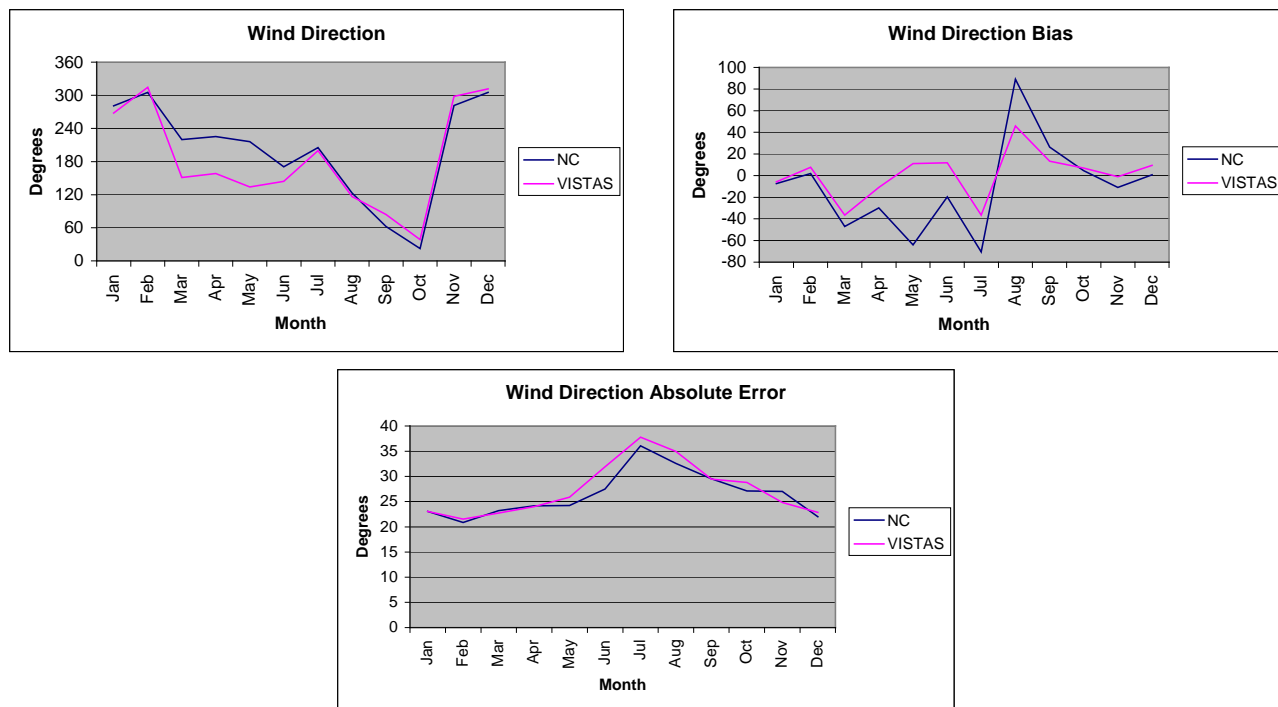


**Figure 2-5 Monthly plots of modeled wind direction, bias and absolute error.**

The wind speed bias in North Carolina was 0.3 to 0.4 meter/second (m/s) higher than wind speeds across the entire VISTAS domain. When considering all wind measurements, the wind speed was .8 to 1.0 m/s too strong. The absolute error is near 1.2 m/s, just above the entire VISTAS domain. When omitting calm observations, the bias falls to 0.2 to 0.5 m/s. The absolute error is near 1.2 m/s, very close to the entire VISTAS domain. When omitting modeled wind speeds below the threshold of the anemometer (<1.5 m/s), the bias is 0.5 to 0.8 m/s. The absolute error is near 1.3 m/s, just above the entire VISTAS domain. Figure 2-6 displays the overall wind speed, wind speed bias and absolute error for North Carolina and the VISTAS modeling domain. Figure 2-7 displays the wind speed when the calm observations are omitted as well as the bias and absolute error. Figure 2-8 displays the wind speed with modeled wind speeds below 1.5 m/s are omitted.

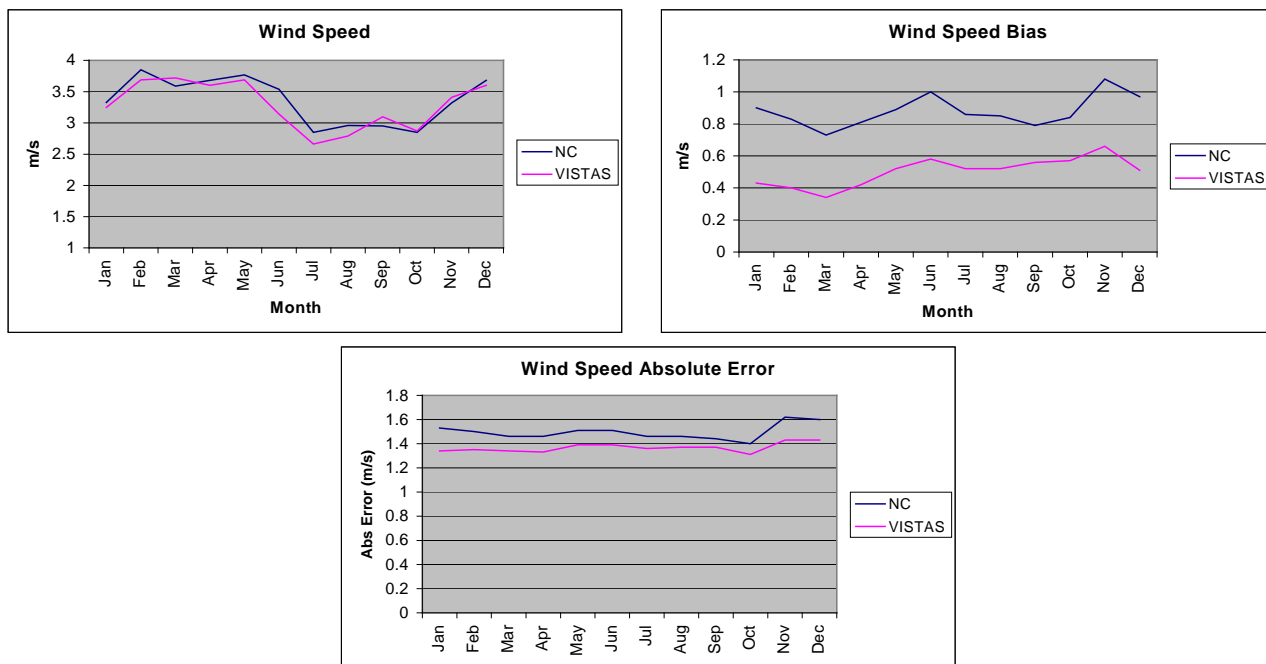


**Figure 2-6 Monthly plots of modeled wind speed, bias and absolute error.**

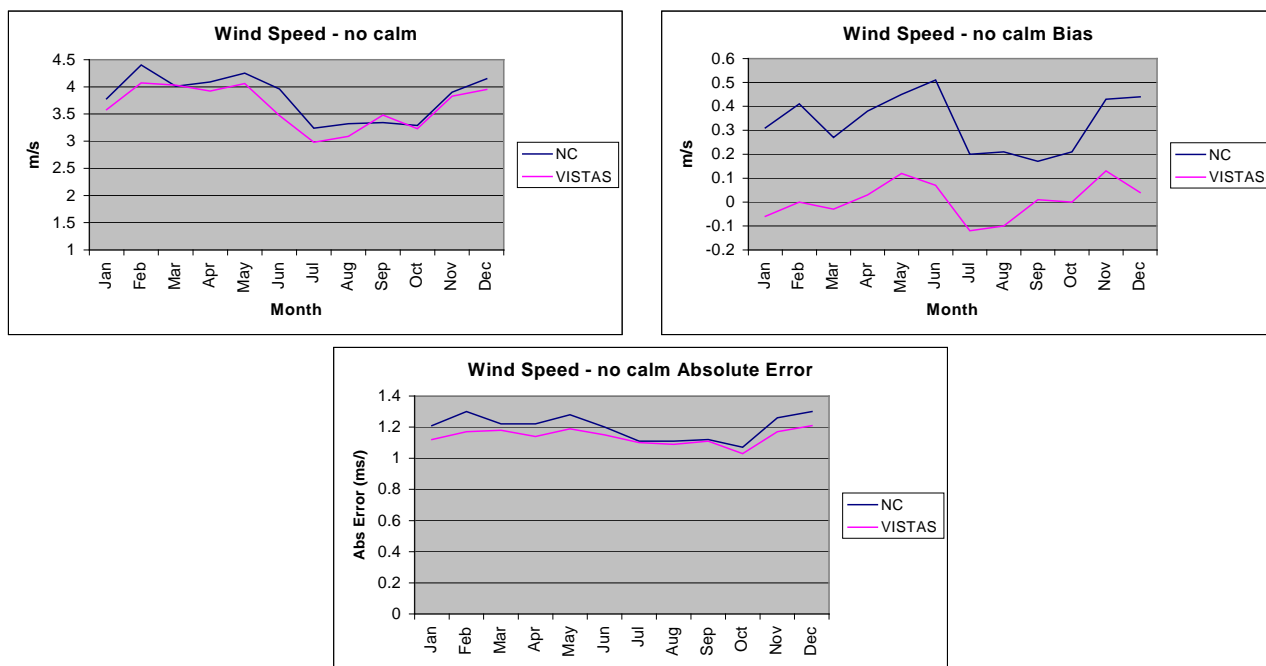


**Figure 2-7 Monthly plots of modeled wind speed with calm observations omitted, bias and absolute error.**

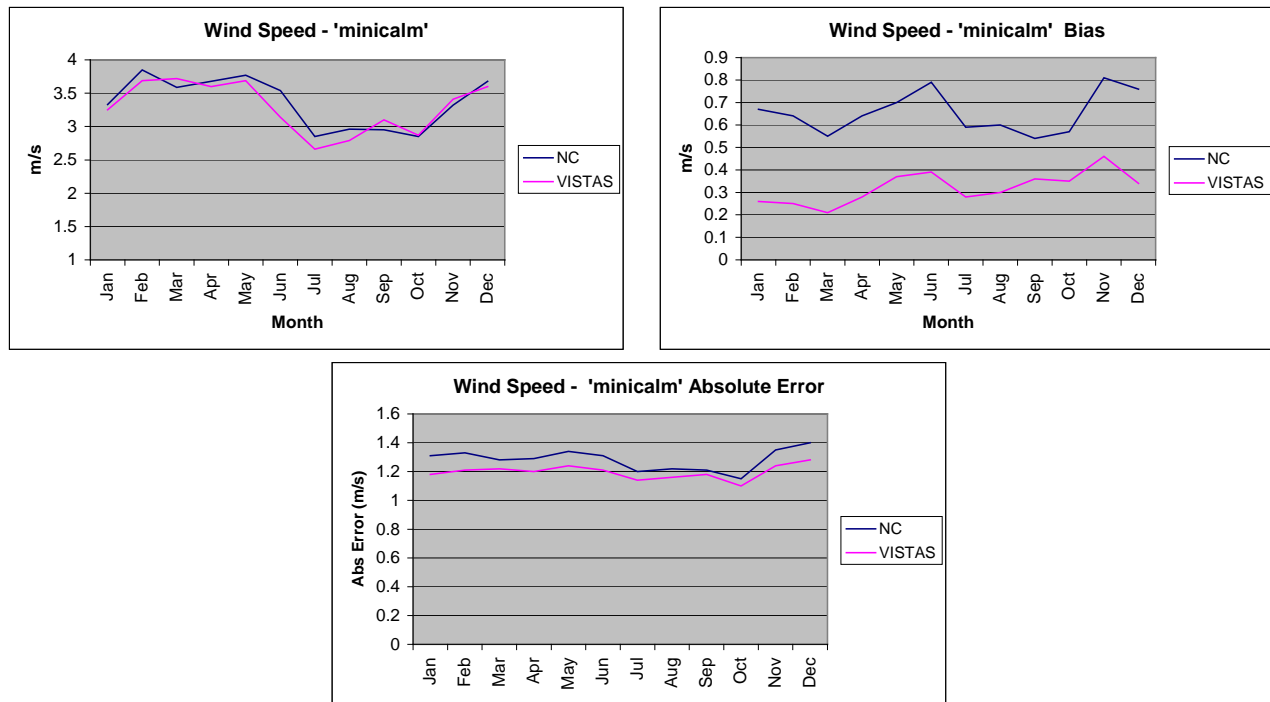


**Figure 2-8 Monthly plots of modeled wind speed with modeled wind speed below 1.5 m/s omitted, bias and absolute error.**

Overall excess wind speeds, increased relative humidity and cloud cover likely lead to under prediction of the daily maximum peak ozone concentration, which will be discussed in the air quality model performance (Appendix J).

### 3 MM5 MODEL PERFORMANCE AT GREENSBORO, NC

An additional way to evaluate model performance is to compare the various parameters to surface observations for a site-specific evaluation. Figures 3-1 and 3-2 show a time series of model and observed metrological data for the Greensboro, North Carolina Automated Surface Observing System (ASOS) site (KGSO). The time series include modeled surface values for temperature, mixing ratio, wind speed, wind direction, relative humidity, cloud cover, and precipitation (blue dashed lines). These model predicted values are compared to actual observations from the Greensboro site (solid black lines). Figure 3-1 depicts two different winter weeks (January 15-21 and November 12-18, 2002), while Figure 3-2 depicts two summer weeks (July 20-26 and August 19-25, 2002). It is important to look at both summer and winter events, as the forcing mechanisms for synoptic features can differ from season to season.

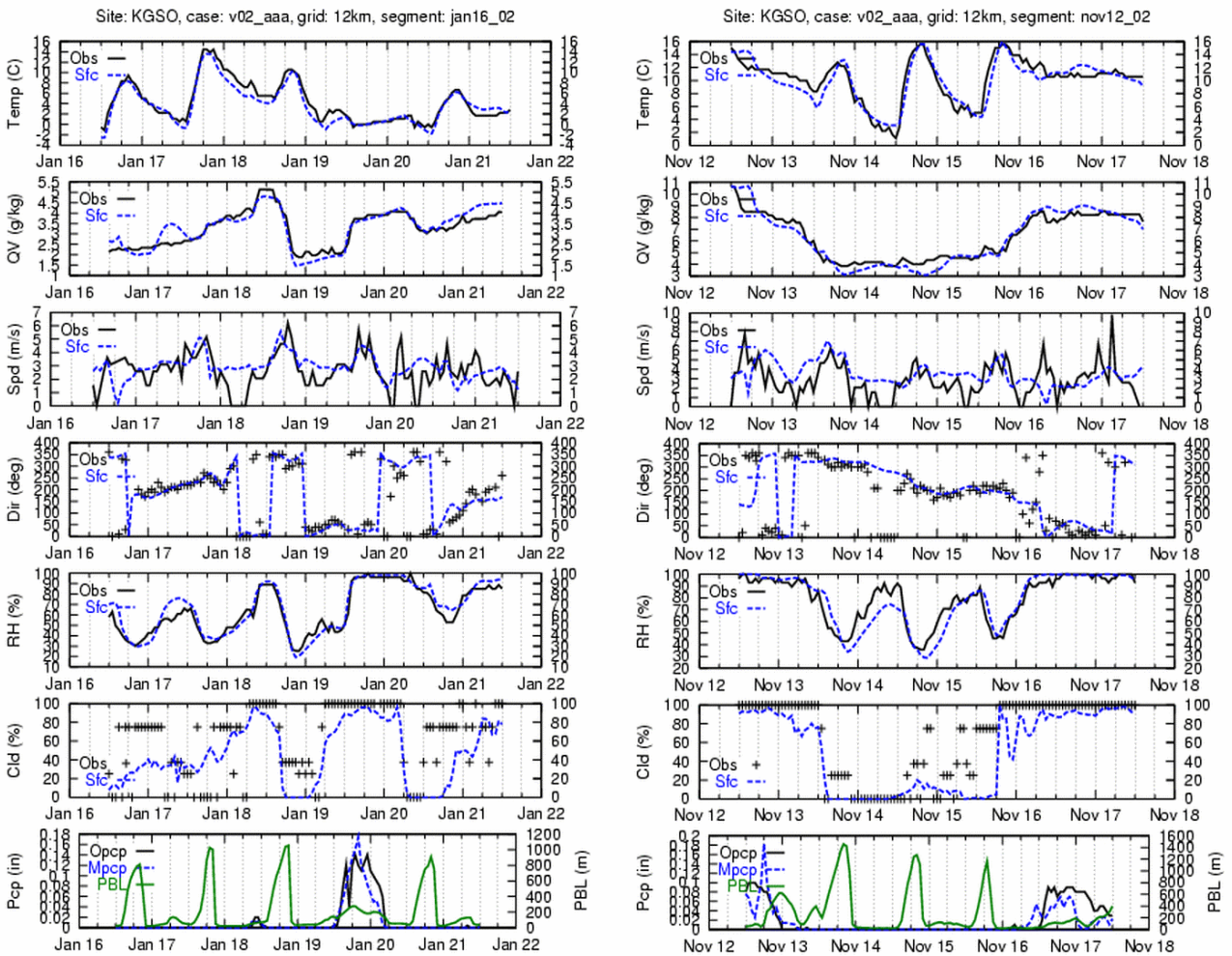


**Figure 3-1 Modeled data compared to surface observations at the Greensboro, NC ASOS site (KGSO) for two weeks typical of winter conditions.**



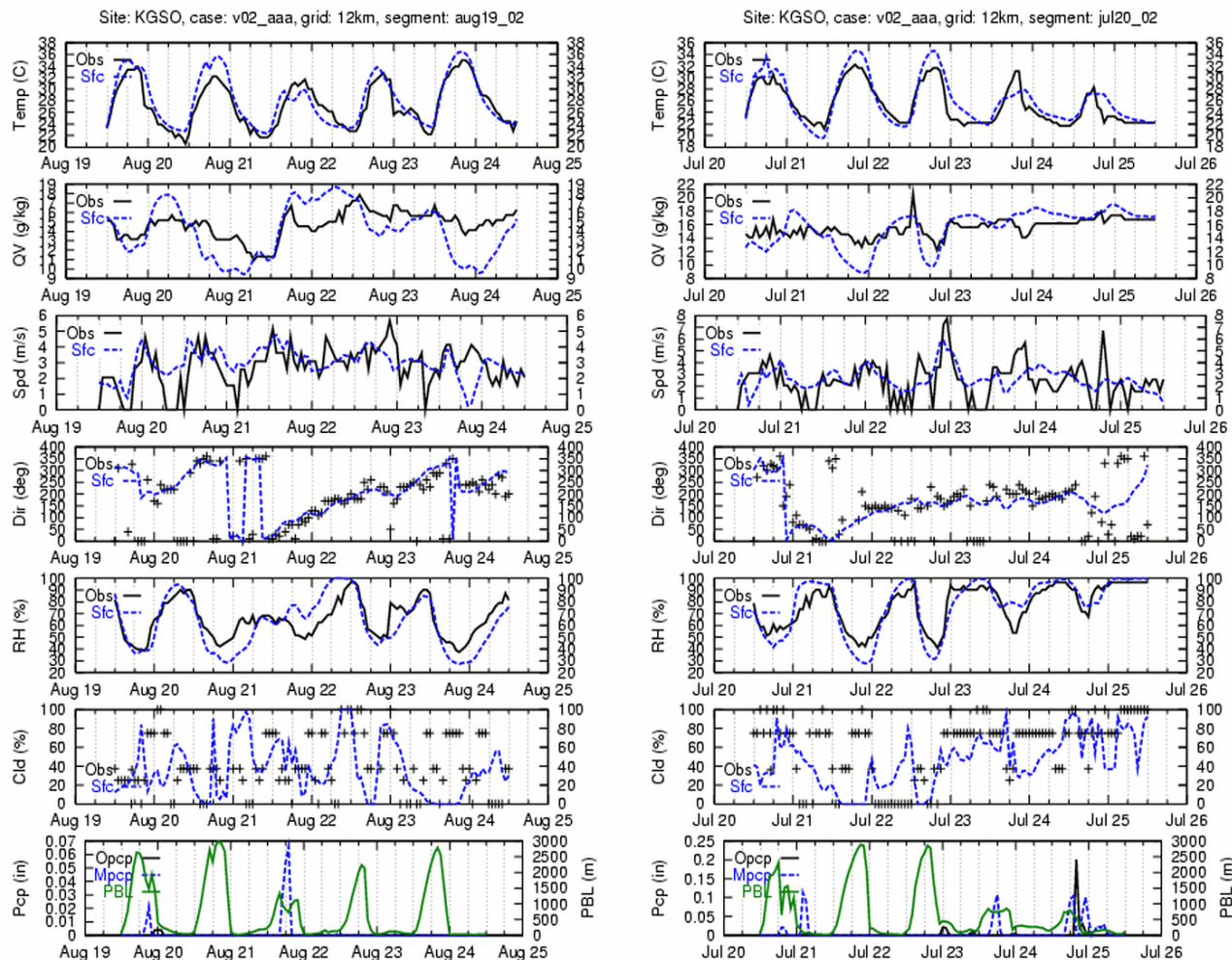


**Figure 3-2 Modeled data compared to surface observations at the Greensboro, NC ASOS site (KGSO) for two weeks typical of summer conditions.**

Generally the time series reflect what was seen on the monthly plots. Overall the plots reflect good model performance for 2002, when compared to modeling standards. Wind direction was close to observed values, and switched at the appropriate time, when frontal boundaries passed through the area. Wind speeds were captured well by the model during the daylight hours, but were often too strong at night.

Model performance was better at capturing the wintertime diurnal temperature trends than the summertime trends. For the summer temperatures the model was generally too cool with the afternoon high temperatures. Mixing ratio was close to observations in the winter, but, again, the model was more variable in the summertime. The diurnal trends in relative humidity were reasonably well captured, though the diurnal ranges were less in the model than with observations.



## 4 UPPER AIR MODEL PERFORMANCE

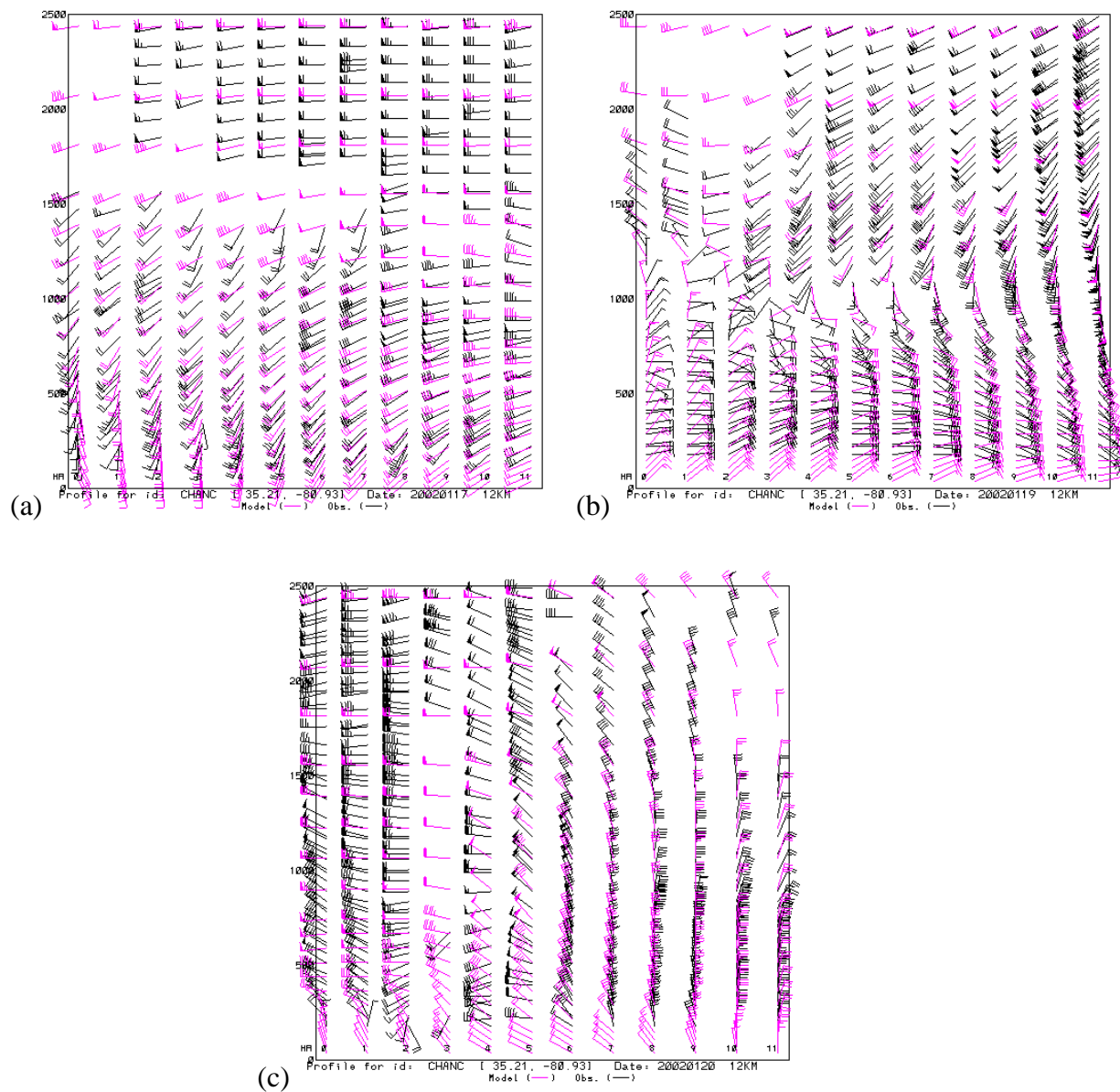
To go further to quantify model performance, upper air data from the model was compared to data from the Charlotte, North Carolina profiler. Figure 4-1 shows a series of profiler plots from the Charlotte, North Carolina profiler. Profilers yield results at a much finer vertical and temporal resolution than do standard rawinsondes (balloons with attached meteorological equipment used to take upper air readings). The profiler data are **not** used to nudge, or correct MM5 modeling results, and in fact cannot effectively be used in that capacity without additional quality control to remove or correct erroneous data. Since the model results will not be artificially biased toward the profiler data because of nudging and the profiler has a high data resolution, it makes an excellent source of data to judge model performance.

Figure 4-1 and 4-2 compare model predicted winds (purple wind barbs) with profiler-derived winds (black wind barbs) over the lowest 2500 meters of the atmosphere. Each plot contains 12 hours of data, with the hour of the observation labeled near the plot bottom, with the hours increasing from left to right. The wind barbs follow the meteorological standard, with a full barb representing a 10-knot (kt) wind, a half barb representing a 5-kt wind, and a full flag representing a 50-kt wind.

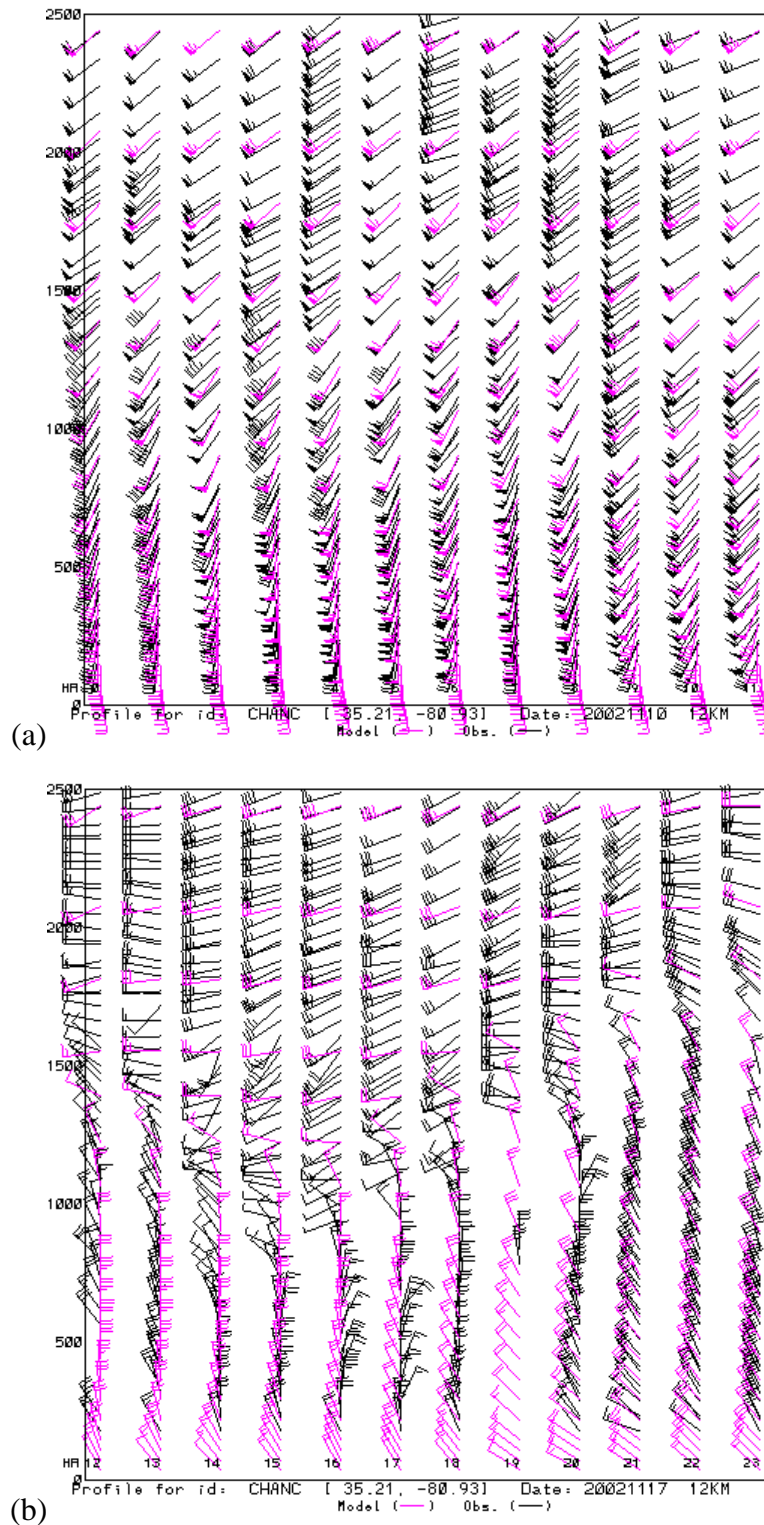
Figure 4-1(a) is from the period of 12 to 23 Coordinated Universal Time (UTC) on January 17, 2002, and depicts the typical wind flow pattern prior to frontal passage. Figure 4-1 (b) is 00-11 UTC on January 19, 2002, shows the disruption to the winds field as a cold front passes through the area, with Figure 4-1(c) (00-11 UTC on January 20, 2002) illustrating the northerly flow typically seen after front passage in the region. The model captures the wind direction fairly well through out the atmosphere. The model winds do become disjointed from the observations in the mid levels during the early hours of the frontal passage on the 19<sup>th</sup> (Figure 4-1(b)).

Figure 4-2(a) represents the time period from 00 UTC to 11 UTC on November 10, 2002, and show the modeling capturing uniform flow through out the atmosphere. Figure 4-2(b) is from seven days later (12-23 UTC on November 17, 2002) and demonstrates the model capturing the disturbance of the uniform flow in the upper levels.

Overall, these Charlotte, North Carolina profiler plots show typical performance in that the model generally matches the profiler winds, but not perfectly. Upper levels winds are captured very well, as are the wind shifts associated with frontal passages. In the subset of days presented here, the model winds are approximately within 20 degrees of the profiler observed winds, and typically are much closer. Unfortunately, it is difficult to know if this slight wind direction bias indicates a model flaw or an issue with the profiler data being representative. It is likely that there are physical mechanisms in the real world of which the model is unaware, which in this case are not being compensated for via nudging.



**Figure 4-1 The Charlotte, NC (CHANC) profiler winds are co-plotted with the 12-km MM5 winds for (a) 12-23 UTC on January 17, 2002, (b) 00-11 UTC on January 19, 2002, and 00-11 UTC on January 20, 2002. .**



**Figure 4-2 The Charlotte, NC (CHANC) profiler winds are co-plotted with the 12-km MM5 winds for (a) 00-11 UTC on November 10, 2002, and (b) 12-23 UTC on November 17, 2002**

## 5 SUMMARY

In general, the meteorological model performed quite well at the 12 km grid resolution. Most of the time the model statistics fell within the expected ranges of error. The NCDAQ believes that the meteorological model performance is adequate for this modeling exercise and should produce credible inputs for the air quality modeling for the attainment demonstration for the Metrolina area.

**ATTACHMENT 1**

**TO**

**APPENDIX I**

# **MM5 2002 Modeling in Support of VISTAS (Visibility Improvement – State and Tribal Association of the Southeast)**

## **Task 3f Deliverable**

Prepared for:

Mr. Mike Abraczinskas  
VISTAS Technical Analysis Workgroup  
NC Division of Air Quality  
1641 Mail Service Center  
Raleigh, NC 27699-1641

Prepared by:

Mr. Don Olerud  
Mr. Aaron Sims  
Baron Advanced Meteorological Systems, LLC  
North Carolina State University  
Marine Earth and Atmospheric Sciences  
1125 Jordan Hall, Campus Box 8208  
Raleigh, North Carolina 27695-8208

August 4, 2004

1 Introduction..... 1

2 Brief Description of the Meteorological Modeling Approach..... 1

3 Results ..... 5

    A. Segment Analyses..... 5

    B. Monthly Analyses ..... 19

        12-km statistical tables..... 21

        36-km statistical tables..... 34

        Statistical discussion..... 46

4 Summary and Conclusions ..... 92

5 Acknowledgements ..... 93

6 References ..... 94

# 1 Introduction

In order to ultimately improve visibility in the southeastern US, the Visibility Improvement State and Tribal Association of the Southeast (VISTAS) (<http://www.vistas-sesarm.org/>) is in the midst of an extensive modeling effort. A 12-month modeling period is deemed necessary to cover an adequate range of visibility impairment. The meteorological component of the modeling is performed by Baron Advanced Meteorological Systems (BAMS) using the PSU/NCAR mesoscale model (MM5) (<http://www.mmm.ucar.edu/mm5/mm5-home.html>). This document evaluates and documents the results of that modeling.

A great deal of effort was expended to determine the optimal MM5 configuration to be implemented for the annual run. The modeling protocol ([http://www.baronams.com/projects/VISTAS/reports/VISTAS\\_TASK3a\\_draft.pdf](http://www.baronams.com/projects/VISTAS/reports/VISTAS_TASK3a_draft.pdf)) examines these sensitivity tests in detail before offering the desired model configuration and evaluation/presentation methodologies. The reader is referred to that document for the details of model implementation.

## 2 Brief Description of the Meteorological Modeling Approach

The meteorological model used in this study is the PSU/NCAR Mesoscale Model (MM5 version 3.6.1+, Grell et al., 1994, MPP version), the same version of the code that was used in the sensitivity modeling. At the time the annual modeling began, the latest released version of the MM5 code was 3.6.2. Most of the v3.6.2 changes are included in the v3.6.1+ version of the code. If NCAR documentation is complete, the only modification not included involves the treatment of sea ice, a change likely to have negligible effect over the southeastern US. The v3.6.1+ code also includes an adapted version of EPA's MPP P-X code, an essential feature that does not readily port into later MM5 versions. The latest v3.6.2 MM5 preprocessors could readily be employed, so we did so.

The modeling domains are shown in figure 1.



Recall from the sensitivity testing that the configuration that produced the most desirable results was px-acm8. This configuration is implemented for the annual run with the following physics options:

<b>Soil:</b>	Pleim-Xiu land surface model
<b>PBL:</b>	Asymmetric Convective Mixing
<b>Radiation:</b>	Rapid Radiative Transfer Model (RRTM)
<b>Cloud:</b>	Kain-Fritsch 2 cumulus parameterization
<b>Microphysics:</b>	Reisner 1 (mixed phase)
<b>Analysis nudging:</b>	
<b>Aloft:</b>	
<b>36km:</b>	t (2.5E-4/s), q (1.0E-5/s), u and v (2.5E-4/s)
<b>12km:</b>	t (1.0E-4/s), q (1.0E-5/s), u and v (1.0E-4/s)
<b>Surface:</b>	
<b>36km:</b>	u and v (2.5E-4/s), T and q not nudged
<b>12km:</b>	u and v (1.0E-4/s), T and q not nudged
<b>Observational nudging:</b>	Not used
<b>Snow effects:</b>	Turned on via IFSNOW = 1
<b>SST:</b>	EDAS 24-hr averaged skin temperatures

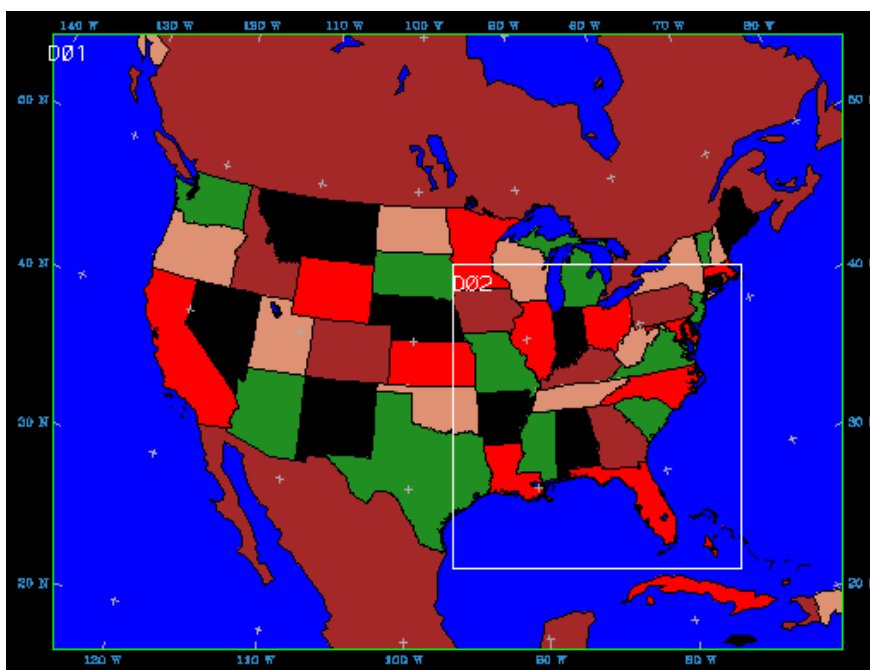


Figure 1. VISTAS 36-km/12-km MM5 modeling domains are shown.

Note that the decision to use sea surface temperatures (SST's) derived from the EDAS skin temperatures was not an arbitrary one. At the time this modeling effort began, most of the other RPO's were planning to use NCEP SST's to avoid problems that might arise from applying skin temperatures as SST's. The 1996 annual modeling effort conducted by Olerud *et al* (2000) suffered from very high inland lake temperatures as the MM5 system erroneously applied land skin temperatures to areas such as the Great Salt Lake. Fortunately the 3.6.2 version of the MM5 preprocessor INTERPF treats skin temperatures in a more appropriate manner, forcing a 24-hour average of skin temperatures if they are being used as a surrogate for SST's. The downside of using the NCEP SST fields is that they have a very coarse resolution of 2.5x2.5 degrees (~270x270 km). Alternatively the EDAS fields are available at 40-km resolution. Figures 2 and 3 show the resultant ground temperatures (equivalent to SST's over water) a few hours into test runs using the alternate SST initializations. The differences between the two approaches are clearly seen in the Gulf of Mexico. Note how appropriately warm the SST's are along the Mexican coast in the EDAS run, while the NCEP run is markedly colder and more "blocky". Similar improvements are seen in the Great Lakes and in the Gulf of California. Overall the EDAS approach seems to be the better approach.

The time-varying preprocessing is performed in six-day chunks (starting at 00Z) using fields created by TERRAIN using the "BotSoil" option from the input ~4km terrain databases. The EDAS analyses files are processed through pregrid and mapped to the MM5 grids via regridder. The fields are "improved" in LITTLE\_R by incorporating the surface, ship, and upper air observations that are available from NCAR. The LITTLE\_R output fields are then interpolated to the MM5 sigma coordinates by INTERPF. MM5 itself is run in 5.5-day segments with a 12-hr overlap from segment to segment. In order to allow sufficient spin-up time for subsequent air quality runs, the modeling initiated at 00Z Dec 17, 2001, continuing through 12Z Jan 1, 2003. With the exception of TERRAIN (which was executed on an SGI machine), MM5 and all its preprocessors/postprocessors were run on a 2.8GHz Xeon Linux cluster, with the core model run on 32 processors via MPP. Complete details regarding model setup and implementation, including namelist examples, are available in the aforementioned modeling protocol.

## Layer 1 TEMPGu

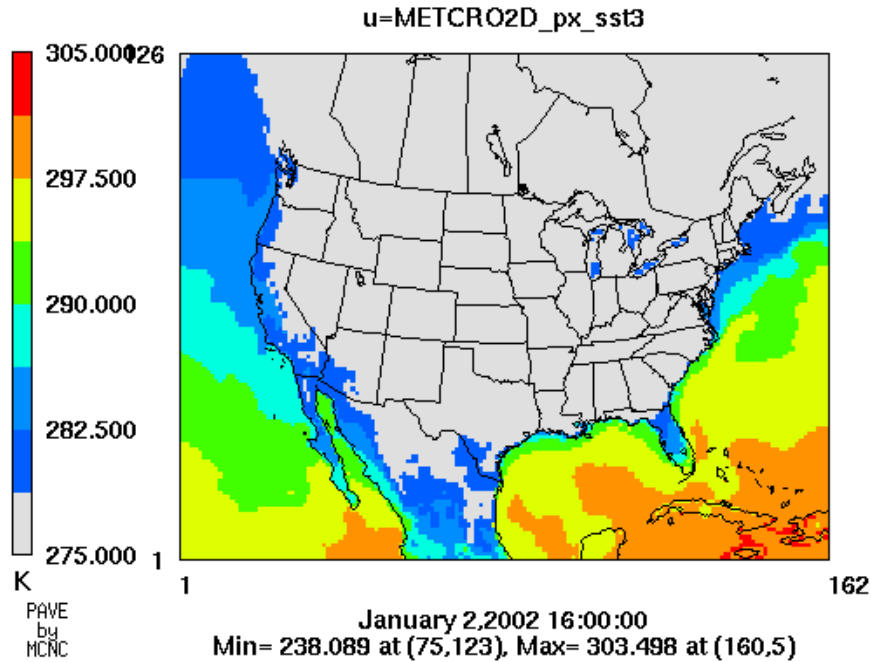


Figure 2. Ground (sea surface) temperatures resulting from an EDAS skin temperature MM5 initialization.

## Layer 1 TEMPGg

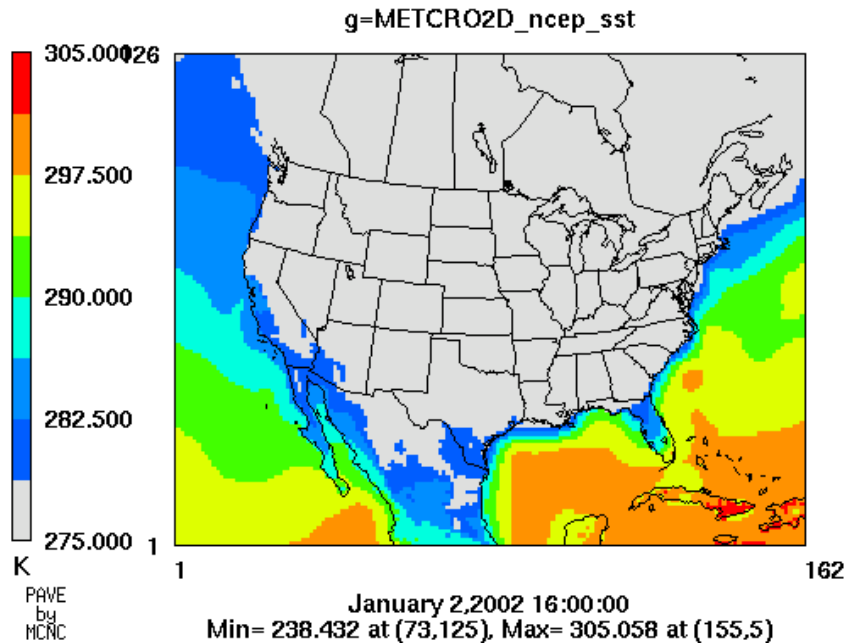


Figure 3. Ground (sea surface) temperatures resulting from an NCEP SST MM5 initialization.

### 3 Results

The amount of data produced in an annual MM5 simulation is foreboding. One needs to consider a variety of primary and secondary meteorological variables, and often these variables need to be examined spatially, vertically, and temporally. Obviously we need to find a way to summarize the results, while concurrently allowing sufficient detail so that possibly important hourly/diurnal variations are not glossed out. To accomplish this we have divided the analyses into two main categories: 1) Segment analyses, 2) Monthly analyses.

#### A. Segment Analyses

The segment analyses examine the useable portion of each 5.5-day segment in considerable detail, focusing on surface data, aloft data, and statistical data. We examine surface data in 6-hourly spatial animations, with observations overlaid when applicable. This allows us to determine qualitatively if the model is replicating the observed spatial pattern, and also if model performance has a noticeable diurnal variation. These animations are available for every Regional Planning Organization (RPO) region (and sometimes sub-RPO region) as appropriate. Figure 4 shows the observing stations color-coded by RPO; the rectangular region plotted for each RPO includes all of its observing sites. The variables plotted as spatial animations include temperature, mixing ratio, wind vectors, cloud fraction, alternative cloud fraction, relative humidity, precipitation, and planetary boundary layer (PBL) height. Of the above variables only PBL height is plotted without observations of some sort.

The number of surface spatial images produced for each segment exceeds 2000, accumulating to over 160,000 images for the span of the entire year. Rather than include a sizeable number of those images in this document, the reader is referred to the annual modeling website to access the animations via convenient pull-down menus ([http://www.baronams.com/projects/VISTAS/select\\_annual\\_product.html](http://www.baronams.com/projects/VISTAS/select_annual_product.html)). Instead, we will show here only a sampling of the types of images that are available on the website, using March 15, 2002, as our sample day. Figure 5 shows the temperature spatial plot for the 12-km VISTAS region for 18Z on our sample day. The synoptic conditions are quite well captured, with cooler temperatures located in the northwestern part of the region and warmer temperatures located in the southwestern part of the region. Close examination reveals a subtle cold bias, illustrated best by the light-red-colored observations in southern Georgia and Florida, overlaid on cooler orange-colored model temperatures. Figure 6 shows a wind plot for the same hour. The model picks up the cold front in southern Illinois quite well, as it does the strong warm advection in the Carolinas. This result is typical of the quality of the model performance.

We also produce time series of key meteorological variables at over 30 sites of interest. Figure 7 shows such a trace for Pittsburgh, PA (KPIT), for the five-day segment encompassing March 15, 2002. For a site like KPIT, whose elevation places it most realistically in an aloft model layer, we include the aloft model data, as well as data from model layer 1. For this segment, the model performs relatively well for most of the meteorological variables. However, a noticeable cold bias is seen on the afternoons of March 13 and 14, leading to a significant overestimation of relative humidity during those periods. Again, this performance is rather typical of the model as a whole. We produce time series plots at both 36-km and 12-km (when applicable) resolutions, as well as figures with both resolutions plotted against the observations to allow for easy intrascale comparisons.

The final surface data product type is what we call a “combination” plot, which is simply a spatial model field juxtaposed with the most appropriate observational image. Figure 8 shows the 24-h CPC accumulated precipitation/model precipitation ending at 12Z March 16, 2002. The model does a nice job in predicting both the magnitude and the spatial extent of the precipitation field. Figure 9 displays the surface analysis field atop the 36-km model pressure/wind fields for 12Z March 15, 2002. In both images the pressure contours are colored blue, precipitation is shown via color shading, and wind barbs are colored black. Certain features (fronts, station data) are only available in the surface analysis. Note that on a synoptic scale the model does quite well replicating the observed features. Figure 10 compares visible satellite imagery over the southeastern U.S. with the 12-km MM5 predicted clouds for 18Z on our sample day. Once again the model does a credible job, though certain areas (e.g., Alabama) exhibit flawed performance. Figure 11 shows infrared satellite imagery compared with 36-km model clouds for 12Z on our sample day. Most of the synoptically induced cloud shields are captured, though there appears to be a general overestimation of cloud coverage in the model. This could be caused by the inability of the satellite to resolve low clouds in its imagery. These combination plots are produced once a day for visible satellite imagery/model clouds (18Z) and 24-h CPC accumulated precipitation/model precipitation (12Z), and twice a day (00Z, 12Z) for surface analysis/model pressure-winds-precipitation and infrared satellite imagery/model clouds.

### Evaluation Sites by RPO

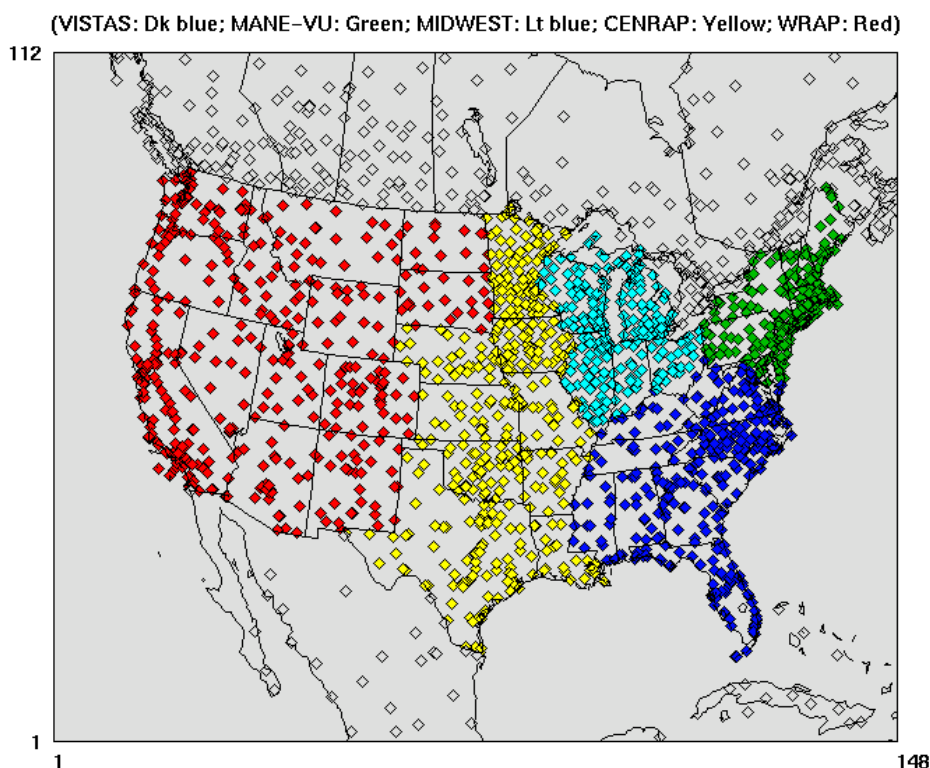


Figure 4. Surface observing network color-coded to represent Regional Planning Organization areas. Dark blue diamonds are in the VISTAS RPO, green diamonds are in the MANE-VU RPO, light blue diamonds are in the MIDWEST RPO, yellow diamonds are in the CENRAP RPO, and red diamonds are in the WRAP RPO. Gray diamonds represent sites out of the US portion of the modeling domain.

## Temperature (w Obs)

(Seg: mar12\_02, VISTAS: 12km, v02\_aaa, Layer 1)

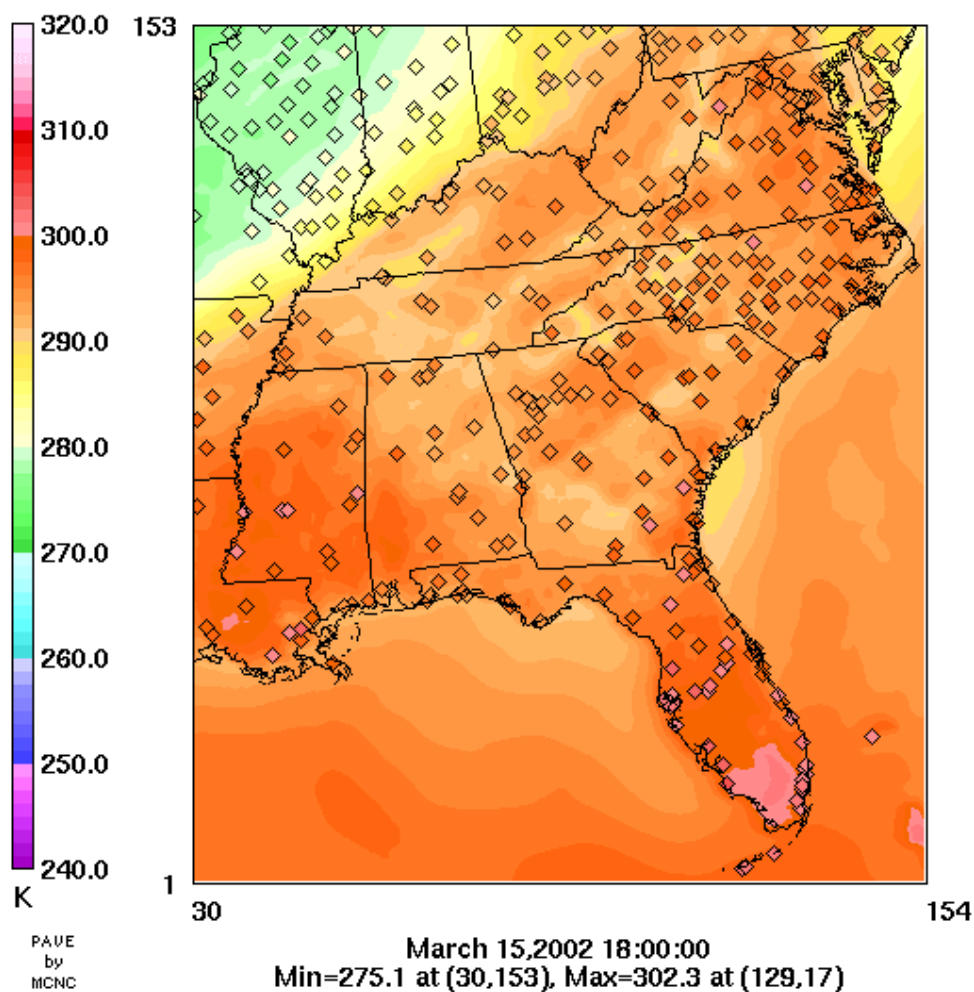


Figure 5. The surface spatial temperature plot over the 12-km VISTAS region is shown for 18UTC March 15, 2002.



## Winds (w Obs)

(Seg: mar12\_02, VISTAS: 12km, v02\_aaa, 10m)

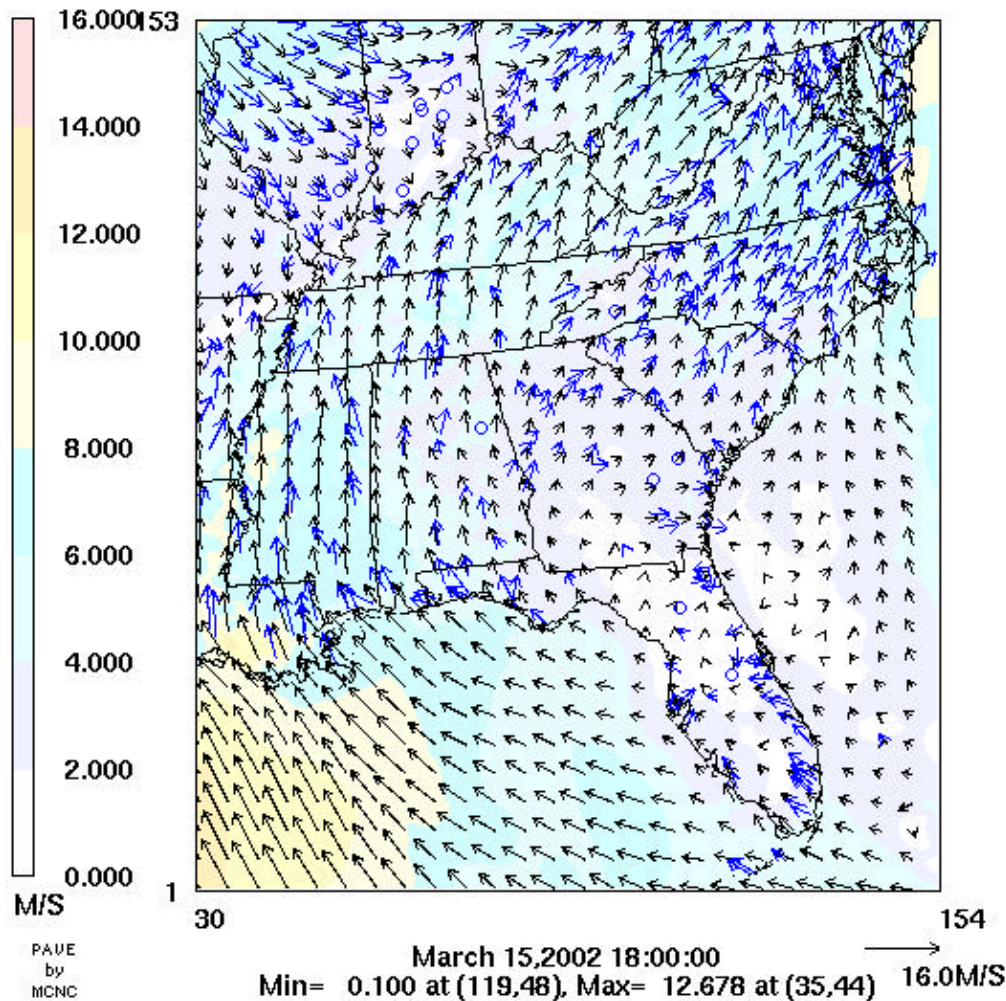


Figure 6. The surface spatial wind plot over the 12-km VISTAS region is shown for 18UTC March 15, 2002. The pastel color scale indicates the model-predicted wind speeds, while wind vectors are displayed in black for the model and blue for the observations.

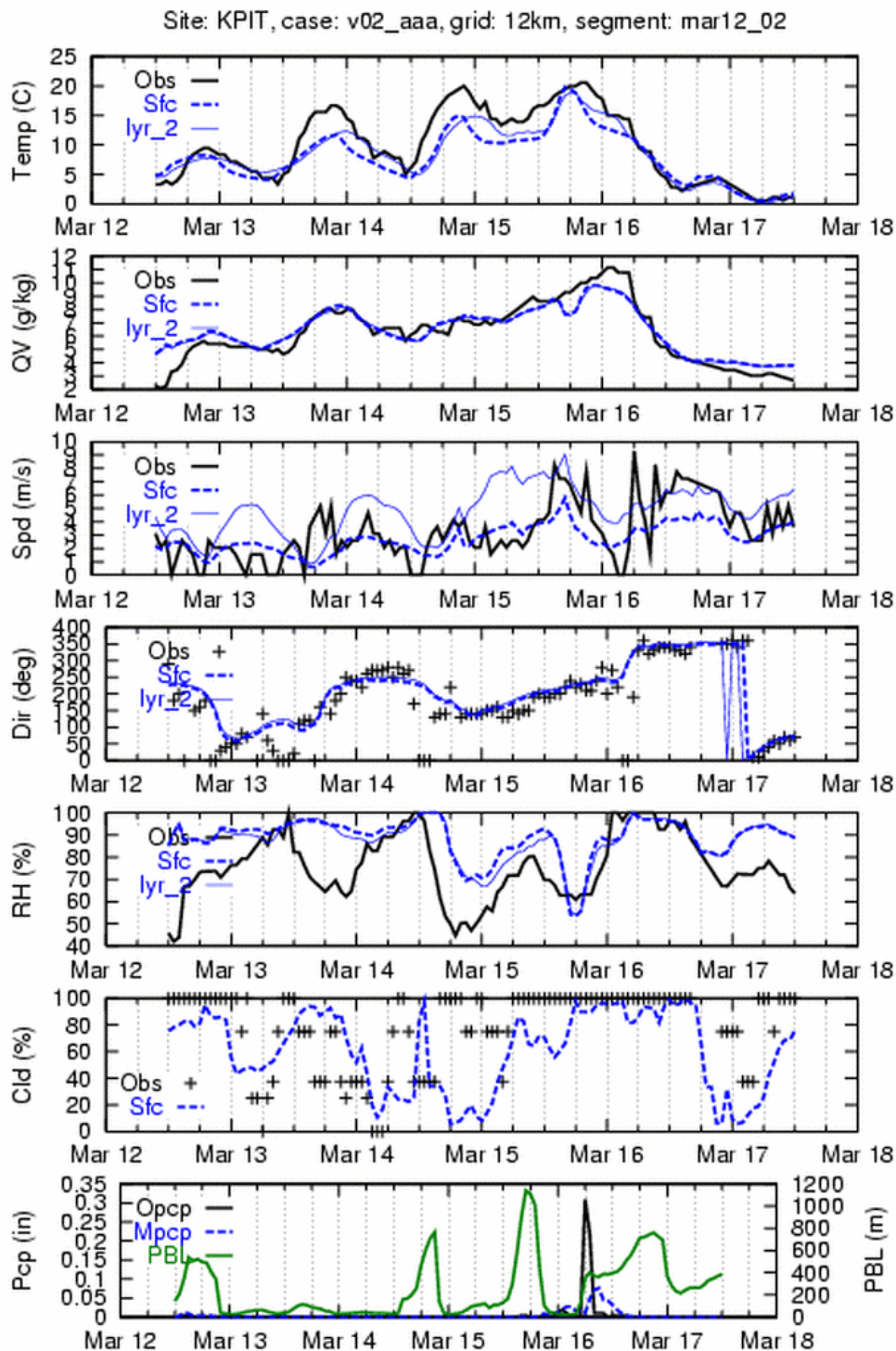
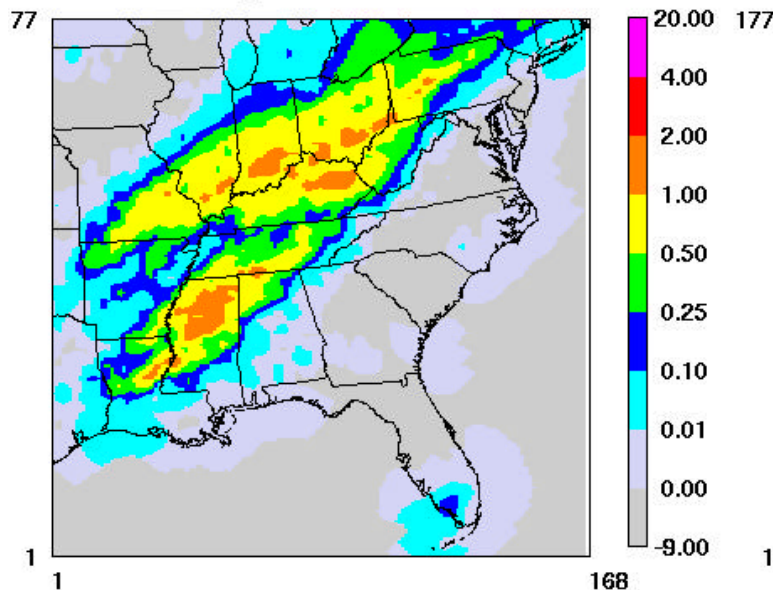


Figure 7. The surface time series trace for Pittsburgh, Pennsylvania is displayed for the March 12-17, 2002 modeling segment. The elevation for this site vertically matches model layer 2 better than layer 1 (i.e. sfc), so both model layers are included in the trace when applicable.



## 24 hr accum precip (in)

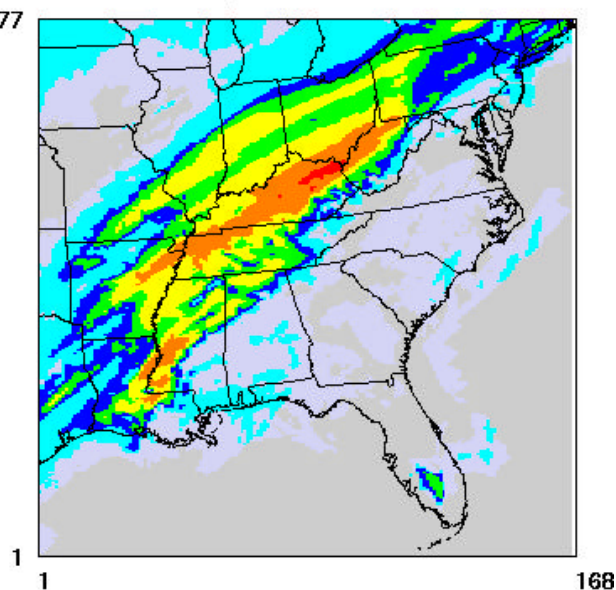
(CPC gridded obs)  
24-hr period ends at 12Z



March 16, 2002 12:00:00  
Min= 0.00 at (1,1), Max= 1.66 at (71,132)

## 24 hr accum precip (in)

(Seg: mar12\_02, v02\_aaa, 12km)  
24-hr period ends at 12Z



March 16, 2002 12:00:00  
Min= 0.00 at (2,1), Max= 2.32 at (87,126)

Figure 8. The 24-h accumulated precipitation (ending at 12UTC March 16, 2002) refashioned from the Climate Prediction Center analyses is displayed next to the 12-km MM5 estimates for the same time period.

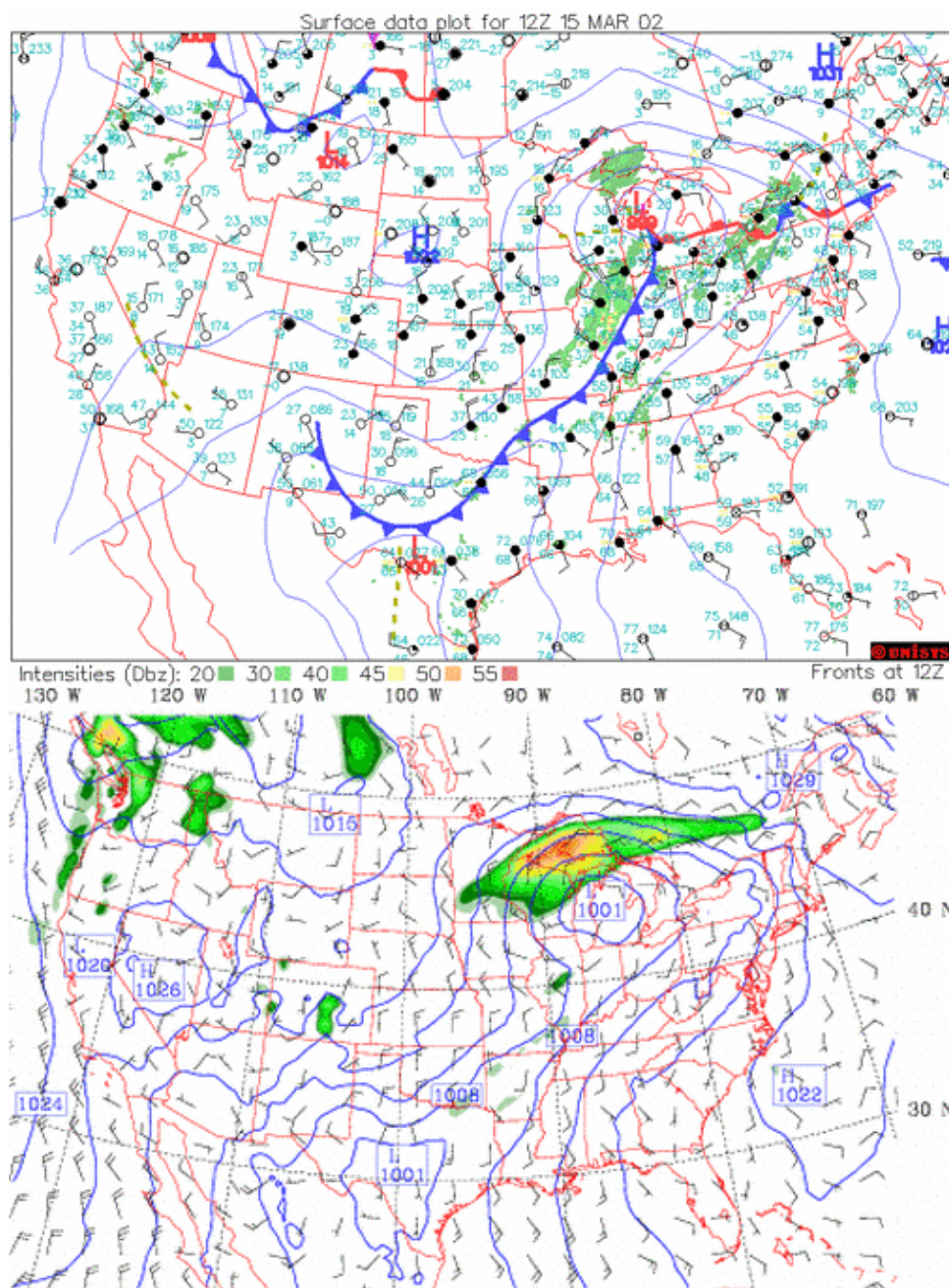


Figure 9. The surface analysis (from Unisys) for 12UTC March 15, 2002 is displayed atop the 36-km MM5 analyses for the same time period. Note that the model precipitation scale does not match the Unisys scale, and also note that the Unisys precipitation characterization is only for the US.



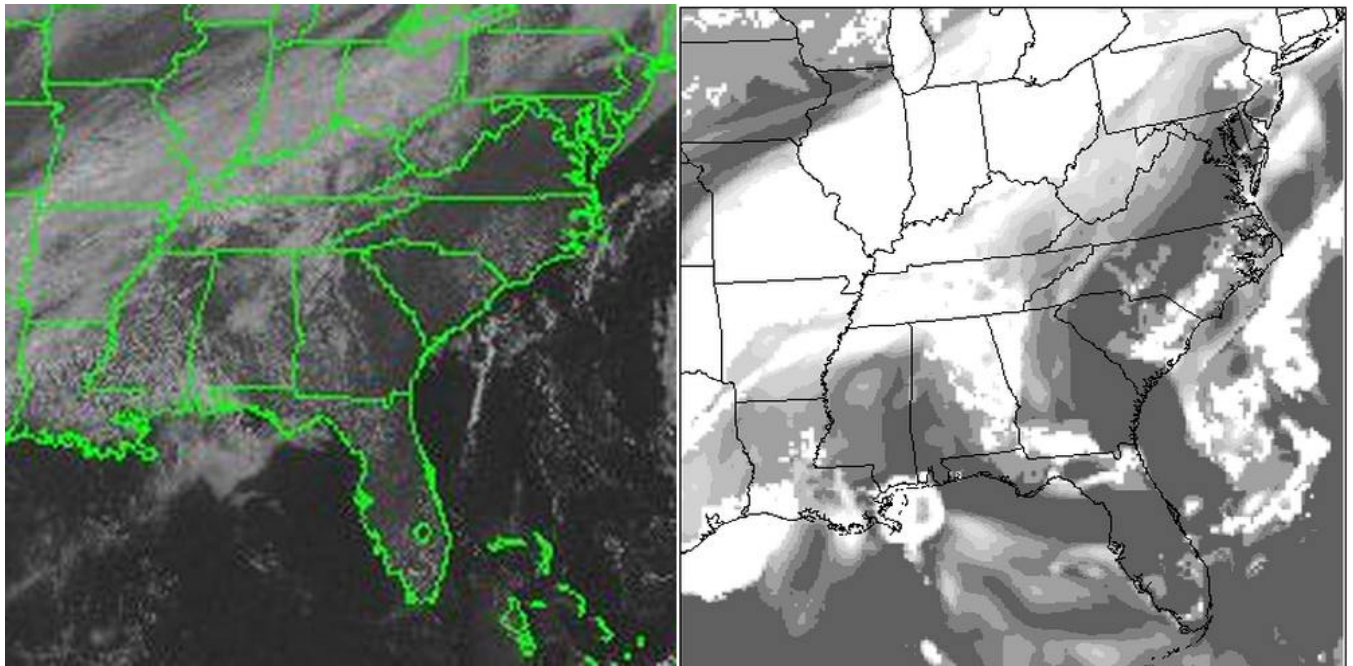


Figure 10. The GOES east visible satellite imagery is juxtaposed with the 12-km MM5 total cloud characterization for 18UTC March 15, 2002.

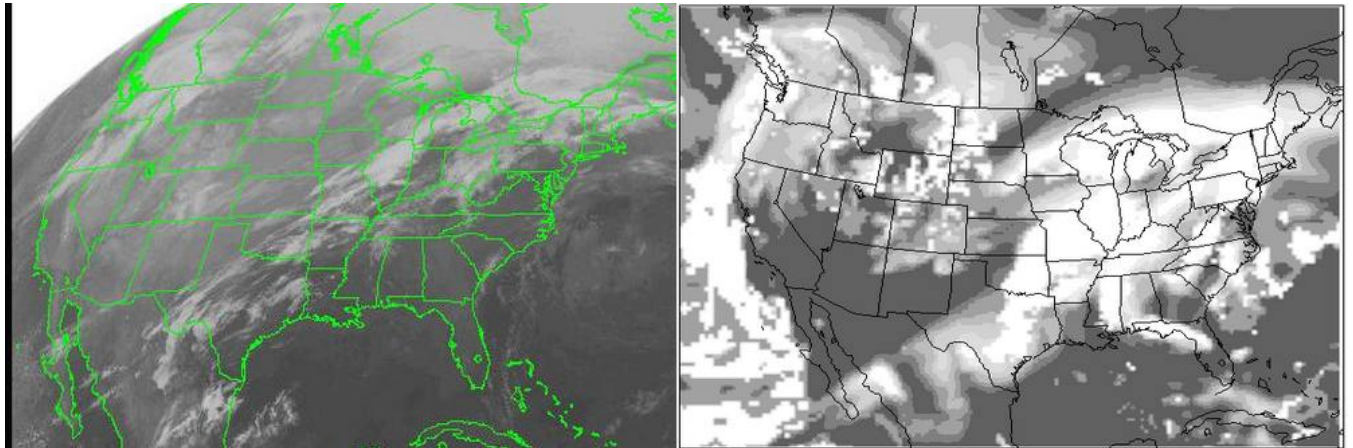


Figure 11. The GOES east infrared satellite imagery is juxtaposed with the 36-km MM5 total cloud characterization for 12UTC March 15, 2002. Note that low clouds may be difficult to see using infrared imagery.

The second segment analyses type is aloft products. These products include spatial analyses, sounding plots, and profiler plots. It is impractical to examine every one of the 34 model layers in detail, so we have decided to focus on three levels aloft for our spatial analyses. The three sigma-layers are layer 9 (~500m), layer 17 (~1600m), and layer 22 (~3400m). This allows us to visualize model performance 1) in the PBL, 2) near the top of/just above the PBL, and 3) in the free troposphere. These aloft spatial plots are very similar in nature to the corresponding plots produced at the surface, though plots for only temperature, mixing ratio, and winds are produced at a 12-hr temporal resolution. Figure 12 shows the wind plot for sigma layer 17 valid at 12Z March 15 for the 12-km grid. The spatial performance aloft is typically outstanding, indicating that the model replicates the observed synoptic pattern. This result is expected considering that we are applying nudging in our model runs.

We also produce a couple of different soundings to examine the ability of the model to capture vertical variations. These plots are made for every rawinsonde site in the VISTAS states, plus a sampling of sites across the country. Not only do we produce full surface-to-100 mb soundings, but we also zoom in on the lower portions of the atmosphere to examine the surface-to-500 mb soundings, as in figure 13. These sounding plots are called skewT's because the temperature scale (solid white line) is skewed and labeled on top of the figure. The pressure lines are also white but are labeled on the left of the plot. The red/pink lines in these plots represent observed/modeled temperatures, while the blue/cyan lines represent observed/modeled dew point temperatures. Observed/modeled wind barbs are offset to the right and are colored yellow and green, respectively. This Greensboro, NC sounding is rather typical in that the model temperature and winds match the observations better than do the dew point trace, and also in that the performance generally improves with height. This is again expected considering that temperature and moisture are not being nudged in the PBL, and that the strength of moisture nudging is much less than it is for temperature or winds.

Figure 14 shows an example of the final aloft evaluation product, the profiler plot. These plots compare model predicted winds with profiler-derived winds over the lowest 2500 meters of the atmosphere. Each plot contains 12 hours of data, with the hour labeled near the plot bottom. The wind barbs follow the meteorological standard, with a full barb representing a 10-kt wind, a half barb representing a 5-kt wind, and a full flag representing a 50-kt wind. Model winds are colored green, and the observed winds are colored white. Profilers yield results at a much finer vertical and temporal resolution than do standard rawinsondes. The profiler data are **not** used to nudge MM5, and in fact cannot effectively be used in that capacity without additional quality control to remove/correct erroneous data. This Raleigh, NC profiler plot shows typical performance in that the model generally matches the profiler winds, but not perfectly. In this case the model winds are biased by ~20 degrees counterclockwise. Unfortunately it is difficult to know if this bias indicates a model flaw or an issue with the profiler data being representative. It is likely that there are physical mechanisms in the real world of which the model is unaware, which in this case are not being compensated for via nudging.

## Wind (w Obs)

(Seg: mar12\_02, 12km, v02\_aaa, Layer 17)

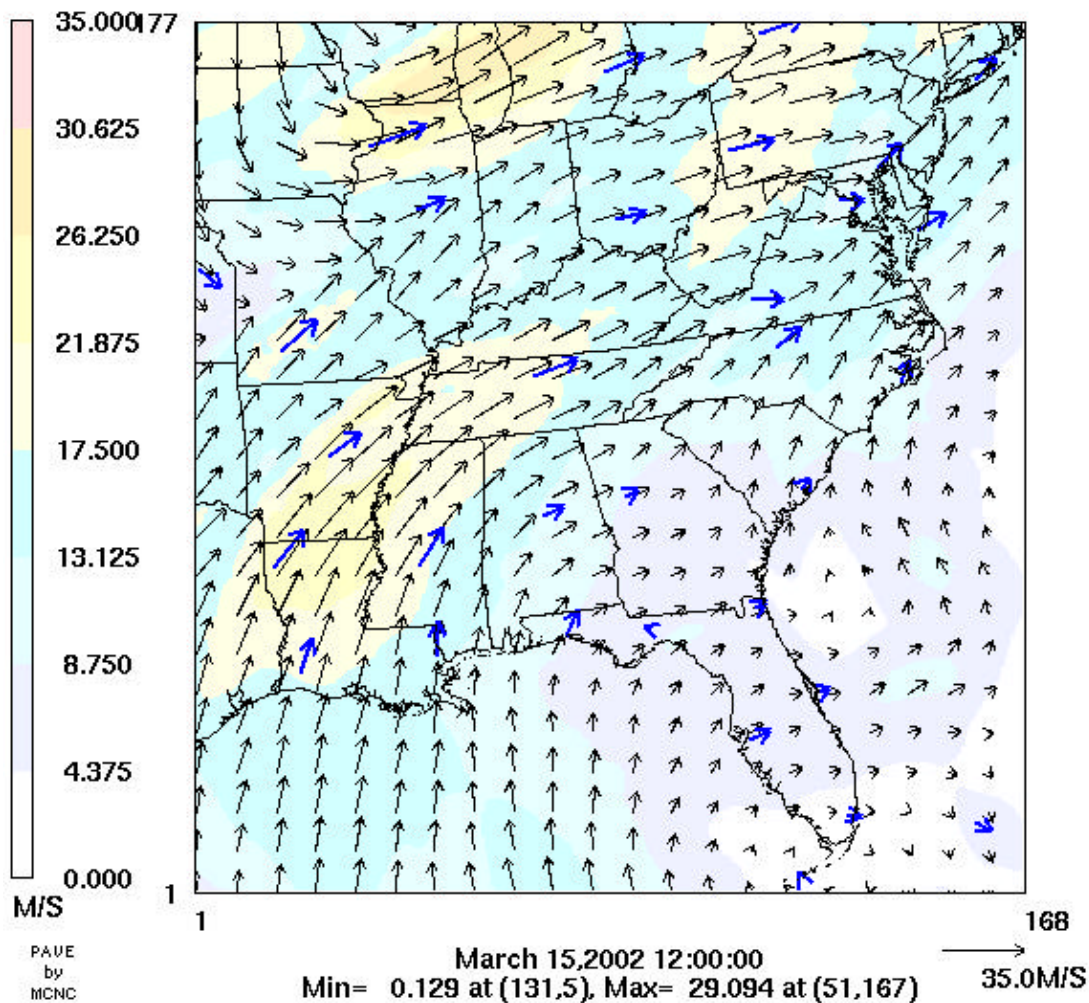


Figure 12. The layer 17 (~1600m) spatial wind plot over the 12-km VISTAS region is shown for 12UTC March 15, 2002. The pastel color scale indicates the model-predicted wind speeds, while wind vectors are displayed in black for the model and blue for the observations.

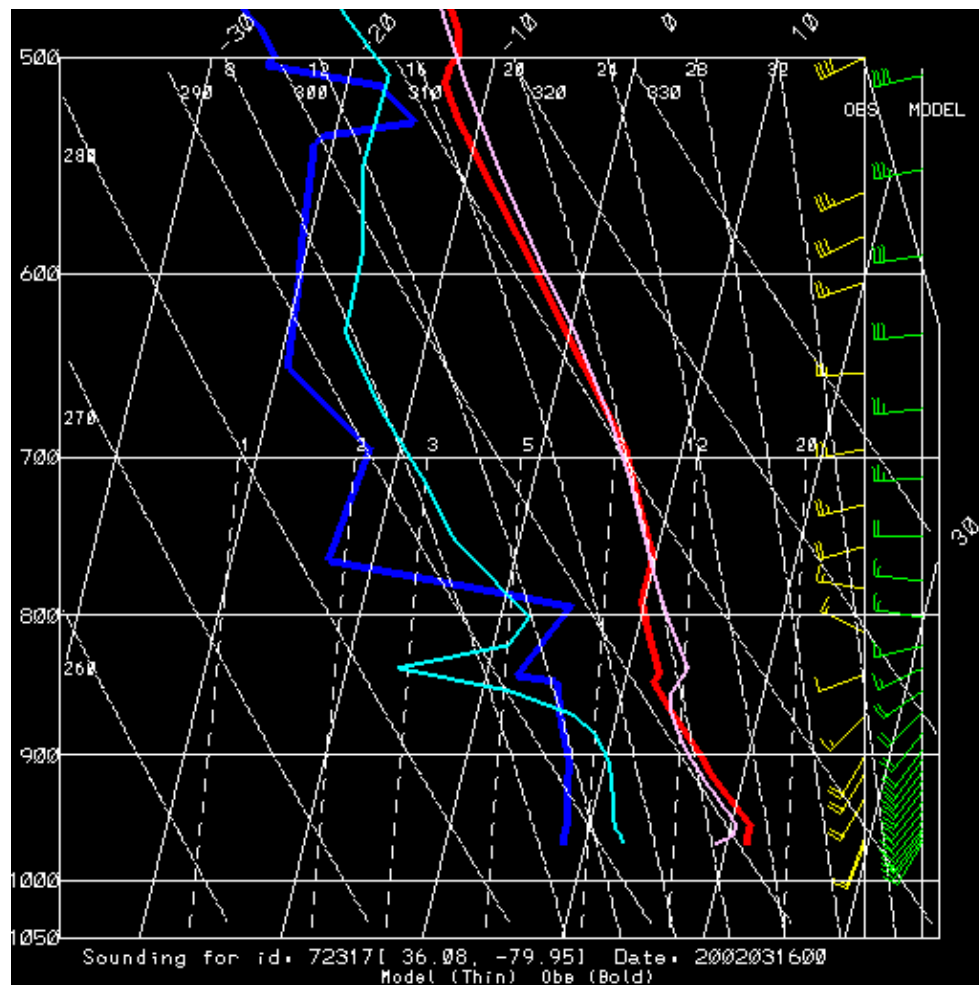


Figure 13. The 500-mb skewt plot for Greensboro, NC (72317) is shown for 00UTC March 16, 2002



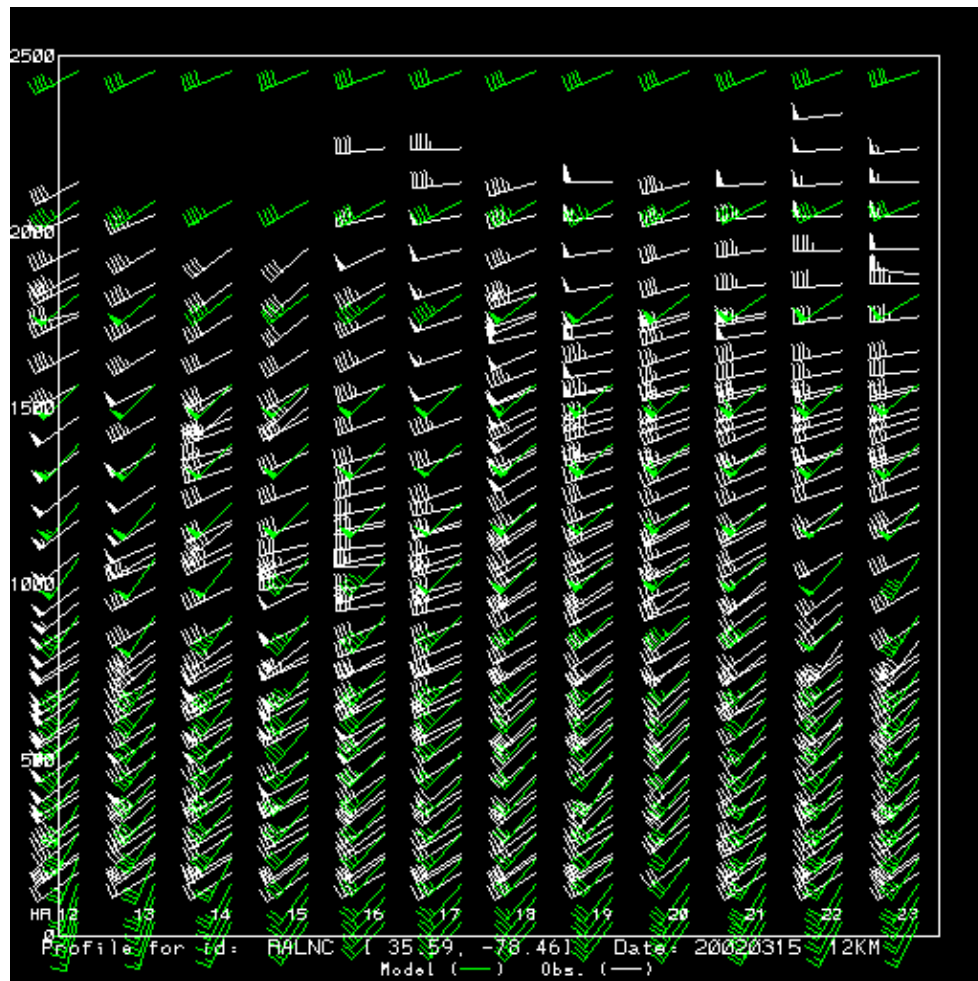


Figure 14. The Raleigh, NC (RALNC) profiler winds are co-plotted with the 12-km MM5 winds for 12-23 UTC on March 15, 2002.

Each modeling segment also contains a variety of statistical products. Table 1 shows the surface summary statistical table (all hours) for the 12-km VISTAS region for the modeling segment containing our sample day. Most of the variable names, while cryptic, are unambiguous and require no further explanation. We should note that CLD refers to the MCIP2.1 variable “CFRAC”, while CLD2 refers to the maximum of MCIP2.1 variables “CFRACH”, “CFRACM”, and “CFRACL”. The latter variable precisely matches the manner in which the observational cloud coverage is calculated, and is generally preferred for the purpose of meteorological analysis. We should also note that “bias” for wind direction should be ignored in favor of “dbias”, the appropriate bias calculation for a non-continuous function line wind direction. Also, “jtot” simply represents the number of model/obs pairs that go into the statistical calculations. While the sample table includes all valid hours within the modeling segment, we also produce tables that include only the 00-11Z hours (to highlight nighttime performance) and 12-23Z hours (to highlight daytime performance). These statistical tables are available for all valid RPO regions and RPO aggregates (i.e. US, Full).

Each modeling segment also contains a full suite of statistical time series plots, both at the surface and aloft. Table 1 revealed a slight positive moisture bias for the March 12-17, 2002 modeling segment, and figure 15 shows that the bias occurs primarily at night and during the first three days of the segment. Figure 16 quantifies the good wind speed performance we normally see aloft. Note that we include the number of valid model/obs pairs in these plots, thus allowing us to better interpret occasional statistic spikes that sometimes occur due to missing observational data. One of the characteristics noted in the sensitivity modeling was a persistent warm bias aloft, especially at layer 22. As expected we note the same signature in the annual modeling, with biases typically ranging from 0.5C-2.5C. It is likely that much of the bias stems from the averaging technique employed (height-weighted, not density-weighted), so the apparent bias should at least be noted but not emphasized. Precipitation statistical time series (not shown) are also routinely produced, but only for the “Full” regions. For a description of the statistical metrics shown below, the reader is referred to Olerud (2003a), available at [http://www.baronams.com/projects/VISTAS/reports/VISTAS\\_TASK1.pdf](http://www.baronams.com/projects/VISTAS/reports/VISTAS_TASK1.pdf).

<b>Total_stats</b>	<b>obsmean</b>	<b>modmean</b>	<b>bias</b>	<b>abserr</b>	<b>r2</b>	<b>ia</b>	<b>rmse</b>	<b>nbias</b>	<b>jtot</b>
TMP-1.5m_(K)	289.46	289.10	-0.36	1.87	0.859	0.951	2.37394	0.00116	30729
QV_(g/kg)	9.57	10.05	0.47	1.06	0.775	0.927	1.40093	-0.07477	30247
RH_(%)	80.80	86.26	5.46	9.42	0.530	0.813	12.98462	-0.09797	30246
WSPD-10m_(m/s)	2.93	3.23	0.29	1.29	0.410	0.767	1.62495	-99.00000	29488
SPD-lyr1_(m/s)	2.93	3.83	0.90	1.51	0.380	0.735	1.89940	-99.00000	29488
CLD_(%)	53.95	54.00	0.05	26.82	0.330	0.764	36.76081	-99.00000	29792
CLD2_(%)	53.95	58.22	4.28	26.36	0.307	0.760	39.19626	-99.00000	29792
TMP-lyr1_(K)	289.46	289.22	-0.24	1.87	0.854	0.949	2.39892	0.00074	30729

<b>Wdir_stats</b>	<b>obsmean</b>	<b>modmean</b>	<b>bias</b>	<b>abserr</b>	<b>ubias</b>	<b>vbias</b>	<b>uerr</b>	<b>verr</b>	<b>newtot</b>	<b>dbias</b>
WDIR_(deg)	190.87	183.85	-7.02	25.40	-0.089	0.314	1.15182	1.26613	29488	2.879

Table 1. Surface summary statistics are shown for the March 12-17, 2002 modeling segment for the 12-km VISTAS region.



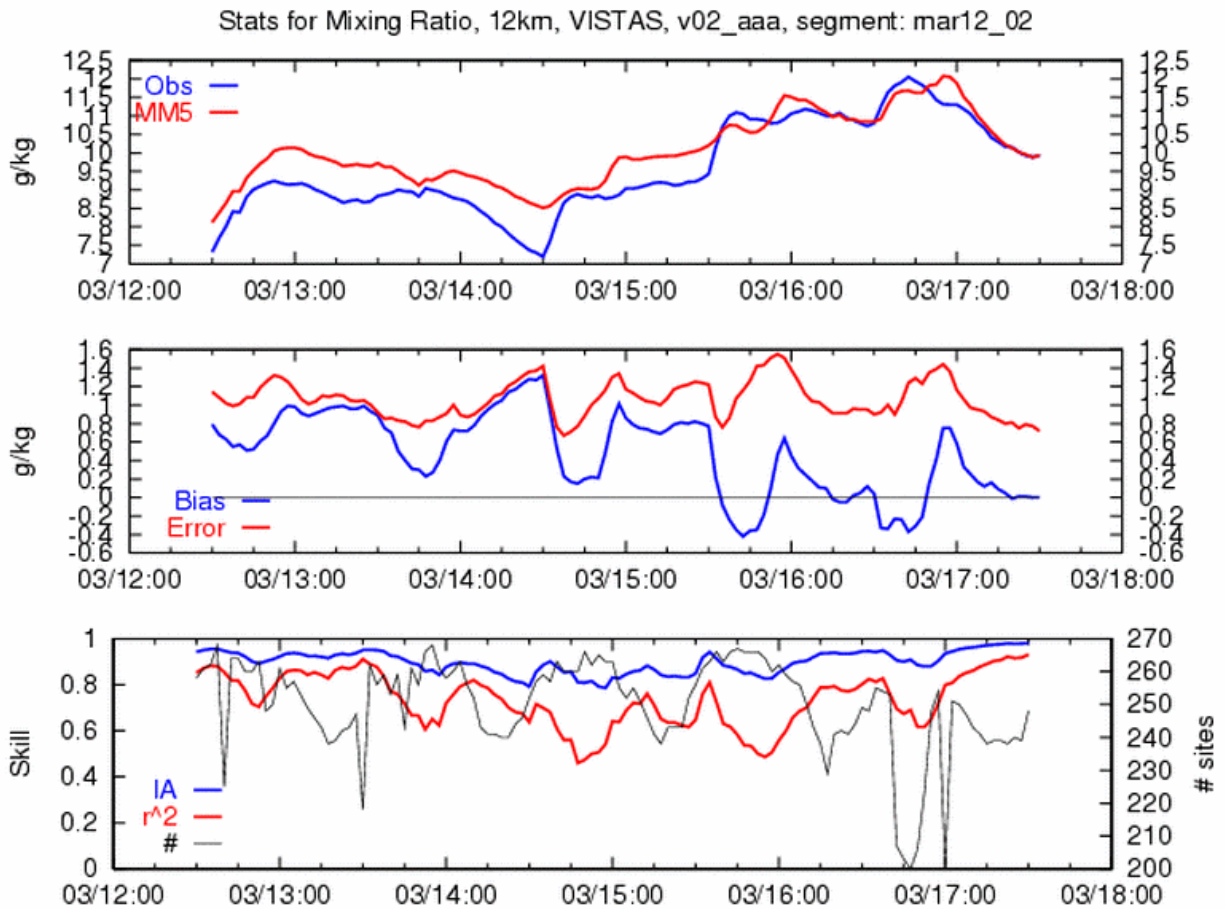


Figure 15. The surface statistical time series plot for water vapor mixing ratio is shown for the March 12-17, 2002 modeling segment for the 12-km VISTAS region.

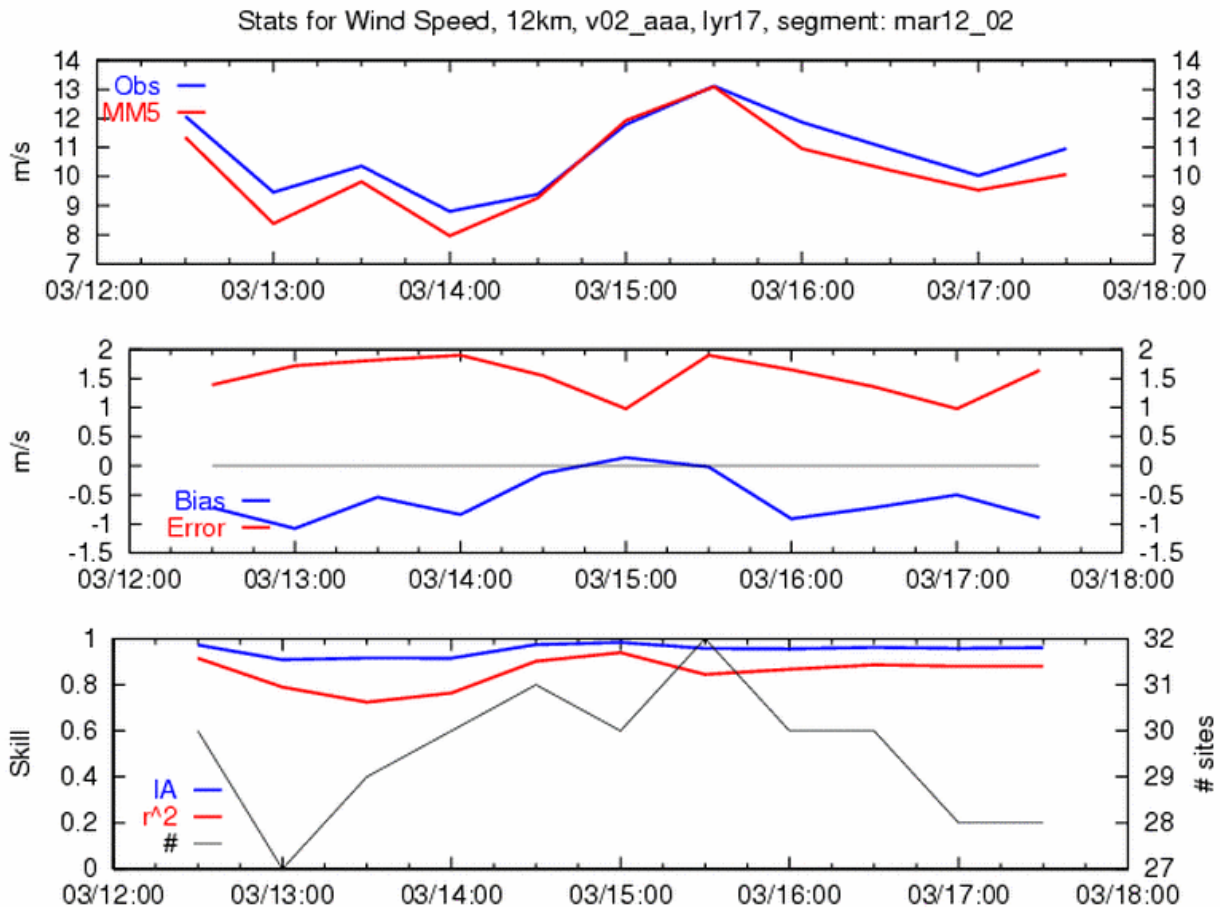


Figure 16. The MM5 sigma layer 17 statistical time series plot for wind speed is shown for the March 12-17, 2002 modeling segment for the 12-km VISTAS region.

## B. Monthly Analyses

Above we included only a sampling of the enormous number of segment analyses plots available. To access model performance in a more complete manner, we have aggregated data into monthly periods. Before examining these results in detail, a couple of points about our statistical processing methodology need to be made. The first involves the manner in which elevation discrepancies between the observations and the model are treated. We have rather arbitrarily decided that if the elevation of an observational site is more than 500 meters different than the model elevation, then that observing site is deemed unrepresentative and is not included in the statistical analyses. Mount Washington, NH (KMWN) is such a station. Even with automated quality control of the observational data, KMWN still occasionally stands out as an unrepresentative site in the MANE-VU spatial analyses plots of temperature and especially winds. If the elevation of a site is within 500 m of the model elevation, we include it in our processing, but not without attempting to account for biases that surely arise solely due to the elevation difference. These biases can be quite large, since people (and therefore airports and other typical observing sites) tend to be located in valleys. There is no easy way to deal with these

elevation differences, but to ignore their effect is probably worse than crudely accounting for them. Our methodology is to apply a standard atmosphere adjustment (6.5C/km) to the elevation differences. Figure 17 shows the magnitude of these adjustments that we subtract from the model temperatures before comparing with the observations. Note that for much of the western U.S., except along the coastline, the majority of sites are adjusted by a factor larger than the “benchmark” standard for temperature bias. This elevation effect is rather small for most of the rest of the country. To illustrate the effect this bias adjustment could make, assume that a station is located at an elevation of 750 m above mean sea level, but the model elevation is 1250 m. The lapse rate adjustment for that site would be -3.25C, and that factor would be subtracted from the standard bias calculation. So if the site reports a temperature of 17C while the model predicts 13C, the reported bias would be -0.75C, not -4.0C.

Another factor to consider in statistically evaluating model performance is the presence of observed calm winds. A calm wind report does not mean that the wind speed is identically 0.0 kts; rather, it means that the true wind speed is less than the instrument threshold. The lowest non-zero wind speed reported is 3 kts. The actual wind speed could thus be 0, 1, or 2 kts. Since the model will never completely “calm out”, this instrument threshold issue introduces a positive wind speed bias to a perfect model simulation. This can play a significant role in the southeastern US, especially at night and in the summer, when stagnant high-pressure systems routinely cause numerous calms to be reported. In an attempt to quantify the magnitude of this effect, we have introduced two additional wind speed metrics to our summary table. The variable “WSPD-no\_calms” quantifies wind speed statistics when all calm reports are thrown out. This approach, however, introduces a negative speed bias, since the < 3 kt winds are removed only in the observations. Probably a less biased approach is to simply assign a 1.5 kt wind speed to all calm reports. The variable “WSPD-min\_calm” quantifies the result when that approach is applied.

We have produced monthly summary statistical tables for all applicable RPO’s and for both grids. Since the precipitation statistics are commiserate with only two grid/scale combinations – 12-km Full and 36-km US – those are the only tables that include said information. In order to gain a thorough statistical overview of model performance throughout the year, tables 2-13 show the January-December 12-km Full statistics. Likewise tables 14-25 show the same for the 36-km US statistics. Recall the meteorological statistical benchmarks reported by Emery (2001):

Wind speed:	RSME	<= 2 m/s,	Bias <= +/- 0.5 m/s,	IA >= 0.6
Wind direction:	Gross Error	<= 30 deg,	Bias <= +/- 10 deg.	
Temperature:	Gross Error	<= 2 K,	Bias <= +/- 0.5 K,	IA >= 0.8
Humidity:	Gross Error	<= 2 g/kg,	Bias <= +/- 1 g/kg,	IA >= 0.6

Note that the benchmarks were developed not to provide a pass/fail standard to which all modeling results should be held, but rather to put the results into an historical context. We also note that only a few of the numerous statistical measures that we show are actually included in the above benchmarks. If a particular relevant metric fails to fall within the benchmarks, that metric will be colored red for easy identification. Even though layer 1 temperature and wind speed are included in the tables, they exist only to put the more relevant 1.5-m temperature/10-m speed statistics in context, so those metrics will not be compared to the benchmarks via color-coding.

## TDIFF

(Std atm temp diff based on model/obs elev ht diff)

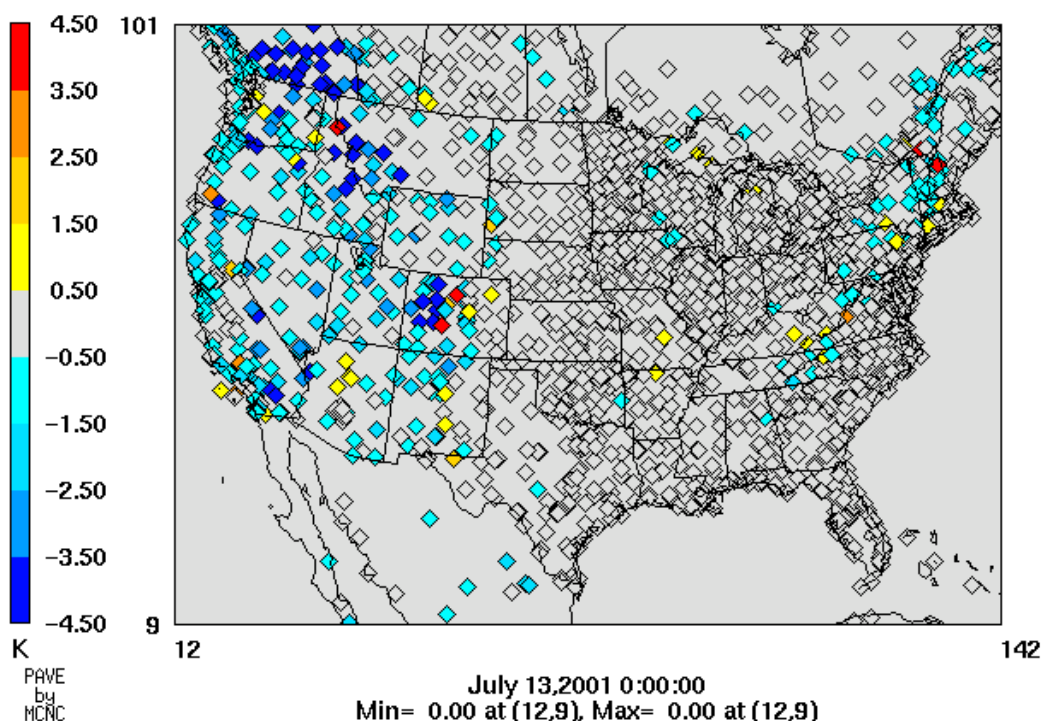


Figure 17. Model/obs elevation differences are converted to temperatures and plotted for the US portion of the 36-km grid. The temperatures are calculated assuming a standard atmosphere lapse rate of 6.5C/km, and practically indicate the temperature biases that might result solely by ignoring elevation-induced temperature effects. All of the observing sites are shown, including those sites that we ignore when calculating statistics due to their elevations being more than 500m different than the corresponding model elevations.

### 12-km statistical tables

Table 2 reveals a significant cold bias for the 12-km Full region. This is not a surprising result considering the results of our sensitivity testing. Note that though the bias is not close to the benchmark, the error (abserr) barely falls beyond its benchmark. The index of agreement (ia) metric is far better than the benchmark. As noted above, the historical context of the benchmarks primarily involves summertime modeling on a smaller scale – both spatially and especially temporally – than what we are doing here. Generally speaking, the increased spatial coverage and longer statistical aggregate time suggest that ia should always easily exceed the benchmarks listed above, and indeed no ia value in any of the following tables are colored red. MM5 cold bias is commonly seen for wintertime simulations, and should not necessarily be considered evidence of a flaw in this particular modeling exercise. The other metrics show overall good statistical performance. Even though precipitation statistics are shown for six threshold levels, meteorologists generally consider only the measurable precipitation level (0.01 inches). We would expect that objective analysis of the observed precipitation would “smear” the spatial extent of measurable precipitation, possibly introducing a perceived dry bias into the 0.01

statistics. This issue should be less significant at higher thresholds. However, at higher thresholds the number of valid model/obs pairs may decrease to a statistically insignificant level. Accordingly the 0.01 and 0.05 inch thresholds will receive most of our attention. For January we find only a very slight positive precipitation bias at those thresholds.

<b>Total_stats</b>	<b>obsmean</b>	<b>modmean</b>	<b>bias</b>	<b>abserr</b>	<b>r2</b>	<b>ia</b>	<b>rmse</b>	<b>nbias</b>	<b>jtot</b>
TMP-1.5m_(K)	277.89	276.87	-1.03	2.05	0.910	0.973	2.70059	0.00364	480126
QV_(g/kg)	4.46	4.63	0.17	0.58	0.936	0.983	0.83009	-0.06401	472271
RH_(%)	72.10	77.66	5.56	12.25	0.470	0.812	15.92663	-0.11393	472217
WSPD-regular_(m/s)	3.51	3.76	0.25	1.31	0.496	0.808	1.67567	-99.00000	466042
WSPD-nocalms_(m/s)	4.14	4.04	-0.10	1.14	0.444	0.805	1.50113	-0.08546	395406
WSPD-mincalm_(m/s)	3.63	3.76	0.13	1.19	0.502	0.823	1.54222	-0.35402	466042
SPD-lyr1_(m/s)	3.63	4.47	0.84	1.43	0.485	0.793	1.80626	-0.64790	466042
CLD_(%)	43.14	37.00	-6.14	24.52	0.414	0.792	35.41226	-99.00000	466016
CLD2_(%)	43.14	40.98	-2.15	23.30	0.411	0.805	35.95408	-99.00000	466016
TMP-lyr1_(K)	277.89	277.39	-0.50	1.97	0.906	0.974	2.58621	0.00173	480126

<b>Wdir_stats</b>	<b>obsmean</b>	<b>modmean</b>	<b>bias</b>	<b>abserr</b>	<b>ubias</b>	<b>vbias</b>	<b>uerr</b>	<b>verr</b>	<b>newtot</b>	<b>dbias</b>
WDIR_(deg)	255.83	254.29	-1.54	19.51	0.039	0.048	1.14482	1.21661	466042	1.667

<b>Pcp threshold (in)</b>	<b>ACC</b>	<b>BIAS</b>	<b>THREAT</b>	<b>ETS</b>	<b>FAR</b>	<b>HK</b>	<b>HSS</b>	<b>POD</b>	<b>HITS</b>	<b>ZEROES</b>	<b>MISSES</b>	<b>FALSES</b>
0.01	0.8665	1.0776	0.6672	0.5387	0.2285	0.7145	0.7002	0.8314	151526	338883	30719	44870
0.05	0.9187	1.0396	0.6962	0.6238	0.1948	0.7792	0.7684	0.8371	105380	414627	20501	25490
0.10	0.9342	1.0168	0.6881	0.6330	0.1915	0.7804	0.7753	0.8221	82119	446660	17770	19449
0.25	0.9555	0.9315	0.6602	0.6266	0.1754	0.7474	0.7705	0.7681	48901	491933	14764	10400
0.50	0.9665	0.9319	0.5626	0.5412	0.2536	0.6800	0.7023	0.6956	24395	522640	10676	8287
1.00	0.9851	0.8378	0.4887	0.4804	0.2799	0.5976	0.6490	0.6033	8042	549542	5288	3126

Table 2. January 2002 statistical table for the 12-km Full region is shown.

Table 3 shows that the cold bias, while smaller, still exists for February 2002 for the 12-km Full region. Most of the other statistics show exceptional performance, though the model does exhibit a slight positive precipitation bias. Very similar results are seen in March 2002 (table 4). By April 2002 (table 5) the cold bias has practically gone. We do note that precipitation biases at higher threshold levels start to become significantly positive. Precipitation biases for May (table 6) are lower at the 0.01 and 0.05 thresholds, while most of the other non-precipitation statistics reveal excellent model performance. The summer months (tables 7-9) reveal good performance for temperature, humidity, and wind speed, but the average directional error has crept up to near or slightly above the benchmark value. This is not surprising given the weak synoptic forcing prevalent during the summer months, meaning that forces that the model does not handle as well often drive the actual wind direction. The other statistical concern involves clouds and precipitation. The model seems to overestimate clouds by a bit, and precipitation becomes significantly biased, but only at higher thresholds. The implication is that the model does a reasonable job in predicting the overall amount of precipitation coverage, but is also too

efficient in producing rainfall when it occurs. This is undoubtedly a convective precipitation problem. Table 10 shows that the summertime precipitation bias has disappeared by September 2002, replaced by a dry bias at the lowest thresholds. All of the other benchmark statistical measures are met, though wind speed bias is at the upper limit of the benchmarks. Table 11 reveals that October 2002 is another dry-biased precipitation month, while we also see evidence that the wintertime cold bias is reappearing. November (table 12) is well modeled statistically except for the cold bias of  $-0.79^{\circ}\text{C}$ , while December (table 13) is even more cold-biased ( $-1.06^{\circ}\text{C}$ ).

<b>Total_stats</b>	<b>obsmean</b>	<b>modmean</b>	<b>bias</b>	<b>abserr</b>	<b>r2</b>	<b>ia</b>	<b>rmse</b>	<b>nbias</b>	<b>jtot</b>
TMP-1.5m_(K)	278.10	277.43	-0.67	1.76	0.915	0.976	2.33970	0.00234	439420
QV_(g/kg)	3.93	3.91	-0.03	0.57	0.909	0.976	0.78907	-0.00807	432003
RH_(%)	65.77	67.39	1.62	12.29	0.542	0.854	16.02342	-0.04847	431961
WSPD-regular_(m/s)	4.05	4.25	0.20	1.33	0.609	0.865	1.70182	-99.00000	425678
WSPD-nocalms_(m/s)	4.69	4.59	-0.10	1.20	0.564	0.859	1.57635	-0.07560	367594
WSPD-mincalm_(m/s)	4.16	4.25	0.09	1.23	0.615	0.874	1.59099	-0.30071	425678
SPD-lyr1_(m/s)	4.16	4.99	0.83	1.45	0.605	0.851	1.83938	-0.57027	425678
CLD_(%)	37.15	30.80	-6.35	24.40	0.368	0.766	35.60085	-99.00000	429885
CLD2_(%)	37.15	34.84	-2.32	23.41	0.375	0.785	35.93363	-99.00000	429885
TMP-lyr1_(K)	278.10	277.74	-0.36	1.80	0.908	0.974	2.36523	0.00123	439420

<b>Wdir_stats</b>	<b>obsmean</b>	<b>modmean</b>	<b>bias</b>	<b>abserr</b>	<b>ubias</b>	<b>vbias</b>	<b>uerr</b>	<b>verr</b>	<b>newtot</b>	<b>dbias</b>
WDIR_(deg)	272.22	274.51	2.29	18.57	-0.079	-0.054	1.16272	1.26860	425678	2.329

<b>Pcp threshold (in)</b>	<b>ACC</b>	<b>BIAS</b>	<b>THREAT</b>	<b>ETS</b>	<b>FAR</b>	<b>HK</b>	<b>HSS</b>	<b>POD</b>	<b>HITS</b>	<b>ZEROES</b>	<b>MISSES</b>	<b>FALSES</b>
0.01	0.8833	1.0906	0.6637	0.5577	0.2353	0.7361	0.7161	0.8340	117691	333894	23429	36210
0.05	0.9186	1.1384	0.6574	0.5909	0.2550	0.7826	0.7428	0.8482	79895	389690	14299	27340
0.10	0.9377	1.1153	0.6596	0.6107	0.2462	0.7947	0.7583	0.8407	61719	417651	11695	20159
0.25	0.9617	1.0924	0.6419	0.6142	0.2512	0.7929	0.7610	0.8181	35114	456524	7809	11777
0.50	0.9751	1.0677	0.5661	0.5503	0.3000	0.7328	0.7099	0.7474	16637	481835	5622	7130
1.00	0.9873	0.8432	0.4215	0.4150	0.3519	0.5414	0.5866	0.5465	4719	500027	3916	2562

Table 3. February 2002 statistical table for the 12-km Full region is shown.



<b>Total_stats</b>	<b>obsmean</b>	<b>modmean</b>	<b>bias</b>	<b>abserr</b>	<b>r2</b>	<b>ia</b>	<b>rmse</b>	<b>nbias</b>	<b>jtot</b>
TMP-1.5m_(K)	280.91	280.26	-0.65	1.76	0.942	0.983	2.32739	0.00225	483897
QV_(g/kg)	5.38	5.38	0.00	0.67	0.936	0.983	0.96168	-0.00419	475077
RH_(%)	69.00	71.47	2.47	11.43	0.617	0.880	15.20245	-0.05256	475043
WSPD-regular_(m/s)	4.13	4.30	0.16	1.34	0.596	0.865	1.73173	-99.00000	467848
WSPD-nocalms_(m/s)	4.70	4.58	-0.12	1.22	0.576	0.866	1.60036	-0.06625	411953
WSPD-mincalm_(m/s)	4.23	4.30	0.07	1.25	0.606	0.874	1.63098	-0.28051	467848
SPD-lyr1_(m/s)	4.23	5.02	0.79	1.46	0.595	0.853	1.87119	-0.53366	467848
CLD_(%)	48.42	42.79	-5.63	24.89	0.410	0.797	35.58189	-99.00000	473232
CLD2_(%)	48.42	47.55	-0.88	23.60	0.405	0.806	36.45646	-99.00000	473232
TMP-lyr1_(K)	280.91	280.41	-0.50	1.77	0.940	0.983	2.32967	0.00170	483897

<b>Wdir_stats</b>	<b>obsmean</b>	<b>modmean</b>	<b>bias</b>	<b>abserr</b>	<b>ubias</b>	<b>vbias</b>	<b>uerr</b>	<b>verr</b>	<b>newtot</b>	<b>dbias</b>
WDIR_(deg)	252.38	245.63	-6.75	20.02	-0.112	0.002	1.21584	1.32478	467848	1.883

<b>Pcp threshold (in)</b>	<b>ACC</b>	<b>BIAS</b>	<b>THREAT</b>	<b>ETS</b>	<b>FAR</b>	<b>HK</b>	<b>HSS</b>	<b>POD</b>	<b>HITS</b>	<b>ZEROES</b>	<b>MISSSES</b>	<b>FALSSES</b>
0.01	0.8473	1.0718	0.6892	0.5217	0.2113	0.6939	0.6857	0.8453	191726	287817	35081	51374
0.05	0.8977	1.0883	0.7138	0.6122	0.2008	0.7791	0.7595	0.8698	144388	363713	21622	36275
0.10	0.9131	1.1050	0.7105	0.6294	0.2087	0.8000	0.7725	0.8744	120658	396180	17334	31826
0.25	0.9240	1.1188	0.6468	0.5867	0.2562	0.7746	0.7395	0.8322	78801	444170	15891	27136
0.50	0.9356	1.1182	0.5179	0.4779	0.3537	0.6809	0.6467	0.7227	39140	490425	15015	21418
1.00	0.9684	0.9143	0.4062	0.3902	0.3952	0.5383	0.5613	0.5529	12229	535891	9887	7991

Table 4. March 2002 statistical table for the 12-km Full region is shown.

<b>Total_stats</b>	<b>obsmean</b>	<b>modmean</b>	<b>bias</b>	<b>abserr</b>	<b>r2</b>	<b>ia</b>	<b>rmse</b>	<b>nbias</b>	<b>jtot</b>
TMP-1.5m_(K)	288.08	287.89	-0.19	1.57	0.943	0.984	2.03842	0.00058	471754
QV_(g/kg)	8.06	8.04	-0.02	1.01	0.901	0.973	1.37537	0.00944	464645
RH_(%)	68.59	69.02	0.43	11.03	0.600	0.877	14.54039	-0.02005	464619
WSPD-regular_(m/s)	3.87	4.05	0.18	1.31	0.567	0.849	1.68699	-99.00000	452937
WSPD-nocalms_(m/s)	4.44	4.33	-0.11	1.18	0.532	0.847	1.55713	-0.07088	394419
WSPD-mincalm_(m/s)	3.97	4.05	0.08	1.22	0.576	0.859	1.57709	-0.29562	452937
SPD-lyr1_(m/s)	3.97	4.75	0.78	1.44	0.560	0.835	1.81917	-0.55694	452937
CLD_(%)	42.90	39.07	-3.84	25.35	0.361	0.775	35.39671	-99.00000	461606
CLD2_(%)	42.90	43.78	0.87	24.80	0.356	0.782	36.59769	-99.00000	461606
TMP-lyr1_(K)	288.08	287.84	-0.23	1.70	0.934	0.982	2.18773	0.00072	471754

<b>Wdir_stats</b>	<b>obsmean</b>	<b>modmean</b>	<b>bias</b>	<b>abserr</b>	<b>ubias</b>	<b>vbias</b>	<b>uerr</b>	<b>verr</b>	<b>newtot</b>	<b>dbias</b>
WDIR_(deg)	209.00	193.43	-15.57	21.59	-0.136	0.128	1.21178	1.32356	452937	1.209

<b>Pcp threshold (in)</b>	<b>ACC</b>	<b>BIAS</b>	<b>THREAT</b>	<b>ETS</b>	<b>FAR</b>	<b>HK</b>	<b>HSS</b>	<b>POD</b>	<b>HITS</b>	<b>ZEROES</b>	<b>MISSES</b>	<b>FALSES</b>
0.01	0.8076	1.0262	0.6342	0.4363	0.2338	0.6096	0.6075	0.7863	182679	259687	49644	55730
0.05	0.8354	1.1194	0.5856	0.4483	0.3007	0.6404	0.6190	0.7828	127452	330107	35373	54808
0.10	0.8506	1.1779	0.5467	0.4363	0.3464	0.6450	0.6075	0.7698	98728	367153	29523	52336
0.25	0.8798	1.2975	0.4620	0.3905	0.4404	0.6314	0.5617	0.7261	56542	425366	21331	44501
0.50	0.9218	1.4147	0.3914	0.3524	0.5198	0.6205	0.5211	0.6793	27536	477396	12999	29809
1.00	0.9662	1.3585	0.2433	0.2303	0.6603	0.4399	0.3744	0.4615	5950	523284	6942	11564

Table 5. April 2002 statistical table for the 12-km Full region is shown.



<b>Total_stats</b>	<b>obsmean</b>	<b>modmean</b>	<b>bias</b>	<b>abserr</b>	<b>r2</b>	<b>ia</b>	<b>rmse</b>	<b>nbias</b>	<b>jtot</b>
TMP-1.5m_(K)	290.70	290.81	0.11	1.55	0.927	0.978	2.00841	-0.00046	488277
QV_(g/kg)	9.39	9.09	-0.30	1.15	0.884	0.968	1.52606	0.03946	478958
RH_(%)	69.69	67.29	-2.40	10.96	0.595	0.872	14.67426	0.02610	478929
WSPD-regular_(m/s)	3.67	3.93	0.27	1.35	0.528	0.834	1.72826	-99.00000	463927
WSPD-nocalms_(m/s)	4.30	4.24	-0.06	1.21	0.486	0.830	1.59112	-0.08440	396047
WSPD-mincalm_(m/s)	3.78	3.93	0.15	1.24	0.537	0.846	1.60626	-0.33737	463927
SPD-lyr1_(m/s)	3.78	4.63	0.85	1.50	0.516	0.813	1.89495	-0.61710	463927
CLD_(%)	38.63	35.77	-2.87	25.27	0.320	0.756	35.53267	-99.00000	476003
CLD2_(%)	38.63	40.09	1.45	25.34	0.314	0.761	37.09673	-99.00000	476003
TMP-lyr1_(K)	290.70	290.72	0.01	1.73	0.908	0.972	2.25051	-0.00014	488277

<b>Wdir_stats</b>	<b>obsmean</b>	<b>modmean</b>	<b>bias</b>	<b>abserr</b>	<b>ubias</b>	<b>vbias</b>	<b>uerr</b>	<b>verr</b>	<b>newtot</b>	<b>dbias</b>
WDIR_(deg)	206.94	181.02	-25.92	24.11	-0.164	0.115	1.25923	1.40530	463927	1.080

<b>Pcp threshold (in)</b>	<b>ACC</b>	<b>BIAS</b>	<b>THREAT</b>	<b>ETS</b>	<b>FAR</b>	<b>HK</b>	<b>HSS</b>	<b>POD</b>	<b>HITS</b>	<b>ZEROES</b>	<b>MISSES</b>	<b>FALSES</b>
0.01	0.8340	0.9283	0.6749	0.4938	0.1630	0.6564	0.6612	0.7770	195088	276929	55993	37988
0.05	0.8521	1.0003	0.6389	0.5019	0.2204	0.6684	0.6684	0.7798	148148	334127	41832	41891
0.10	0.8583	1.0352	0.6011	0.4836	0.2619	0.6589	0.6519	0.7641	120906	364870	37328	42894
0.25	0.8762	1.1044	0.5184	0.4349	0.3495	0.6306	0.6062	0.7185	75403	420541	29549	40505
0.50	0.9033	1.2099	0.3998	0.3488	0.4783	0.5654	0.5172	0.6311	36459	474799	21308	33432
1.00	0.9563	1.3192	0.3034	0.2847	0.5908	0.5114	0.4432	0.5398	10760	530531	9172	15535

Table 6. May 2002 statistical table for the 12-km Full region is shown.

<b>Total_stats</b>	<b>obsmean</b>	<b>modmean</b>	<b>bias</b>	<b>abserr</b>	<b>r2</b>	<b>ia</b>	<b>rmse</b>	<b>nbias</b>	<b>jtot</b>
TMP-1.5m_(K)	296.64	296.72	0.08	1.44	0.881	0.964	1.86762	-0.00033	471541
QV_(g/kg)	13.30	13.15	-0.15	1.44	0.725	0.920	1.89633	0.00405	461949
RH_(%)	72.31	71.57	-0.75	9.56	0.591	0.876	12.56255	-0.00780	461910
WSPD-regular_(m/s)	2.92	3.29	0.38	1.32	0.436	0.786	1.67923	-99.00000	444811
WSPD-nocalms_(m/s)	3.66	3.59	-0.06	1.12	0.401	0.792	1.48413	-0.08254	354602
WSPD-mincalm_(m/s)	3.07	3.29	0.22	1.17	0.450	0.807	1.50996	-0.41357	444811
SPD-lyr1_(m/s)	3.07	3.91	0.84	1.42	0.430	0.769	1.79058	-0.72151	444811
CLD_(%)	30.69	34.39	3.70	26.76	0.204	0.682	35.47783	-99.00000	459618
CLD2_(%)	30.69	39.99	9.30	28.21	0.204	0.685	38.29418	-99.00000	459618
TMP-lyr1_(K)	296.64	296.69	0.05	1.70	0.842	0.947	2.17950	-0.00026	471541

<b>Wdir_stats</b>	<b>obsmean</b>	<b>modmean</b>	<b>bias</b>	<b>abserr</b>	<b>ubias</b>	<b>vbias</b>	<b>uerr</b>	<b>verr</b>	<b>newtot</b>	<b>dbias</b>
WDIR_(deg)	190.75	177.00	-13.74	29.29	-0.152	0.269	1.26252	1.38427	444811	1.992

<b>Pcp threshold (in)</b>	<b>ACC</b>	<b>BIAS</b>	<b>THREAT</b>	<b>ETS</b>	<b>FAR</b>	<b>HK</b>	<b>HSS</b>	<b>POD</b>	<b>HITS</b>	<b>ZEROES</b>	<b>MISSES</b>	<b>FALSES</b>
0.01	0.7755	0.9138	0.6134	0.3794	0.2038	0.5491	0.5501	0.7276	195087	229708	73022	49923
0.05	0.7767	1.0503	0.5372	0.3529	0.3178	0.5274	0.5217	0.7165	141983	283458	56166	66133
0.10	0.7788	1.1554	0.4730	0.3187	0.4009	0.5058	0.4833	0.6922	108783	317778	48376	72803
0.25	0.8040	1.4082	0.3460	0.2467	0.5604	0.4603	0.3958	0.6191	56808	383576	34951	72405
0.50	0.8608	1.7966	0.2320	0.1802	0.7069	0.4164	0.3053	0.5266	23033	448451	20707	55549
1.00	0.9414	2.5649	0.1274	0.1121	0.8429	0.3560	0.2016	0.4029	4687	510957	6946	25150

Table 7. June 2002 statistical table for the 12-km Full region is shown.

<b>Total_stats</b>	<b>obsmean</b>	<b>modmean</b>	<b>bias</b>	<b>abserr</b>	<b>r2</b>	<b>ia</b>	<b>rmse</b>	<b>nbias</b>	<b>jtot</b>
TMP-1.5m_(K)	298.81	298.76	-0.06	1.45	0.845	0.952	1.87971	0.00014	487170
QV_(g/kg)	15.27	15.10	-0.17	1.57	0.665	0.901	2.05339	0.00492	478167
RH_(%)	73.17	72.91	-0.26	9.27	0.582	0.872	12.17288	-0.01525	478139
WSPD-regular_(m/s)	2.54	2.93	0.38	1.28	0.376	0.753	1.62831	-99.00000	456961
WSPD-nocalms_(m/s)	3.35	3.23	-0.11	1.07	0.330	0.756	1.42205	-0.06657	347258
WSPD-mincalm_(m/s)	2.73	2.93	0.20	1.11	0.389	0.779	1.43773	-0.41674	456961
SPD-lyr1_(m/s)	2.73	3.50	0.77	1.35	0.369	0.742	1.69625	-0.73414	456961
CLD_(%)	26.37	31.74	5.37	27.26	0.134	0.625	35.75912	-99.00000	473107
CLD2_(%)	26.37	37.08	10.71	29.06	0.139	0.633	38.65865	-99.00000	473107
TMP-lyr1_(K)	298.81	298.75	-0.06	1.73	0.797	0.928	2.19164	0.00012	487170

<b>Wdir_stats</b>	<b>obsmean</b>	<b>modmean</b>	<b>bias</b>	<b>abserr</b>	<b>ubias</b>	<b>vbias</b>	<b>uerr</b>	<b>verr</b>	<b>newtot</b>	<b>dbias</b>
WDIR_(deg)	222.63	203.14	-19.49	31.93	0.000	0.358	1.21420	1.32984	456961	1.568

<b>Pcp threshold (in)</b>	<b>ACC</b>	<b>BIAS</b>	<b>THREAT</b>	<b>ETS</b>	<b>FAR</b>	<b>HK</b>	<b>HSS</b>	<b>POD</b>	<b>HITS</b>	<b>ZEROES</b>	<b>MISSES</b>	<b>FALSES</b>
0.01	0.7420	0.9319	0.6036	0.3189	0.2197	0.4865	0.4836	0.7272	222407	197539	83444	62608
0.05	0.7300	1.0806	0.5090	0.2857	0.3505	0.4505	0.4445	0.7018	158414	254768	67312	85504
0.10	0.7307	1.1879	0.4407	0.2562	0.4366	0.4285	0.4079	0.6692	120096	293476	59356	93070
0.25	0.7569	1.4958	0.3029	0.1874	0.6121	0.3764	0.3156	0.5802	59791	368606	43254	94347
0.50	0.8266	2.0711	0.1711	0.1154	0.7834	0.3080	0.2069	0.4487	20260	447587	24894	73257
1.00	0.9318	3.4324	0.0636	0.0500	0.9227	0.2088	0.0952	0.2652	2623	524776	7269	31330

Table 8. July 2002 statistical table for the 12-km Full region is shown.

<b>Total_stats</b>	<b>obsmean</b>	<b>modmean</b>	<b>bias</b>	<b>abserr</b>	<b>r2</b>	<b>ia</b>	<b>rmse</b>	<b>nbias</b>	<b>jtot</b>
TMP-1.5m_(K)	297.71	297.68	-0.04	1.41	0.866	0.960	1.85205	0.00008	490592
QV_(g/kg)	14.47	14.21	-0.26	1.49	0.693	0.909	1.97951	0.01051	481892
RH_(%)	74.14	73.09	-1.05	9.39	0.589	0.874	12.36538	-0.00380	481863
WSPD-regular_(m/s)	2.59	3.00	0.42	1.29	0.372	0.745	1.64195	-99.00000	462138
WSPD-nocalms_(m/s)	3.37	3.29	-0.08	1.06	0.333	0.757	1.41078	-0.08320	354549
WSPD-mincalm_(m/s)	2.77	3.00	0.24	1.12	0.386	0.773	1.44531	-0.45255	462138
SPD-lyr1_(m/s)	2.77	3.60	0.83	1.38	0.358	0.730	1.72670	-0.78282	462138
CLD_(%)	28.95	32.65	3.70	26.76	0.189	0.670	35.27541	-99.00000	476106
CLD2_(%)	28.95	37.91	8.96	28.12	0.191	0.676	37.87040	-99.00000	476106
TMP-lyr1_(K)	297.71	297.74	0.02	1.71	0.818	0.939	2.19548	-0.00016	490592

<b>Wdir_stats</b>	<b>obsmean</b>	<b>modmean</b>	<b>bias</b>	<b>abserr</b>	<b>ubias</b>	<b>vbias</b>	<b>uerr</b>	<b>verr</b>	<b>newtot</b>	<b>dbias</b>
WDIR_(deg)	110.50	135.85	25.35	30.52	-0.086	0.290	1.21190	1.32377	462138	1.738

<b>Pcp threshold (in)</b>	<b>ACC</b>	<b>BIAS</b>	<b>THREAT</b>	<b>ETS</b>	<b>FAR</b>	<b>HK</b>	<b>HSS</b>	<b>POD</b>	<b>HITS</b>	<b>ZEROES</b>	<b>MISSES</b>	<b>FALSES</b>
0.01	0.7482	0.8859	0.5595	0.3261	0.2363	0.4889	0.4918	0.6766	181007	242460	86534	55997
0.05	0.7523	1.0274	0.4737	0.2932	0.3657	0.4564	0.4534	0.6517	126184	299638	67440	72736
0.10	0.7593	1.1264	0.4096	0.2603	0.4514	0.4295	0.4131	0.6179	94535	335199	58464	77800
0.25	0.7952	1.3602	0.2926	0.1979	0.6072	0.3787	0.3304	0.5343	47945	402146	41791	74116
0.50	0.8644	1.6680	0.1977	0.1494	0.7360	0.3396	0.2599	0.4404	18911	470333	24034	52720
1.00	0.9473	1.9173	0.1125	0.0976	0.8461	0.2575	0.1778	0.2951	3786	532358	9043	20811

Table 9. August 2002 statistical table for the 12-km Full region is shown.

<b>Total_stats</b>	<b>obsmean</b>	<b>modmean</b>	<b>bias</b>	<b>abserr</b>	<b>r2</b>	<b>ia</b>	<b>rmse</b>	<b>nbias</b>	<b>jtot</b>
TMP-1.5m_(K)	295.09	294.96	-0.13	1.41	0.905	0.973	1.81645	0.00039	476372
QV_(g/kg)	12.69	12.23	-0.46	1.31	0.825	0.949	1.73622	0.02804	467739
RH_(%)	74.86	72.05	-2.81	10.02	0.584	0.870	13.40506	0.02058	467717
WSPD-regular_(m/s)	2.69	3.19	0.50	1.31	0.457	0.788	1.65562	-99.00000	451873
WSPD-nocalms_(m/s)	3.53	3.54	0.01	1.08	0.419	0.800	1.41941	-0.11001	344231
WSPD-mincalm_(m/s)	2.88	3.19	0.31	1.14	0.473	0.813	1.45720	-0.47861	451873
SPD-lyr1_(m/s)	2.88	3.82	0.95	1.44	0.438	0.764	1.80178	-0.82303	451873
CLD_(%)	32.74	32.19	-0.56	25.00	0.288	0.732	34.68699	-99.00000	460857
CLD2_(%)	32.74	37.16	4.41	25.29	0.291	0.743	36.41303	-99.00000	460857
TMP-lyr1_(K)	295.09	295.23	0.14	1.81	0.843	0.950	2.35419	-0.00055	476372

<b>Wdir_stats</b>	<b>obsmean</b>	<b>modmean</b>	<b>bias</b>	<b>abserr</b>	<b>ubias</b>	<b>vbias</b>	<b>uerr</b>	<b>verr</b>	<b>newtot</b>	<b>dbias</b>
WDIR_(deg)	86.12	108.62	22.50	27.24	-0.225	0.249	1.17785	1.30454	451873	2.484

<b>Pcp threshold (in)</b>	<b>ACC</b>	<b>BIAS</b>	<b>THREAT</b>	<b>ETS</b>	<b>FAR</b>	<b>HK</b>	<b>HSS</b>	<b>POD</b>	<b>HITS</b>	<b>ZEROES</b>	<b>MISSES</b>	<b>FALSES</b>
0.01	0.7973	0.8291	0.5570	0.3891	0.2108	0.5429	0.5602	0.6544	139609	297101	73743	37287
0.05	0.8216	0.9114	0.4963	0.3721	0.3044	0.5275	0.5423	0.6340	96280	353734	55592	42134
0.10	0.8382	0.9384	0.4571	0.3552	0.3521	0.5127	0.5242	0.6081	74599	384524	48085	40532
0.25	0.8687	0.9700	0.3816	0.3119	0.4390	0.4697	0.4755	0.5441	44365	431484	37167	34724
0.50	0.9062	1.0036	0.3123	0.2694	0.5250	0.4251	0.4244	0.4768	23315	473073	25587	25765
1.00	0.9524	0.9859	0.2434	0.2246	0.6056	0.3643	0.3668	0.3888	8397	513246	13201	12896

Table 10. September 2002 statistical table for the 12-km Full region is shown.

<b>Total_stats</b>	<b>obsmean</b>	<b>modmean</b>	<b>bias</b>	<b>abserr</b>	<b>r2</b>	<b>ia</b>	<b>rmse</b>	<b>nbias</b>	<b>jtot</b>
TMP-1.5m_(K)	287.55	287.06	-0.48	1.43	0.949	0.986	1.82413	0.00165	494315
QV_(g/kg)	9.05	8.61	-0.43	0.96	0.930	0.980	1.30642	0.05585	485751
RH_(%)	79.12	76.52	-2.60	10.56	0.488	0.827	14.51381	0.02483	485734
WSPD-regular_(m/s)	2.84	3.28	0.44	1.27	0.485	0.803	1.61567	-99.00000	473203
WSPD-nocalms_(m/s)	3.61	3.61	0.00	1.06	0.448	0.813	1.40056	-0.10252	372607
WSPD-mincalm_(m/s)	3.01	3.28	0.28	1.12	0.500	0.826	1.43520	-0.43255	473203
SPD-lyr1_(m/s)	3.01	3.89	0.88	1.38	0.475	0.785	1.73316	-0.74139	473203
CLD_(%)	53.80	49.66	-4.14	24.97	0.420	0.798	34.21059	-99.00000	477460
CLD2_(%)	53.80	56.68	2.88	22.91	0.420	0.810	35.15409	-99.00000	477460
TMP-lyr1_(K)	287.55	287.27	-0.28	1.60	0.932	0.982	2.05254	0.00092	494315

<b>Wdir_stats</b>	<b>obsmean</b>	<b>modmean</b>	<b>bias</b>	<b>abserr</b>	<b>ubias</b>	<b>vbias</b>	<b>uerr</b>	<b>verr</b>	<b>newtot</b>	<b>dbias</b>
WDIR_(deg)	16.35	26.54	10.19	24.40	-0.144	-0.030	1.12207	1.21988	473203	2.365

<b>Pcp threshold (in)</b>	<b>ACC</b>	<b>BIAS</b>	<b>THREAT</b>	<b>ETS</b>	<b>FAR</b>	<b>HK</b>	<b>HSS</b>	<b>POD</b>	<b>HITS</b>	<b>ZEROES</b>	<b>MISSES</b>	<b>FALSES</b>
0.01	0.8026	0.8851	0.6429	0.4317	0.1666	0.6007	0.6031	0.7377	201122	253161	71522	40193
0.05	0.8360	0.8813	0.5965	0.4563	0.2024	0.6090	0.6266	0.7029	137196	336001	57989	34812
0.10	0.8504	0.8643	0.5488	0.4375	0.2357	0.5831	0.6087	0.6606	102992	378320	52918	31768
0.25	0.8760	0.7899	0.4406	0.3690	0.3070	0.4948	0.5391	0.5474	55292	440507	45708	24491
0.50	0.9110	0.6908	0.3192	0.2796	0.4078	0.3771	0.4370	0.4091	23629	491971	34127	16271
1.00	0.9607	0.6572	0.1878	0.1743	0.6013	0.2479	0.2969	0.2621	5149	538586	14499	7764

Table 11. October 2002 statistical table for the 12-km Full region is shown.

<b>Total_stats</b>	<b>obsmean</b>	<b>modmean</b>	<b>bias</b>	<b>abserr</b>	<b>r2</b>	<b>ia</b>	<b>rmse</b>	<b>nbias</b>	<b>jtot</b>
TMP-1.5m_(K)	280.90	280.12	-0.79	1.72	0.922	0.977	2.21495	0.00277	479161
QV_(g/kg)	5.42	5.18	-0.23	0.66	0.926	0.979	0.90901	0.04068	471466
RH_(%)	74.26	73.05	-1.21	11.81	0.438	0.813	15.76113	0.00046	471439
WSPD-regular_(m/s)	3.40	3.82	0.42	1.34	0.542	0.830	1.71160	-99.00000	462666
WSPD-nocalms_(m/s)	4.12	4.16	0.04	1.15	0.502	0.835	1.51639	-0.12069	381354
WSPD-mincalm_(m/s)	3.53	3.82	0.29	1.21	0.553	0.846	1.55902	-0.42682	462666
SPD-lyr1_(m/s)	3.53	4.51	0.98	1.49	0.535	0.809	1.87939	-0.73215	462666
CLD_(%)	45.82	37.87	-7.95	24.67	0.424	0.795	35.43811	-99.00000	467013
CLD2_(%)	45.82	43.10	-2.73	22.91	0.428	0.813	35.53258	-99.00000	467013
TMP-lyr1_(K)	280.90	280.52	-0.38	1.85	0.898	0.972	2.38565	0.00131	479161

<b>Wdir_stats</b>	<b>obsmean</b>	<b>modmean</b>	<b>bias</b>	<b>abserr</b>	<b>ubias</b>	<b>vbias</b>	<b>uerr</b>	<b>verr</b>	<b>newtot</b>	<b>dbias</b>
WDIR_(deg)	277.08	277.80	0.72	20.66	0.027	-0.020	1.15565	1.25453	462666	2.515

<b>Pcp threshold (in)</b>	<b>ACC</b>	<b>BIAS</b>	<b>THREAT</b>	<b>ETS</b>	<b>FAR</b>	<b>HK</b>	<b>HSS</b>	<b>POD</b>	<b>HITS</b>	<b>ZEROES</b>	<b>MISSES</b>	<b>FALSES</b>
0.01	0.8769	0.9480	0.6846	0.5639	0.1649	0.7120	0.7212	0.7916	146380	333922	38526	28912
0.05	0.9096	0.9321	0.6686	0.5911	0.1694	0.7255	0.7430	0.7742	99891	398342	29134	20373
0.10	0.9208	0.9069	0.6362	0.5744	0.1824	0.7035	0.7296	0.7414	75817	428568	26440	16915
0.25	0.9445	0.8604	0.5935	0.5551	0.1947	0.6707	0.7139	0.6929	44395	472936	19675	10734
0.50	0.9571	0.7312	0.4682	0.4447	0.2450	0.5389	0.6156	0.5521	20675	503583	16774	6708
1.00	0.9779	0.5857	0.2346	0.2267	0.4856	0.2948	0.3696	0.3013	3704	531950	8590	3496

Table 12. November 2002 statistical table for the 12-km Full region is shown.

<b>Total_stats</b>	<b>obsmean</b>	<b>modmean</b>	<b>bias</b>	<b>abserr</b>	<b>r2</b>	<b>ia</b>	<b>rmse</b>	<b>nbias</b>	<b>jtot</b>
TMP-1.5m_(K)	276.76	275.70	-1.06	1.95	0.908	0.971	2.56867	0.00379	490016
QV_(g/kg)	4.13	4.12	-0.01	0.54	0.922	0.979	0.77691	-0.02104	480644
RH_(%)	73.55	76.81	3.26	11.85	0.457	0.817	15.42577	-0.07090	480593
WSPD-regular_(m/s)	3.68	3.96	0.28	1.37	0.523	0.824	1.75923	-99.00000	472282
WSPD-nocalms_(m/s)	4.33	4.27	-0.07	1.21	0.477	0.822	1.59735	-0.09683	400659
WSPD-mincalm_(m/s)	3.79	3.96	0.17	1.25	0.531	0.838	1.62973	-0.37147	472282
SPD-lyr1_(m/s)	3.79	4.68	0.88	1.49	0.517	0.809	1.89879	-0.66217	472282
CLD_(%)	47.06	37.81	-9.25	24.93	0.422	0.794	36.50302	-99.00000	475867
CLD2_(%)	47.06	42.34	-4.72	22.98	0.430	0.813	36.21823	-99.00000	475867
TMP-lyr1_(K)	276.76	276.21	-0.55	1.89	0.903	0.973	2.44788	0.00191	490016

<b>Wdir_stats</b>	<b>obsmean</b>	<b>modmean</b>	<b>bias</b>	<b>abserr</b>	<b>ubias</b>	<b>vbias</b>	<b>uerr</b>	<b>verr</b>	<b>newtot</b>	<b>dbias</b>
WDIR_(deg)	269.54	273.18	3.64	19.78	0.017	-0.062	1.22383	1.22865	472282	3.167

<b>Pcp threshold (in)</b>	<b>ACC</b>	<b>BIAS</b>	<b>THREAT</b>	<b>ETS</b>	<b>FAR</b>	<b>HK</b>	<b>HSS</b>	<b>POD</b>	<b>HITS</b>	<b>ZEROES</b>	<b>MISSES</b>	<b>FALSES</b>
0.01	0.8719	0.9854	0.6815	0.5550	0.1834	0.7113	0.7138	0.8047	155162	338324	37659	34853
0.05	0.9272	0.9768	0.7395	0.6697	0.1397	0.7959	0.8021	0.8404	117008	407773	22222	18995
0.10	0.9416	0.9751	0.7472	0.6931	0.1338	0.8111	0.8187	0.8447	97741	435189	17976	15092
0.25	0.9521	0.9389	0.7128	0.6728	0.1406	0.7841	0.8044	0.8069	67294	471593	16102	11009
0.50	0.9534	0.8980	0.5857	0.5543	0.2193	0.6806	0.7133	0.7010	37253	502394	15886	10465
1.00	0.9735	0.7084	0.4464	0.4326	0.2556	0.5196	0.6040	0.5273	12104	538885	10852	4157

Table 13. December 2002 statistical table for the 12-km Full region is shown.



### 36-km statistical tables

Tables 14-25 show the monthly summary statistical tables for the 36-km US region. The overall performance is generally similar to that seen for the 12-km Full statistics. The wintertime cold biases are not quite as strong, but they still exist. The wind direction errors are also slightly larger, presumably due to the inclusion of more difficult sites to model (e.g. western mountain sites). Wind speeds tend to be lower with respect to the observations (i.e. lower bias number) at 36-km than was the case at 12-km. This is due to the higher nudging strength applied at 36-km, which has the practical effect of reducing wind speeds while deflecting the model winds toward the observations. Finally, the cloud (CLD2) summer high bias is dampened considerably from what is observed at 12-km resolution.

Total_stats	obsmean	modmean	bias	abserr	r2	ia	rmse	nbias	jtot
TMP-1.5m_(K)	276.06	275.33	-0.73	2.09	0.907	0.974	2.79742	0.00261	946480
QV_(g/kg)	3.85	3.99	0.14	0.56	0.918	0.978	0.81239	-0.06870	935823
RH_(%)	70.82	74.27	3.44	12.03	0.518	0.843	15.80381	-0.08749	935716
WSPD-regular_(m/s)	3.54	3.50	-0.04	1.32	0.524	0.814	1.72335	-99.00000	918366
WSPD-nocalms_(m/s)	4.22	3.79	-0.43	1.20	0.478	0.802	1.60926	0.00338	770354
WSPD-mincalm_(m/s)	3.67	3.50	-0.17	1.21	0.530	0.826	1.60455	-0.24553	918366
SPD-lyr1_(m/s)	3.67	4.18	0.51	1.40	0.450	0.797	1.84380	-0.54357	918366
CLD_(%)	42.82	33.74	-9.07	26.44	0.377	0.760	36.90822	-99.00000	913447
CLD2_(%)	42.82	38.09	-4.73	24.98	0.377	0.782	36.84609	-99.00000	913447
TMP-lyr1_(K)	276.06	276.14	0.08	1.99	0.907	0.975	2.67626	-0.00037	946480

Wdir_stats	obsmean	modmean	bias	abserr	ubias	vbias	uerr	verr	newtot	dbias
WDIR_(deg)	264.82	259.87	-4.95	25.19	0.080	0.113	1.25187	1.29823	918366	2.476

Pcp threshold (in)	ACC	BIAS	THREAT	ETS	FAR	HK	HSS	POD	HITS	ZEROES	MISSES	FALSES
0.01	0.8249	1.0210	0.5781	0.4312	0.2748	0.6058	0.6025	0.7404	48455	118152	16993	18365
0.05	0.8921	1.1151	0.5631	0.4858	0.3167	0.6831	0.6539	0.7620	28092	152080	8774	13019
0.10	0.9219	1.1637	0.5486	0.4967	0.3413	0.7104	0.6638	0.7665	19163	167036	5837	9929
0.25	0.9615	1.1017	0.5535	0.5290	0.3203	0.7247	0.6920	0.7488	9642	184544	3235	4544
0.50	0.9798	1.0355	0.5207	0.5087	0.3270	0.6860	0.6744	0.6970	4432	193453	1927	2153
1.00	0.9922	0.8983	0.4498	0.4457	0.3443	0.5856	0.6166	0.5890	1291	199095	901	678

Table 14. January 2002 statistical table for the 36-km US region is shown.

<b>Total_stats</b>	<b>obsmean</b>	<b>modmean</b>	<b>bias</b>	<b>abserr</b>	<b>r2</b>	<b>ia</b>	<b>rmse</b>	<b>nbias</b>	<b>jtot</b>
TMP-1.5m_(K)	276.77	276.25	-0.52	1.96	0.907	0.975	2.65000	0.00183	865039
QV_(g/kg)	3.53	3.55	0.02	0.58	0.874	0.966	0.81379	-0.04582	854281
RH_(%)	64.85	66.53	1.68	12.78	0.547	0.858	16.69427	-0.06509	854194
WSPD-regular_(m/s)	4.01	3.89	-0.12	1.37	0.613	0.859	1.78559	-99.00000	837617
WSPD-nocalms_(m/s)	4.71	4.24	-0.47	1.27	0.578	0.850	1.70210	0.01323	713258
WSPD-mincalm_(m/s)	4.12	3.89	-0.23	1.26	0.620	0.867	1.68347	-0.20926	837617
SPD-lyr1_(m/s)	4.12	4.59	0.47	1.43	0.560	0.850	1.88236	-0.48598	837617
CLD_(%)	35.11	28.38	-6.73	24.41	0.363	0.755	35.27850	-99.00000	839881
CLD2_(%)	35.11	32.50	-2.62	23.39	0.369	0.779	35.42045	-99.00000	839881
TMP-lyr1_(K)	276.77	276.90	0.13	1.95	0.901	0.973	2.66067	-0.00055	865039

<b>Wdir_stats</b>	<b>obsmean</b>	<b>modmean</b>	<b>bias</b>	<b>abserr</b>	<b>ubias</b>	<b>vbias</b>	<b>uerr</b>	<b>verr</b>	<b>newtot</b>	<b>dbias</b>
WDIR_(deg)	283.05	279.59	-3.46	24.27	-0.017	0.077	1.28521	1.35146	837617	2.566

<b>Pcp threshold (in)</b>	<b>ACC</b>	<b>BIAS</b>	<b>THREAT</b>	<b>ETS</b>	<b>FAR</b>	<b>HK</b>	<b>HSS</b>	<b>POD</b>	<b>HITS</b>	<b>ZEROES</b>	<b>MISSES</b>	<b>FALSES</b>
0.01	0.8525	0.9578	0.5749	0.4584	0.2539	0.6205	0.6287	0.7146	36377	119141	14525	12377
0.05	0.9053	1.1405	0.5585	0.4927	0.3275	0.6979	0.6601	0.7671	21851	143294	6636	10639
0.10	0.9322	1.2237	0.5545	0.5099	0.3518	0.7420	0.6754	0.7932	15395	154657	4013	8355
0.25	0.9644	1.2517	0.5419	0.5200	0.3678	0.7655	0.6842	0.7914	7688	168233	2027	4472
0.50	0.9828	1.2082	0.4975	0.4878	0.3928	0.7224	0.6557	0.7336	3101	176187	1126	2006
1.00	0.9936	0.9948	0.3988	0.3956	0.4284	0.5655	0.5670	0.5687	770	180489	584	577

Table 15. February 2002 statistical table for the 36-km US region is shown.

<b>Total_stats</b>	<b>obsmean</b>	<b>modmean</b>	<b>bias</b>	<b>abserr</b>	<b>r2</b>	<b>ia</b>	<b>rmse</b>	<b>nbias</b>	<b>jtot</b>
TMP-1.5m_(K)	278.72	278.15	-0.57	1.90	0.936	0.983	2.60455	0.00200	954172
QV_(g/kg)	4.44	4.45	0.01	0.63	0.924	0.980	0.92272	-0.02995	941638
RH_(%)	65.84	68.32	2.48	11.58	0.638	0.890	15.35492	-0.06849	941570
WSPD-regular_(m/s)	4.22	3.99	-0.24	1.38	0.606	0.860	1.80846	-99.00000	921790
WSPD-nocalms_(m/s)	4.83	4.28	-0.55	1.30	0.579	0.851	1.74057	0.03515	806024
WSPD-mincalm_(m/s)	4.32	3.99	-0.33	1.29	0.614	0.866	1.72353	-0.15606	921790
SPD-lyr1_(m/s)	4.32	4.69	0.37	1.43	0.554	0.852	1.89848	-0.41354	921790
CLD_(%)	44.56	35.62	-8.94	25.31	0.412	0.783	35.65981	-99.00000	926303
CLD2_(%)	44.56	40.19	-4.38	23.81	0.410	0.801	35.71257	-99.00000	926303
TMP-lyr1_(K)	278.72	278.54	-0.18	1.80	0.942	0.985	2.42655	0.00057	954172

<b>Wdir_stats</b>	<b>obsmean</b>	<b>modmean</b>	<b>bias</b>	<b>abserr</b>	<b>ubias</b>	<b>vbias</b>	<b>uerr</b>	<b>verr</b>	<b>newtot</b>	<b>dbias</b>
WDIR_(deg)	273.61	270.52	-3.09	24.53	0.015	0.030	1.32654	1.39867	921790	2.697

<b>Pcp threshold (in)</b>	<b>ACC</b>	<b>BIAS</b>	<b>THREAT</b>	<b>ETS</b>	<b>FAR</b>	<b>HK</b>	<b>HSS</b>	<b>POD</b>	<b>HITS</b>	<b>ZEROES</b>	<b>MISSES</b>	<b>FALSES</b>
0.01	0.8267	1.0198	0.6305	0.4632	0.2341	0.6356	0.6332	0.7811	59710	107264	16738	18253
0.05	0.8720	1.1866	0.5879	0.4885	0.3178	0.6997	0.6563	0.8096	36878	139236	8675	17176
0.10	0.8979	1.3045	0.5590	0.4882	0.3666	0.7374	0.6561	0.8263	26139	155201	5496	15129
0.25	0.9403	1.3553	0.5393	0.5019	0.3912	0.7762	0.6684	0.8252	14102	175815	2988	9060
0.50	0.9652	1.2754	0.4742	0.4549	0.4261	0.7076	0.6253	0.7319	6346	188583	2324	4712
1.00	0.9869	1.0177	0.4083	0.4018	0.4251	0.5783	0.5733	0.5850	1820	197508	1291	1346

Table 16. March 2002 statistical table for the 36-km US region is shown.

<b>Total_stats</b>	<b>obsmean</b>	<b>modmean</b>	<b>bias</b>	<b>abserr</b>	<b>r2</b>	<b>ia</b>	<b>rmse</b>	<b>nbias</b>	<b>jtot</b>
TMP-1.5m_(K)	286.16	286.00	-0.16	1.66	0.936	0.983	2.24593	0.00050	929547
QV_(g/kg)	6.82	6.82	0.00	0.92	0.902	0.974	1.29698	-0.00510	919347
RH_(%)	65.36	66.02	0.67	10.76	0.667	0.902	14.31827	-0.03816	919278
WSPD-regular_(m/s)	4.15	3.93	-0.21	1.34	0.612	0.863	1.74615	-99.00000	892333
WSPD-nocalms_(m/s)	4.73	4.22	-0.51	1.26	0.584	0.854	1.68282	0.03235	782189
WSPD-mincalm_(m/s)	4.24	3.93	-0.31	1.25	0.621	0.870	1.66103	-0.15123	892333
SPD-lyr1_(m/s)	4.24	4.61	0.37	1.40	0.562	0.855	1.83303	-0.39942	892333
CLD_(%)	42.55	34.17	-8.39	25.90	0.361	0.762	36.09765	-99.00000	903391
CLD2_(%)	42.55	38.54	-4.01	24.98	0.355	0.777	36.57596	-99.00000	903391
TMP-lyr1_(K)	286.16	286.06	-0.10	1.73	0.934	0.982	2.28581	0.00028	929547

<b>Wdir_stats</b>	<b>obsmean</b>	<b>modmean</b>	<b>bias</b>	<b>abserr</b>	<b>ubias</b>	<b>vbias</b>	<b>uerr</b>	<b>verr</b>	<b>newtot</b>	<b>dbias</b>
WDIR_(deg)	218.87	219.95	1.08	25.42	0.030	0.015	1.32221	1.40175	892333	2.539

<b>Pcp threshold (in)</b>	<b>ACC</b>	<b>BIAS</b>	<b>THREAT</b>	<b>ETS</b>	<b>FAR</b>	<b>HK</b>	<b>HSS</b>	<b>POD</b>	<b>HITS</b>	<b>ZEROES</b>	<b>MISSES</b>	<b>FALSES</b>
0.01	0.8084	0.9982	0.5969	0.4217	0.2518	0.5930	0.5932	0.7469	55447	102558	18789	18656
0.05	0.8484	1.1845	0.5447	0.4328	0.3497	0.6427	0.6042	0.7703	35439	130384	10570	19057
0.10	0.8711	1.3047	0.4992	0.4163	0.4118	0.6594	0.5878	0.7674	25113	145145	7610	17582
0.25	0.9135	1.5165	0.4157	0.3710	0.5127	0.6683	0.5412	0.7389	12033	166504	4251	12662
0.50	0.9549	1.5555	0.3597	0.3392	0.5654	0.6417	0.5065	0.6760	4953	181679	2374	6444
1.00	0.9859	1.4007	0.2714	0.2658	0.6341	0.5033	0.4200	0.5125	1027	191666	977	1780

Table 17. April 2002 statistical table for the 36-km US region is shown.

<b>Total_stats</b>	<b>obsmean</b>	<b>modmean</b>	<b>bias</b>	<b>abserr</b>	<b>r2</b>	<b>ia</b>	<b>rmse</b>	<b>nbias</b>	<b>jtot</b>
TMP-1.5m_(K)	289.31	289.43	0.12	1.60	0.931	0.981	2.10449	-0.00050	958163
QV_(g/kg)	7.91	7.68	-0.23	1.07	0.890	0.970	1.44575	0.02491	947550
RH_(%)	64.05	62.34	-1.72	10.64	0.684	0.907	14.30719	0.00226	947477
WSPD-regular_(m/s)	4.03	3.93	-0.10	1.40	0.560	0.847	1.81702	-99.00000	911895
WSPD-nocalms_(m/s)	4.64	4.21	-0.43	1.30	0.530	0.838	1.73692	0.00811	791445
WSPD-mincalm_(m/s)	4.13	3.93	-0.21	1.30	0.569	0.855	1.72139	-0.20846	911895
SPD-lyr1_(m/s)	4.13	4.60	0.47	1.49	0.515	0.834	1.93289	-0.46539	911895
CLD_(%)	36.37	29.96	-6.40	24.97	0.319	0.744	35.40861	-99.00000	931303
CLD2_(%)	36.37	33.85	-2.51	24.78	0.311	0.755	36.39382	-99.00000	931303
TMP-lyr1_(K)	289.31	289.35	0.04	1.75	0.919	0.976	2.29601	-0.00024	958163

<b>Wdir_stats</b>	<b>obsmean</b>	<b>modmean</b>	<b>bias</b>	<b>abserr</b>	<b>ubias</b>	<b>vbias</b>	<b>uerr</b>	<b>verr</b>	<b>newtot</b>	<b>dbias</b>
WDIR_(deg)	217.14	217.14	0.00	28.17	0.020	0.026	1.40364	1.50237	911895	2.332

<b>Pcp threshold (in)</b>	<b>ACC</b>	<b>BIAS</b>	<b>THREAT</b>	<b>ETS</b>	<b>FAR</b>	<b>HK</b>	<b>HSS</b>	<b>POD</b>	<b>HITS</b>	<b>ZEROES</b>	<b>MISSES</b>	<b>FALSES</b>
0.01	0.8152	0.9412	0.5960	0.4301	0.2298	0.5945	0.6015	0.7249	55064	109575	20898	16428
0.05	0.8541	1.1208	0.5521	0.4433	0.3269	0.6397	0.6142	0.7544	36311	136195	11823	17636
0.10	0.8742	1.2297	0.5151	0.4314	0.3836	0.6572	0.6027	0.7581	26982	149584	8611	16788
0.25	0.9079	1.4068	0.4342	0.3841	0.4821	0.6558	0.5550	0.7286	14267	169104	5314	13280
0.50	0.9413	1.4939	0.3309	0.3050	0.5849	0.5772	0.4675	0.6201	5860	184258	3590	8257
1.00	0.9797	1.4468	0.2626	0.2547	0.6483	0.4954	0.4060	0.5089	1460	196405	1409	2691

Table 18. May 2002 statistical table for the 36-km US region is shown.

<b>Total_stats</b>	<b>obsmean</b>	<b>modmean</b>	<b>bias</b>	<b>abserr</b>	<b>r2</b>	<b>ia</b>	<b>rmse</b>	<b>nbias</b>	<b>jtot</b>
TMP-1.5m_(K)	295.48	295.48	0.00	1.57	0.905	0.972	2.07234	-0.00007	924881
QV_(g/kg)	11.37	11.22	-0.15	1.42	0.809	0.947	1.88997	-0.00201	913811
RH_(%)	65.90	65.46	-0.44	9.66	0.713	0.918	12.88463	-0.02752	913725
WSPD-regular_(m/s)	3.46	3.37	-0.09	1.38	0.485	0.808	1.79191	-99.00000	874547
WSPD-nocalms_(m/s)	4.16	3.65	-0.50	1.26	0.455	0.799	1.69961	0.03324	728033
WSPD-mincalm_(m/s)	3.59	3.37	-0.22	1.26	0.496	0.820	1.67297	-0.23146	874547
SPD-lyr1_(m/s)	3.59	3.99	0.40	1.42	0.442	0.801	1.85255	-0.50409	874547
CLD_(%)	28.63	26.95	-1.68	24.07	0.246	0.706	33.91846	-99.00000	898454
CLD2_(%)	28.63	30.99	2.37	24.85	0.237	0.713	35.81057	-99.00000	898454
TMP-lyr1_(K)	295.48	295.49	0.00	1.79	0.884	0.963	2.32985	-0.00012	924881

<b>Wdir_stats</b>	<b>obsmean</b>	<b>modmean</b>	<b>bias</b>	<b>abserr</b>	<b>ubias</b>	<b>vbias</b>	<b>uerr</b>	<b>verr</b>	<b>newtot</b>	<b>dbias</b>
WDIR_(deg)	193.94	192.30	-1.63	32.18	-0.007	0.067	1.39309	1.48954	874547	3.031

<b>Pcp threshold (in)</b>	<b>ACC</b>	<b>BIAS</b>	<b>THREAT</b>	<b>ETS</b>	<b>FAR</b>	<b>HK</b>	<b>HSS</b>	<b>POD</b>	<b>HITS</b>	<b>ZEROES</b>	<b>MISSES</b>	<b>FALSES</b>
0.01	0.7824	0.9828	0.5708	0.3755	0.2669	0.5444	0.5460	0.7205	56558	96360	21940	20592
0.05	0.8079	1.2337	0.4989	0.3634	0.3973	0.5737	0.5330	0.7435	37382	120528	12896	24644
0.10	0.8219	1.3960	0.4398	0.3329	0.4758	0.5750	0.4995	0.7319	27327	133312	10012	24799
0.25	0.8594	1.6809	0.3368	0.2724	0.5982	0.5567	0.4281	0.6755	13952	154027	6703	20768
0.50	0.9088	2.0457	0.2393	0.2071	0.7125	0.5134	0.3432	0.5882	5611	172005	3929	13905
1.00	0.9662	2.4301	0.1435	0.1343	0.8228	0.4039	0.2368	0.4305	1106	187744	1463	5137

Table 19. June 2002 statistical table for the 36-km US region is shown.

Total_stats	obsmean	modmean	bias	abserr	r2	ia	rmse	nbias	jtot
TMP-1.5m_(K)	297.91	297.76	-0.14	1.60	0.872	0.962	2.11752	0.00041	955148
QV_(g/kg)	13.39	13.24	-0.15	1.58	0.751	0.930	2.11797	-0.00406	944939
RH_(%)	67.31	67.50	0.19	9.64	0.682	0.907	12.80378	-0.03968	944878
WSPD-regular_(m/s)	3.04	2.95	-0.09	1.34	0.400	0.762	1.73542	-99.00000	899474
WSPD-nocalms_(m/s)	3.78	3.22	-0.56	1.21	0.356	0.746	1.64473	0.05924	723951
WSPD-mincalm_(m/s)	3.19	2.95	-0.24	1.20	0.410	0.777	1.60245	-0.22406	899474
SPD-lyr1_(m/s)	3.19	3.53	0.33	1.35	0.356	0.759	1.75191	-0.50492	899474
CLD_(%)	24.62	24.44	-0.18	24.38	0.156	0.640	34.00370	-99.00000	926991
CLD2_(%)	24.62	28.38	3.75	25.64	0.151	0.648	36.11977	-99.00000	926991
TMP-lyr1_(K)	297.91	297.81	-0.10	1.83	0.847	0.949	2.36812	0.00023	955148

Wdir_stats	obsmean	modmean	bias	abserr	ubias	vbias	uerr	verr	newtot	dbias
WDIR_(deg)	204.25	201.88	-2.37	34.47	0.030	0.142	1.34061	1.42832	899474	2.280

Pcp threshold (in)	ACC	BIAS	THREAT	ETS	FAR	HK	HSS	POD	HITS	ZEROES	MISSES	FALSES
0.01	0.7476	0.9451	0.5523	0.3223	0.2677	0.4851	0.4875	0.6921	62895	88091	27983	22996
0.05	0.7587	1.2031	0.4515	0.2879	0.4304	0.4739	0.4471	0.6853	40113	113117	18422	30313
0.10	0.7730	1.4150	0.3813	0.2548	0.5288	0.4679	0.4061	0.6667	28260	127859	14128	31718
0.25	0.8184	1.9454	0.2615	0.1904	0.6862	0.4534	0.3199	0.6105	12986	152299	8285	28395
0.50	0.8826	2.6541	0.1634	0.1306	0.8066	0.4131	0.2310	0.5132	4631	173621	4393	19320
1.00	0.9576	3.3732	0.0868	0.0779	0.8965	0.3139	0.1445	0.3492	814	192585	1517	7049

Table 20. July 2002 statistical table for the 36-km US region is shown.

Total_stats	obsmean	modmean	bias	abserr	r2	ia	rmse	nbias	jtot
TMP-1.5m_(K)	296.55	296.44	-0.11	1.58	0.888	0.967	2.09779	0.00032	960510
QV_(g/kg)	12.52	12.27	-0.24	1.48	0.790	0.941	1.97364	0.00548	950621
RH_(%)	67.96	67.18	-0.78	9.72	0.694	0.911	12.90850	-0.01967	950558
WSPD-regular_(m/s)	3.05	2.99	-0.06	1.35	0.425	0.771	1.74270	-99.00000	906887
WSPD-nocalms_(m/s)	3.81	3.26	-0.55	1.21	0.393	0.763	1.63919	0.05181	725907
WSPD-mincalm_(m/s)	3.20	2.99	-0.21	1.21	0.437	0.788	1.60231	-0.24946	906887
SPD-lyr1_(m/s)	3.20	3.57	0.37	1.36	0.379	0.768	1.76247	-0.54113	906887
CLD_(%)	26.25	24.33	-1.91	24.51	0.181	0.657	34.36785	-99.00000	931042
CLD2_(%)	26.25	28.01	1.76	25.46	0.173	0.666	36.13303	-99.00000	931042
TMP-lyr1_(K)	296.55	296.59	0.04	1.86	0.858	0.953	2.41966	-0.00022	960510

Wdir_stats	obsmean	modmean	bias	abserr	ubias	vbias	uerr	verr	newtot	dbias
WDIR_(deg)	167.86	171.10	3.24	33.78	0.009	0.102	1.32762	1.42218	906887	3.122

Pcp threshold (in)	ACC	BIAS	THREAT	ETS	FAR	HK	HSS	POD	HITS	ZEROES	MISSES	FALSES
0.01	0.7562	0.9062	0.5188	0.3209	0.2815	0.4785	0.4858	0.6512	53092	99635	28441	20797
0.05	0.7872	1.1566	0.4367	0.3012	0.4332	0.4871	0.4630	0.6556	33316	125680	17505	25464
0.10	0.8074	1.3391	0.3731	0.2696	0.5253	0.4808	0.4246	0.6356	23160	139898	13276	25631
0.25	0.8532	1.7417	0.2679	0.2088	0.6674	0.4606	0.3455	0.5793	10848	161475	7877	21765
0.50	0.9084	2.1723	0.1836	0.1549	0.7734	0.4187	0.2683	0.4921	4162	179299	4295	14209
1.00	0.9668	2.4277	0.1036	0.0951	0.8675	0.2963	0.1738	0.3217	774	194492	1632	5067

Table 21. August 2002 statistical table for the 36-km US region is shown.



Total_stats	obsmean	modmean	bias	abserr	r2	ia	rmse	nbias	jtot
TMP-1.5m_(K)	293.58	293.42	-0.16	1.58	0.912	0.975	2.06790	0.00048	929086
QV_(g/kg)	10.83	10.46	-0.37	1.29	0.846	0.956	1.71890	0.02128	919288
RH_(%)	69.16	66.62	-2.54	10.45	0.658	0.897	13.97618	0.00755	919236
WSPD-regular_(m/s)	3.02	3.10	0.08	1.34	0.458	0.792	1.71472	-99.00000	883516
WSPD-nocalms_(m/s)	3.82	3.41	-0.41	1.18	0.425	0.788	1.57921	0.01471	696986
WSPD-mincalm_(m/s)	3.18	3.10	-0.08	1.19	0.470	0.810	1.56122	-0.30124	883516
SPD-lyr1_(m/s)	3.18	3.71	0.53	1.39	0.408	0.780	1.79446	-0.61312	883516
CLD_(%)	29.50	25.83	-3.67	23.12	0.302	0.731	33.43845	-99.00000	899879
CLD2_(%)	29.50	29.86	0.36	23.20	0.301	0.747	34.53160	-99.00000	899879
TMP-lyr1_(K)	293.58	293.81	0.23	1.93	0.870	0.960	2.54493	-0.00089	929086

Wdir_stats	obsmean	modmean	bias	abserr	ubias	vbias	uerr	verr	newtot	dbias
WDIR_(deg)	163.97	165.42	1.45	32.11	-0.032	0.139	1.28408	1.40265	883516	3.668

Pcp threshold (in)	ACC	BIAS	THREAT	ETS	FAR	HK	HSS	POD	HITS	ZEROES	MISSES	FALSES
0.01	0.8003	0.8586	0.5336	0.3779	0.2468	0.5309	0.5485	0.6467	44672	111738	24405	14635
0.05	0.8407	1.0137	0.4776	0.3733	0.3579	0.5463	0.5436	0.6509	28470	135839	15270	15871
0.10	0.8623	1.0778	0.4339	0.3531	0.4167	0.5381	0.5219	0.6287	20626	147912	12180	14732
0.25	0.9000	1.1628	0.3456	0.2972	0.5223	0.4916	0.4582	0.5554	10320	165585	8260	11285
0.50	0.9389	1.1899	0.2671	0.2419	0.6120	0.4247	0.3896	0.4617	4356	179144	5079	6871
1.00	0.9770	1.0315	0.2235	0.2148	0.6403	0.3591	0.3536	0.3711	1294	189660	2193	2303

Table 22. September 2002 statistical table for the 36-km US region is shown.

<b>Total_stats</b>	<b>obsmean</b>	<b>modmean</b>	<b>bias</b>	<b>abserr</b>	<b>r2</b>	<b>ia</b>	<b>rmse</b>	<b>nbias</b>	<b>jtot</b>
TMP-1.5m_(K)	285.40	285.08	-0.32	1.55	0.943	0.985	2.03521	0.00108	964996
QV_(g/kg)	7.50	7.16	-0.33	0.87	0.928	0.980	1.20843	0.04233	955278
RH_(%)	74.45	71.76	-2.70	10.68	0.610	0.879	14.57492	0.02312	955236
WSPD-regular_(m/s)	3.03	3.12	0.09	1.30	0.473	0.802	1.67285	-99.00000	923832
WSPD-nocalms_(m/s)	3.80	3.43	-0.37	1.15	0.444	0.800	1.53473	0.00948	737154
WSPD-mincalm_(m/s)	3.19	3.12	-0.07	1.16	0.486	0.820	1.52445	-0.28620	923832
SPD-lyr1_(m/s)	3.19	3.70	0.51	1.34	0.430	0.791	1.73976	-0.57562	923832
CLD_(%)	50.27	40.31	-9.96	25.83	0.419	0.787	35.86313	-99.00000	931672
CLD2_(%)	50.27	46.22	-4.05	23.51	0.419	0.808	35.72335	-99.00000	931672
TMP-lyr1_(K)	285.40	285.47	0.08	1.72	0.925	0.980	2.30551	-0.00034	964996

<b>Wdir_stats</b>	<b>obsmean</b>	<b>modmean</b>	<b>bias</b>	<b>abserr</b>	<b>ubias</b>	<b>vbias</b>	<b>uerr</b>	<b>verr</b>	<b>newtot</b>	<b>dbias</b>
WDIR_(deg)	356.76	358.78	2.02	29.70	-0.017	-0.010	1.23321	1.29759	923832	3.563

<b>Pcp threshold (in)</b>	<b>ACC</b>	<b>BIAS</b>	<b>THREAT</b>	<b>ETS</b>	<b>FAR</b>	<b>HK</b>	<b>HSS</b>	<b>POD</b>	<b>HITS</b>	<b>ZEROES</b>	<b>MISSES</b>	<b>FALSES</b>
0.01	0.8122	0.8706	0.6085	0.4336	0.1872	0.5933	0.6049	0.7077	58955	105082	24354	13574
0.05	0.8581	0.9508	0.5610	0.4534	0.2626	0.6139	0.6239	0.7011	36627	136674	15618	13046
0.10	0.8849	0.9993	0.5264	0.4484	0.3100	0.6190	0.6191	0.6895	25835	152891	11633	11606
0.25	0.9210	0.9882	0.4400	0.3958	0.3853	0.5641	0.5671	0.6075	12534	173476	8099	7856
0.50	0.9514	0.8581	0.3354	0.3131	0.4561	0.4449	0.4769	0.4667	4958	187183	5666	4158
1.00	0.9803	0.6871	0.2018	0.1949	0.5877	0.2761	0.3262	0.2833	1004	196990	2540	1431

Table 23. October 2002 statistical table for the 36-km US region is shown.

<b>Total_stats</b>	<b>obsmean</b>	<b>modmean</b>	<b>bias</b>	<b>abserr</b>	<b>r2</b>	<b>ia</b>	<b>rmse</b>	<b>nbias</b>	<b>jtot</b>
TMP-1.5m_(K)	279.74	279.25	-0.49	1.79	0.915	0.977	2.37599	0.00170	934494
QV_(g/kg)	4.76	4.59	-0.17	0.67	0.893	0.971	0.94236	0.01688	924789
RH_(%)	70.91	69.36	-1.55	12.34	0.509	0.843	16.52333	-0.00149	924726
WSPD-regular_(m/s)	3.41	3.57	0.16	1.38	0.511	0.817	1.79044	-99.00000	902729
WSPD-nocalms_(m/s)	4.17	3.89	-0.28	1.22	0.481	0.817	1.63401	-0.03680	738455
WSPD-mincalm_(m/s)	3.55	3.57	0.01	1.25	0.521	0.831	1.64849	-0.34529	902729
SPD-lyr1_(m/s)	3.55	4.21	0.66	1.47	0.466	0.801	1.91359	-0.64066	902729
CLD_(%)	42.57	33.28	-9.29	25.15	0.409	0.778	35.89886	-99.00000	905626
CLD2_(%)	42.57	38.15	-4.42	23.44	0.414	0.801	35.60152	-99.00000	905626
TMP-lyr1_(K)	279.74	279.89	0.15	1.96	0.891	0.971	2.62297	-0.00060	934494

<b>Wdir_stats</b>	<b>obsmean</b>	<b>modmean</b>	<b>bias</b>	<b>abserr</b>	<b>ubias</b>	<b>vbias</b>	<b>uerr</b>	<b>verr</b>	<b>newtot</b>	<b>dbias</b>
WDIR_(deg)	283.05	278.32	-4.73	27.07	0.017	0.089	1.30490	1.34806	902729	2.845

<b>Pcp threshold (in)</b>	<b>ACC</b>	<b>BIAS</b>	<b>THREAT</b>	<b>ETS</b>	<b>FAR</b>	<b>HK</b>	<b>HSS</b>	<b>POD</b>	<b>HITS</b>	<b>ZEROES</b>	<b>MISSES</b>	<b>FALSES</b>
0.01	0.8568	0.9102	0.5941	0.4771	0.2179	0.6291	0.6460	0.7119	40966	126490	16580	11414
0.05	0.9081	0.9997	0.5827	0.5159	0.2636	0.6806	0.6807	0.7362	25072	152420	8984	8974
0.10	0.9318	1.0067	0.5733	0.5265	0.2736	0.6918	0.6898	0.7312	17896	164233	6579	6742
0.25	0.9598	0.9568	0.5415	0.5163	0.2816	0.6674	0.6810	0.6874	9290	178294	4225	3641
0.50	0.9753	0.8611	0.4589	0.4455	0.3202	0.5752	0.6164	0.5854	4093	186530	2899	1928
1.00	0.9888	0.6679	0.2512	0.2470	0.4986	0.3311	0.3961	0.3348	736	192520	1462	732

Table 24. November 2002 statistical table for the 36-km US region is shown.

<b>Total_stats</b>	<b>obsmean</b>	<b>modmean</b>	<b>bias</b>	<b>abserr</b>	<b>r2</b>	<b>ia</b>	<b>rmse</b>	<b>nbias</b>	<b>jtot</b>
TMP-1.5m_(K)	275.83	275.14	-0.69	1.93	0.905	0.973	2.59378	0.00247	958013
QV_(g/kg)	3.88	3.91	0.03	0.55	0.901	0.974	0.77852	-0.04232	947441
RH_(%)	73.34	75.58	2.24	11.92	0.460	0.821	15.53317	-0.05973	947352
WSPD-regular_(m/s)	3.58	3.68	0.09	1.41	0.511	0.818	1.82360	-99.00000	926398
WSPD-nocalms_(m/s)	4.31	4.00	-0.31	1.26	0.475	0.813	1.68927	-0.03069	770288
WSPD-mincalm_(m/s)	3.71	3.68	-0.04	1.28	0.519	0.831	1.69570	-0.31577	926398
SPD-lyr1_(m/s)	3.71	4.34	0.63	1.50	0.458	0.800	1.96714	-0.60378	926398
CLD_(%)	45.18	34.24	-10.94	25.85	0.412	0.777	36.91812	-99.00000	927290
CLD2_(%)	45.18	39.01	-6.17	23.73	0.422	0.803	36.17173	-99.00000	927290
TMP-lyr1_(K)	275.83	275.89	0.06	1.91	0.898	0.973	2.55529	-0.00029	958013

<b>Wdir_stats</b>	<b>obsmean</b>	<b>modmean</b>	<b>bias</b>	<b>abserr</b>	<b>ubias</b>	<b>vbias</b>	<b>uerr</b>	<b>verr</b>	<b>newtot</b>	<b>dbias</b>
WDIR_(deg)	263.56	257.97	-5.58	26.09	0.101	0.108	1.34565	1.34846	926398	3.811

<b>Pcp threshold (in)</b>	<b>ACC</b>	<b>BIAS</b>	<b>THREAT</b>	<b>ETS</b>	<b>FAR</b>	<b>HK</b>	<b>HSS</b>	<b>POD</b>	<b>HITS</b>	<b>ZEROES</b>	<b>MISSES</b>	<b>FALSES</b>
0.01	0.8502	0.8932	0.6244	0.4908	0.1853	0.6416	0.6585	0.7277	50306	121397	18823	11439
0.05	0.9058	0.9930	0.6346	0.5586	0.2207	0.7150	0.7168	0.7738	33048	149892	9663	9362
0.10	0.9282	1.0277	0.6335	0.5785	0.2348	0.7412	0.7329	0.7864	25052	162420	6805	7688
0.25	0.9558	1.0133	0.6225	0.5910	0.2377	0.7473	0.7429	0.7724	14717	178322	4336	4590
0.50	0.9716	0.9856	0.5760	0.5576	0.2637	0.7111	0.7160	0.7257	7800	188424	2948	2793
1.00	0.9859	0.8220	0.4762	0.4685	0.2850	0.5825	0.6380	0.5878	2592	196522	1818	1033

Table 25. December 2002 statistical table for the 36-km US region is shown.

## **Statistical discussion**

### ***Temperature***

Now that we have a general overview of model performance, let's turn our attention to how specific statistical quantities vary throughout the year. To do this we will focus on the VISTAS region, cleanly comparing results at the 36-km and 12-km resolutions. Figure 18 shows how monthly temperature biases vary throughout 2002. Note that biases are generally small, never exceeding  $\pm 0.8^\circ\text{C}$ . Nonetheless the model shows a clear predilection towards being too cold in the winter months, and the problem is exacerbated at 12-km. Presumably the increased temperature nudging strength aloft ( $2.5 \text{ E-}4/\text{s}$  vs.  $1.0 \text{ E-}4/\text{s}$ ) enables the coarser grid to be slightly less biased. Model biases for the May-August period are practically 0.0 at both resolutions. The seasonal aggregation of temperature biases quantifies the same result in a bar chart (figure 19).

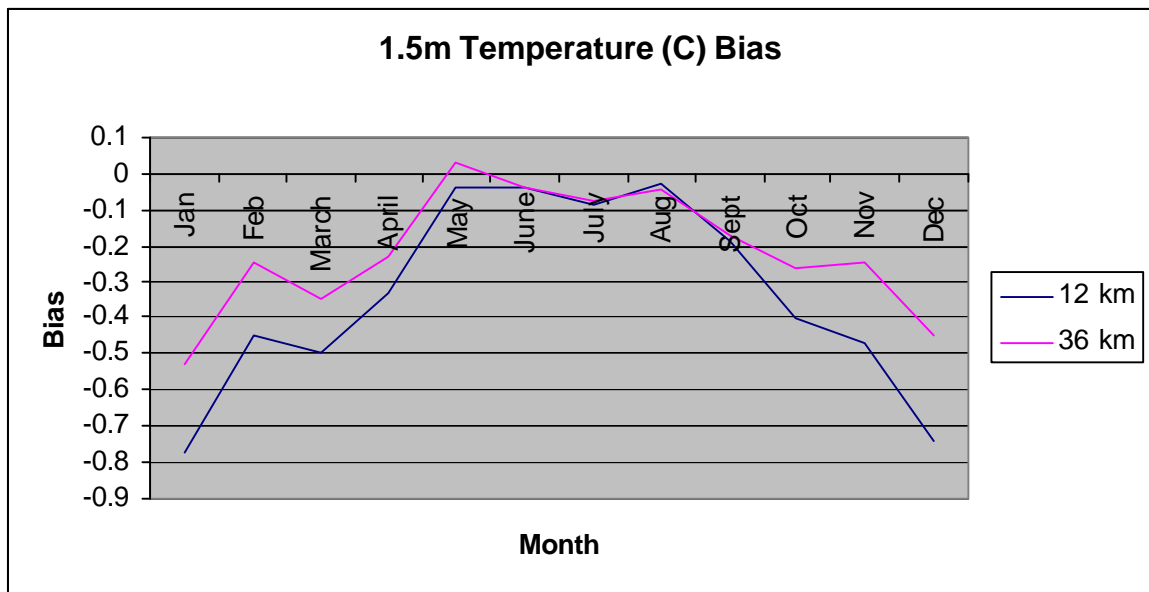


Figure 18. VISTAS region monthly temperature biases are plotted for both 12-km and 36-km resolutions.

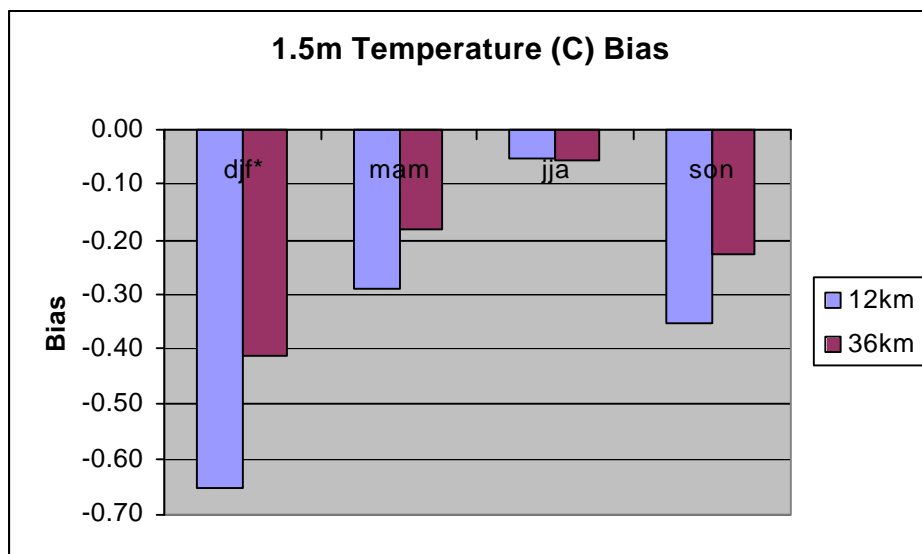


Figure 19. Seasonally aggregated VISTAS region temperature biases are shown for both the 36-km and 12-km grids.  
 \* All months are in 2002, so the winter (djf) bar graph represents a discontinuous time period.

To examine the temperature biases in greater detail, consider the day (12Z-23Z) and night (00Z-11Z) bias traces for the 12-km grid in figure 20. Clearly model performance for the daytime period is the primary reason for the wintertime cold bias. The daytime cold bias is persistent from month to month, but in the summer the model is only relatively weakly biased. The nighttime trace reveals that over the entire year the model is unbiased, being slightly low biased in the winter and slightly warm biased in the summer. There could be at least four physical mechanisms that could lead to a daytime cold bias: 1) Too cold soil initial conditions, 2) Too moist soil initial conditions, 3) Too many daytime clouds, and 4) Poor treatment of snow related processes. Once we examine the full suite of summary statistical products we will have a better idea of what is really going on. In the grand scheme of things the model temperature performance appears to be line with what we expect given the state of the art in MM5 applications. Figure 21 indicates similar temperature biases for the VISTAS region at 36-km resolution, though the magnitude of the wintertime biases are damped.

Figure 22 displays the January 2002 aggregate temperature biases for each station within the 12-km domain. Most of the sites in the VISTAS states display the cold bias, but the biases are definitely larger for sites in the northern VISTAS states, especially so for sites in western NC and VA. Given the significant snowfall that fell in this area early in the month, it seems likely that less than optimum treatment of snow/snow melt might contribute to the cold biases.

To complete our statistical analyses of temperature, we have included a series of “Bakergrams” in figures 23-26 for the 12-km VISTAS region. These images place daily statistics into a tile plot in a calendar-like layout. In this way we can effectively summarize performance for the entire year in one plot. Figure 23 shows the temperature bias Bakergram. Note how small the biases are in the summer, while the wintertime cold biases are easily seen. The temperature errors (figure 24) and RMSE (figure 26) are also greatest in the winter. Figure 25 indicates that the model skill in predicting temperature is fairly high every day of the year.



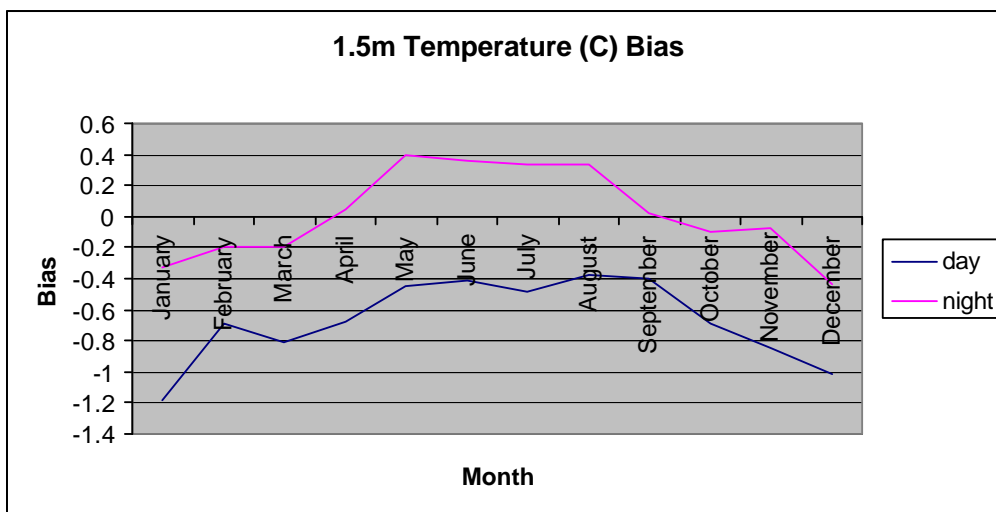


Figure 20. Monthly temperature biases for the 12-km VISTAS region are plotted. The “day” period is defined to be 12Z-23Z, while “night” is defined to be 00Z-11Z.

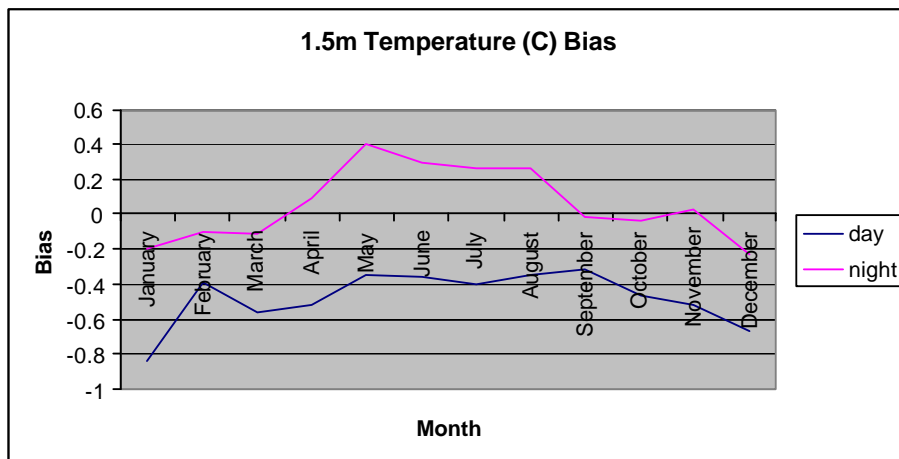


Figure 21. Monthly temperature biases for the 36-km VISTAS region are plotted. The “day” period is defined to be 12Z-23Z, while “night” is defined to be 00Z-11Z.

## Temperature Bias (Composite)

(jan02, Full: 12km, v02\_aaa, 1.5m)

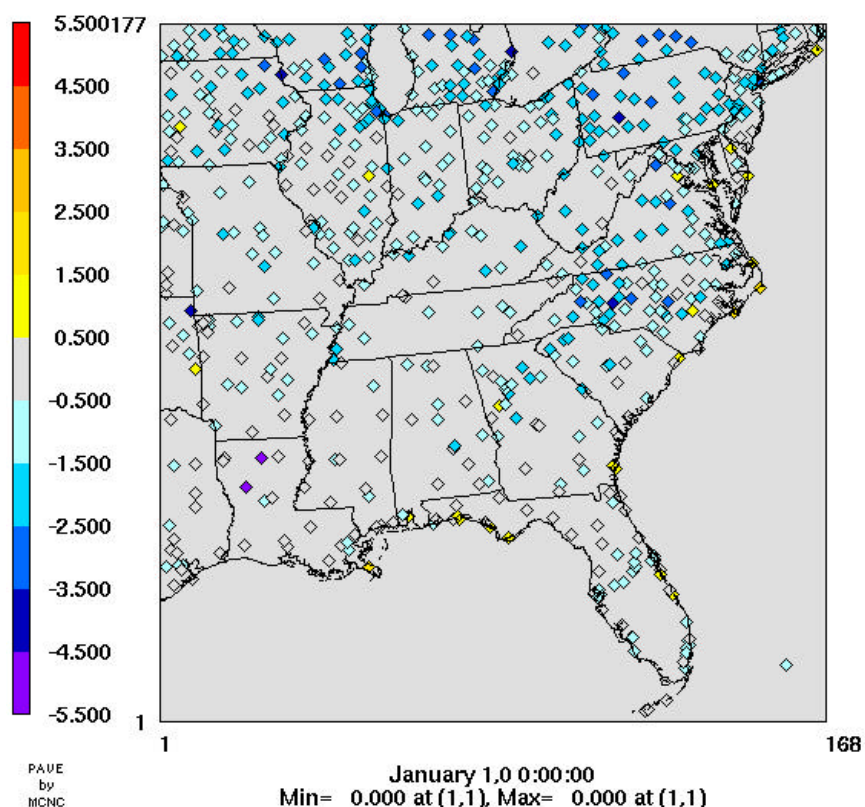


Figure 22. Site-specific temperature biases (K) for January 2002 are displayed for each site in the 12-km grid. Note that the PAVE date label (January 1, 0) is nonsensical and should be ignored since it is only a placeholder.

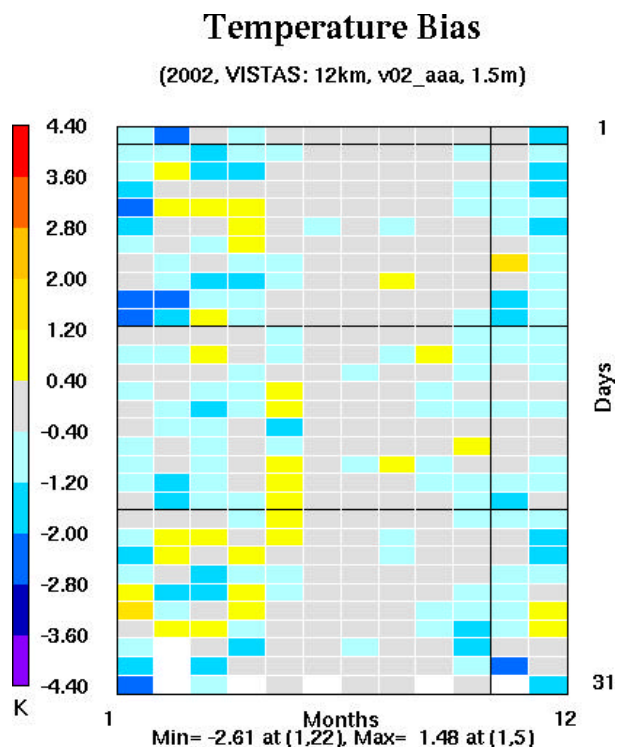


Figure 23. The 2002 12-km VISTAS “Bakergram” for temperature biases are plotted. The data are shown in a calendar-like layout so that the upper left cell represents the bias on the first day of January.

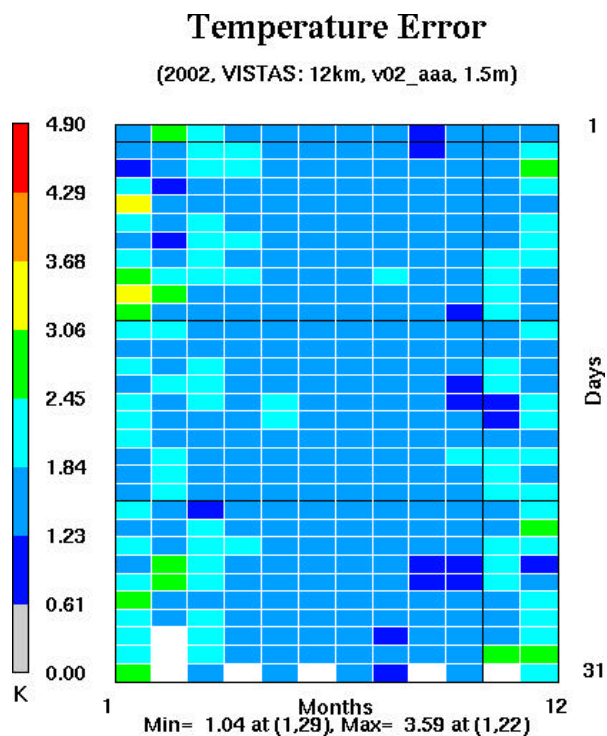


Figure 24. The 2002 12-km VISTAS “Bakergram” for temperature errors are plotted. The data are shown in a calendar-like layout so that the upper left cell represents the bias on the first day of January.

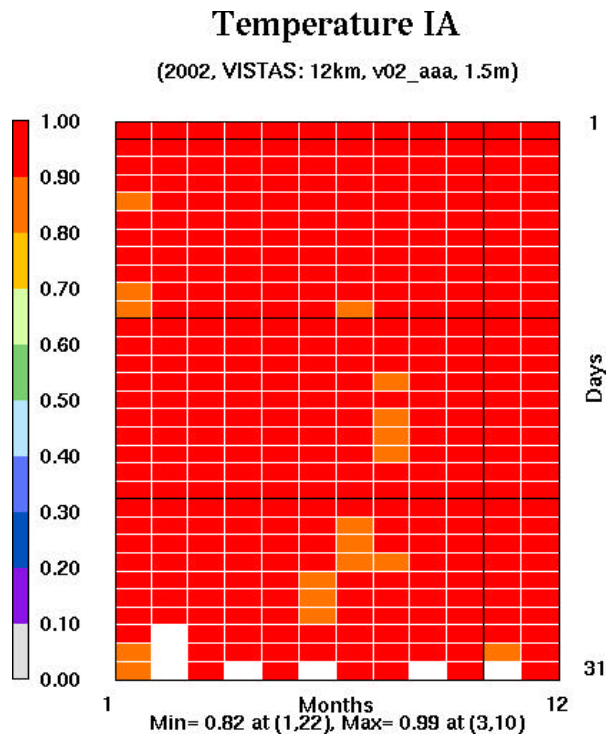


Figure 25. The 2002 12-km VISTAS “Bakergram” for temperature index of agreement is plotted. The data are shown in a calendar-like layout so that the upper left cell represents the bias on the first day of January.

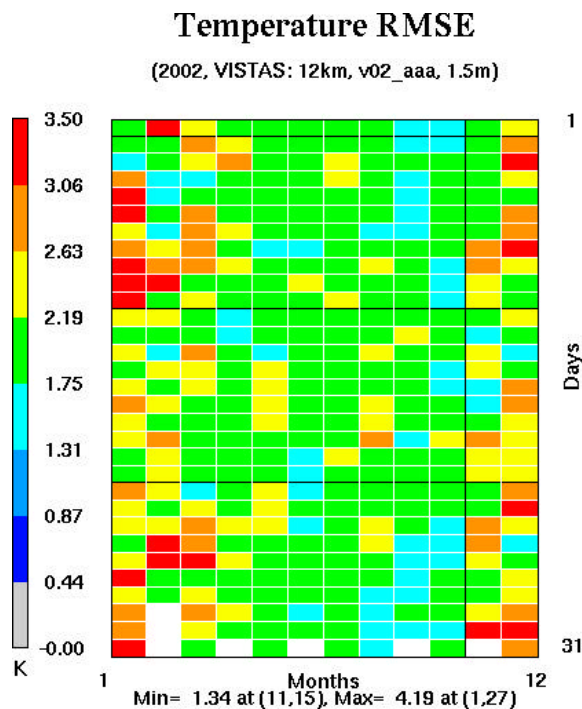


Figure 26. The 2002 12-km VISTAS “Bakergram” for temperature root mean square error is plotted. The data are shown in a calendar-like layout so that the upper left cell represents the bias on the first day of January.

## Mixing Ratio

Figure 27 shows the mixing ratio bias trace over for 2002 for both model resolutions for the VISTAS region. The model exhibits a slight positive bias in January, especially at 36-km resolution. Considering that the average observed mixing ratio in January is on the order of 4 g/kg, this bias is more significant than an equivalent bias in July, when average observed mixing ratios are on the order of 15 g/kg. Might this positive moisture bias be the root cause of the temperature cold bias? Probably not, since the cold bias was larger in the 12-km grid, not the 36-km grid where the moisture bias is more significant.

Another striking observation about the mixing ratio bias traces is the low biases noted in the fall months, shown well in figure 28. These values easily fall within the benchmark expectation of  $\pm 1.0$  g/kg, but it is curious that the model shows that signature. Figures 29-30 show that the model is systemically dry-biased during the afternoon for non-winter months. Usually one associates such a feature with too much mixing (or too efficient mixing) in the model, thus bringing dry air from aloft to the surface. For most of the year the model is slightly moist biased at night, but in the fall the night shows a slight dry bias. The combination leads to the overall dry bias noted for that season. Figure 31 displays the site-specific moisture biases for September over the 12-km grid. Virginia and western North Carolina show the largest dry bias, while many areas (eastern NC, northern FL, MI) show a moist bias. Such spatial discrepancies in model performance over small areas suggest that either the model is failing to capture smaller-scale variations properly, or that the model is introducing smaller-scale variations where none exist. One of the striking differences between eastern North Carolina (moist bias) and western North Carolina (dry bias) is the soil types prevalent in those areas. Perhaps there are issues with the soil moisture/temperature initializations that lead to the performance differences over small areas? Figure 32 shows the September “Bakergram” for moisture bias over the 12-km VISTAS region. These plots display hourly biases in a tile plot format, with the day of the month increasing from left to right, and the UTC hour of the day increasing from top to bottom. Recall that the model is run in 5-day segments such that every fifth day at 13Z results from a new segment are introduced. The first new segment in September starts on the 3<sup>rd</sup>. Moisture biases tend to significantly worsen at the beginning of a segment than they are at the end of a segment, indicating that there does indeed seem to be soil initialization issues that are affecting the model.

The annual Bakergrams for mixing ratio (figures 33-36) clearly indicate the autumn dry bias. Because mixing ratio nonlinearly increases with temperature, larger errors are found in the summer. The index of agreement (IA) metric (figure 35) can be a little misleading at times in that it determines the skill in replicating the observational variations. So in the heat of summer there is relatively little difference in mixing ratio across the VISTAS region, meaning that IA could become low even when the model error is small. Therefore the most disconcerting mixing ratio statistic is the fall dry bias, even though the errors are lower in the fall than in the summer, and the IA is higher in the fall than in the summer.

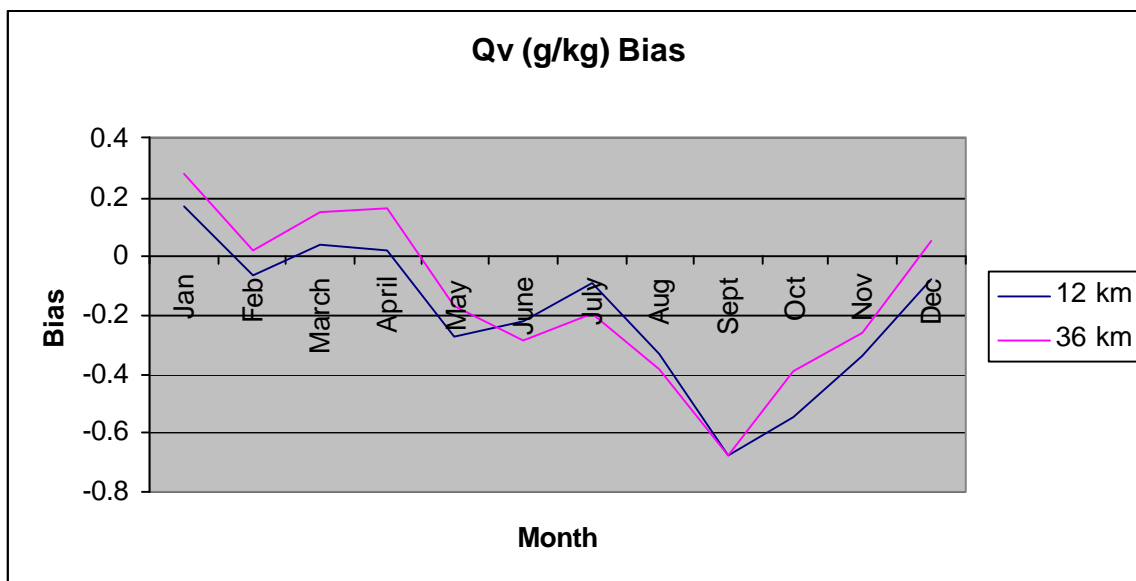


Figure 27. VISTAS region monthly mixing ratio biases are plotted for both 12-km and 36-km resolutions.

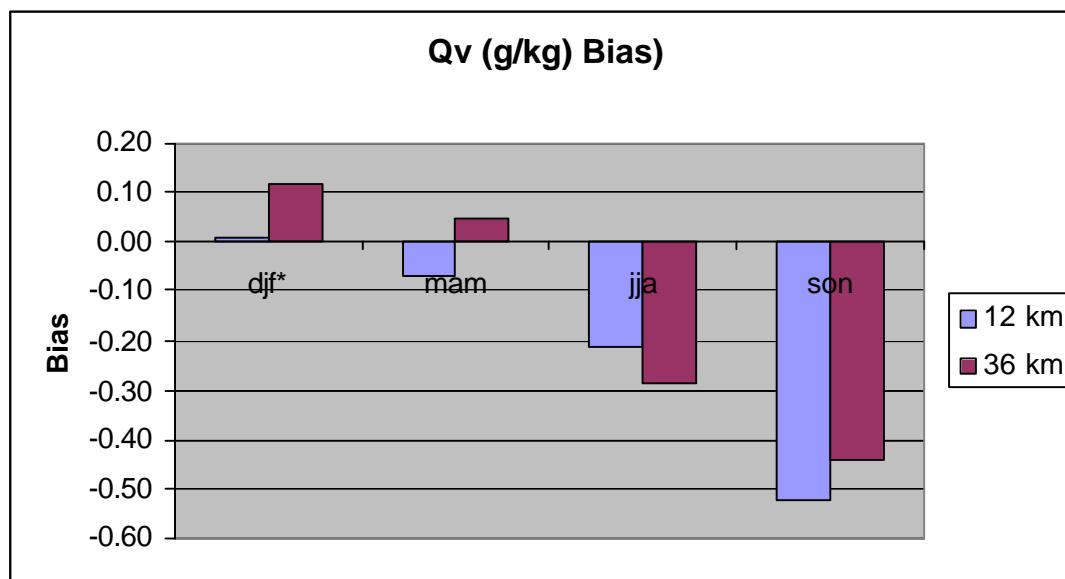


Figure 28. Seasonally aggregated VISTAS region mixing ratio biases are shown for both the 36-km and 12-km grids.

\* All months are in 2002, so the winter (djf) bar graph represents a discontinuous time period.

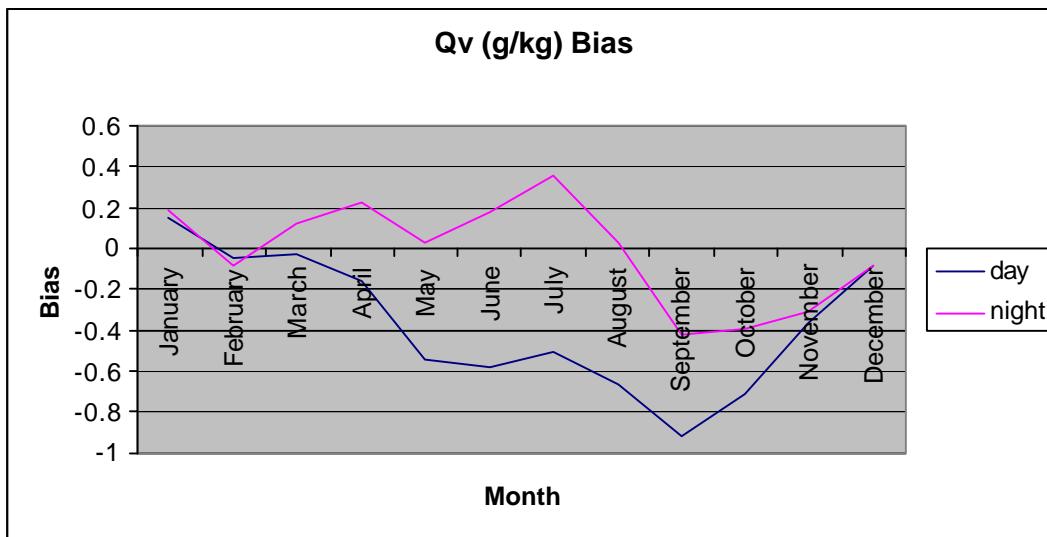


Figure 29. Monthly mixing ratio biases for the 12-km VISTAS region are plotted. The “day” period is defined to be 12Z-23Z, while “night” is defined to be 00Z-11Z.

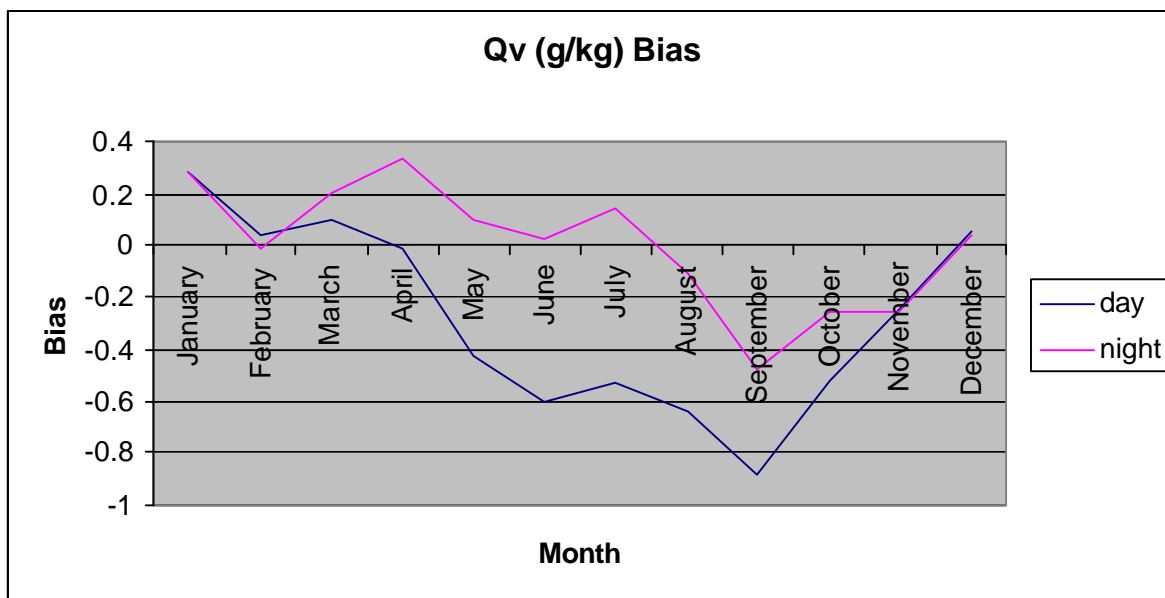


Figure 30. Monthly mixing ratio biases for the 36-km VISTAS region are plotted. The “day” period is defined to be 12Z-23Z, while “night” is defined to be 00Z-11Z.



## Mixing Ratio Bias (Composite)

(sep02, Full: 12km, v02\_aaa, Layer 1)

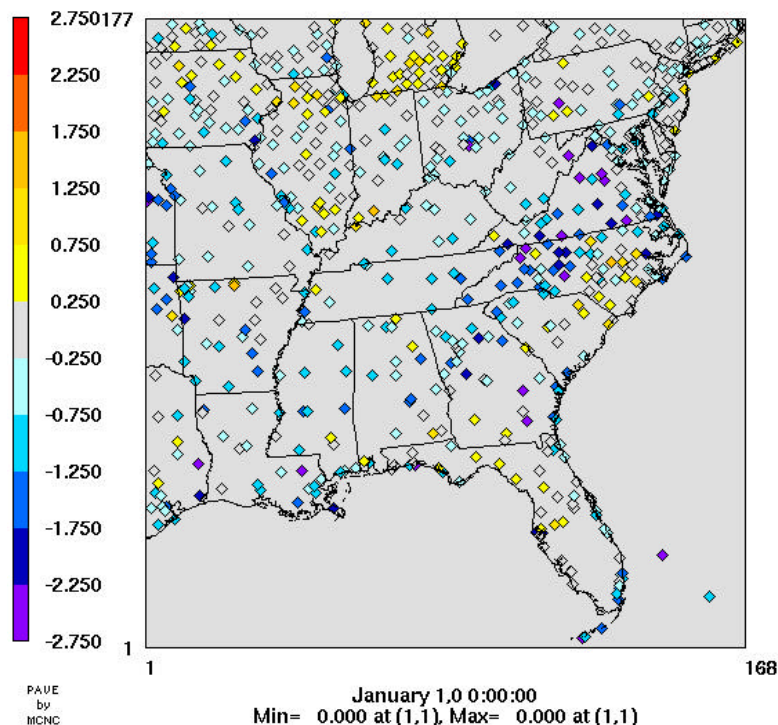


Figure 31. Site-specific mixing ratio biases (g/kg) for September 2002 are displayed for each site in the 12-km grid. Note that the PAVE date label (January 1, 0) is nonsensical and should be ignored since it is only a placeholder.

## Mixing Ratio Bias

(sep02, VISTAS: 12km, v02\_aaa, Layer 1)

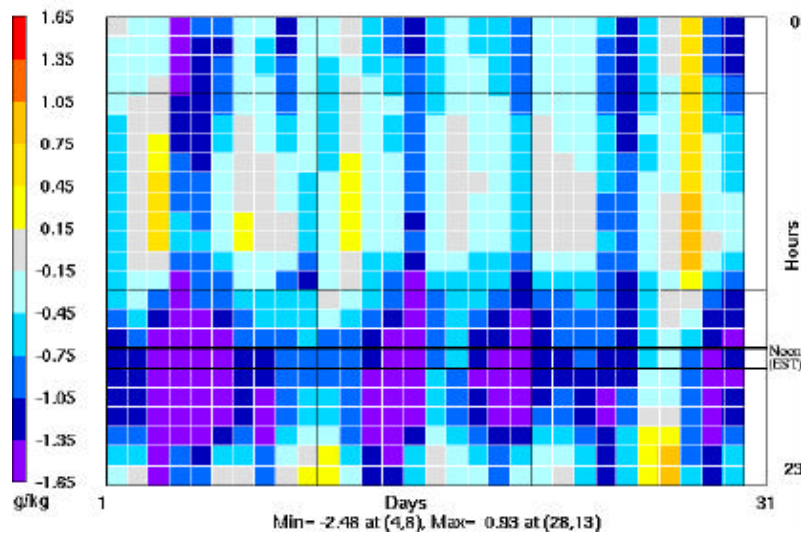


Figure 32. The September 2002 12-km VISTAS “Bakergram” for mixing ratio biases (g/kg) is plotted. The hourly biases are shown in a calendar-like layout so that the upper left cell represents the 00Z bias on the first day of the month.

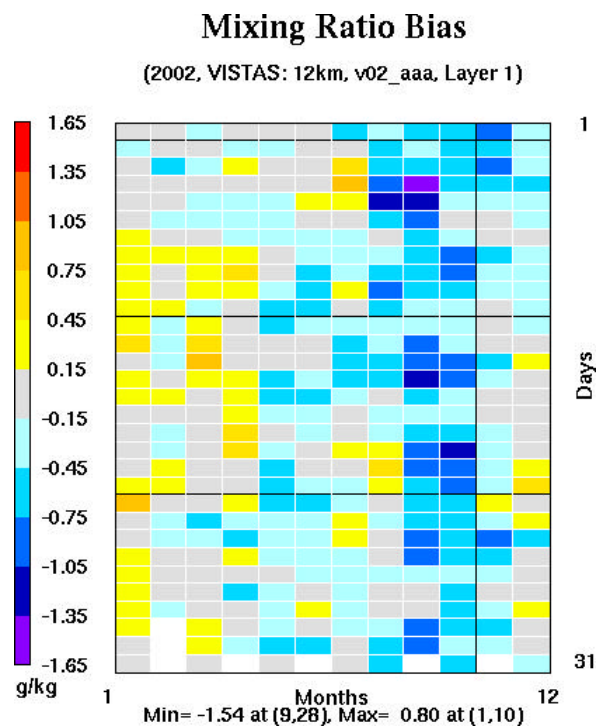


Figure 33. The 2002 12-km VISTAS “Bakergram” for mixing ratio bias is plotted. The data are shown in a calendar-like layout so that the upper left cell represents the bias on the first day of January.

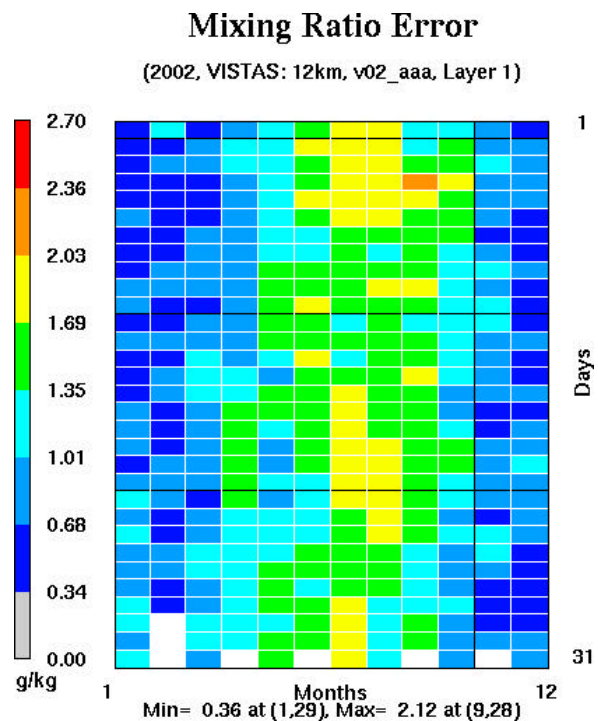


Figure 34. The 2002 12-km VISTAS “Bakergram” for mixing ratio error is plotted. The data are shown in a calendar-like layout so that the upper left cell represents the bias on the first day of January.

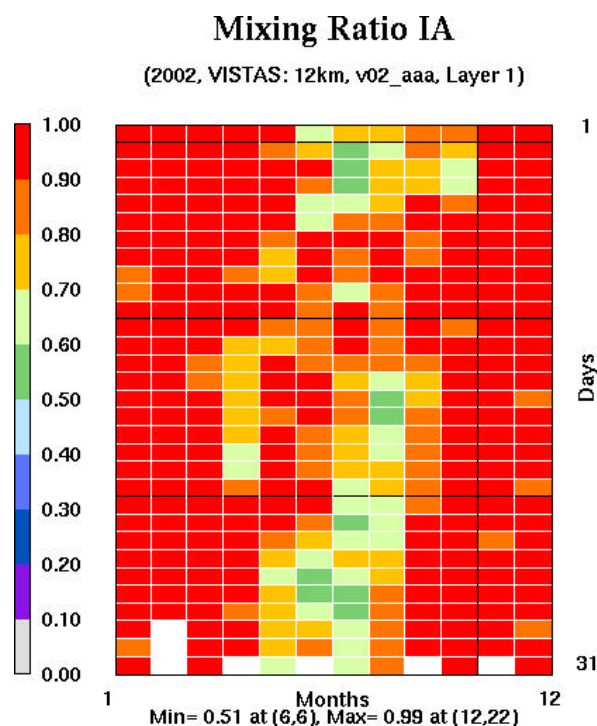


Figure 35. The 2002 12-km VISTAS “Bakergram” for mixing ratio index of agreement is plotted. The data are shown in a calendar-like layout so that the upper left cell represents the bias on the first day of January.

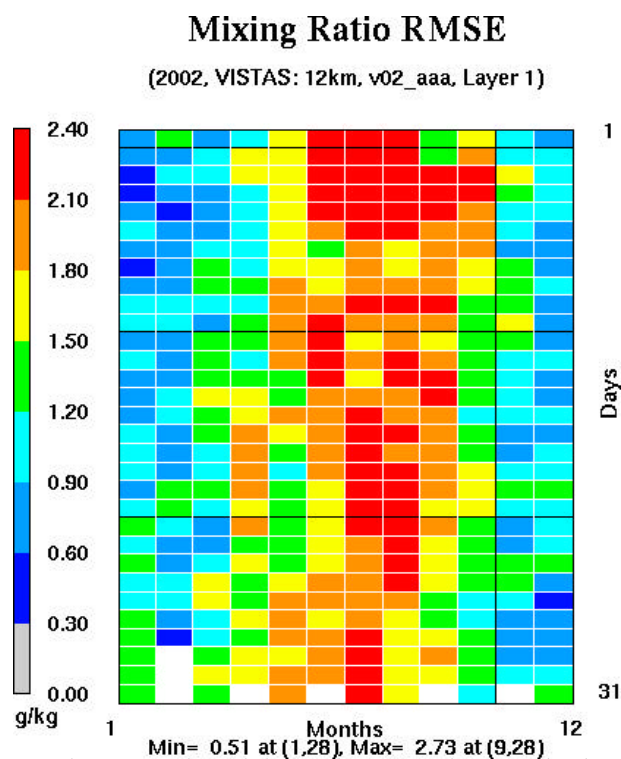


Figure 36. The 2002 12-km VISTAS “Bakergram” for mixing ratio RMSE is plotted. The data are shown in a calendar-like layout so that the upper left cell represents the bias on the first day of January.

## Relative Humidity

With the January cold/dry bias, we would expect that relative humidity would be high biased. Figure 37 indicates that is indeed the case. Generally, however, relative humidity is unbiased. The fall dry bias noted above does result in a low RH bias (figure 38) that is especially noticeable in November. The model tends to be positively biased during the daytime and negatively biased at night (figure 39). Spatially (figure 40) the model is actually slightly high biased just north of the VISTAS states, but the heart of the region from Virginia to Mississippi is biased low. The November relative humidity bias Bakergram (figure 41) shows some segment initialization signatures, but not as decisively as was seen in the mixing ratio September Bakergram (figure 32). Completing our suite of relative humidity plots are the annual Bakergrams (figures 42-45).

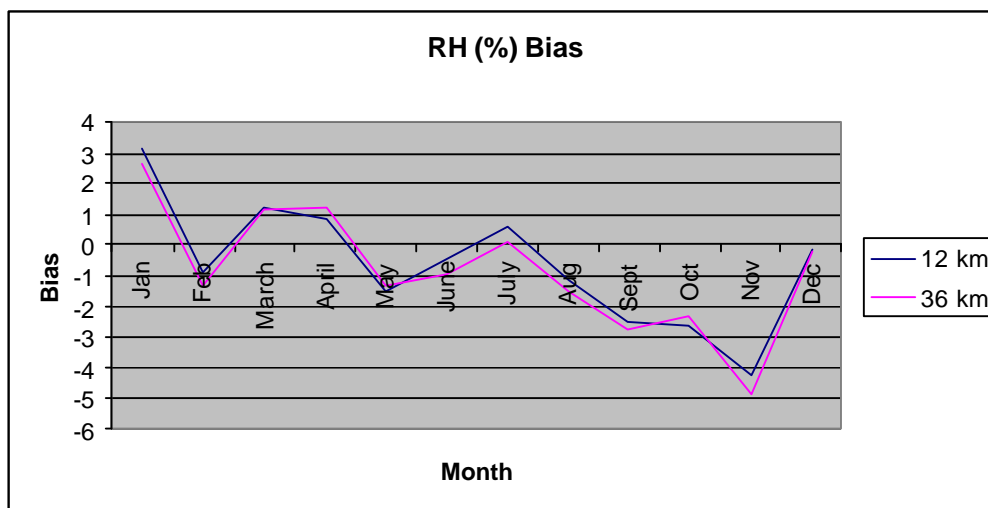


Figure 37. VISTAS region relative humidity biases (%) are plotted for both 12-km and 36-km resolutions.

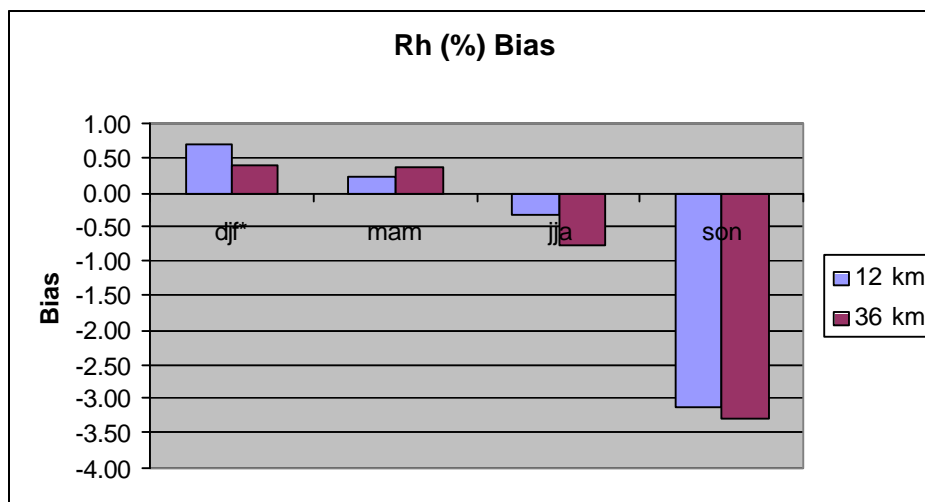


Figure 38. Seasonally aggregated VISTAS region relative humidity biases are shown. All months are in 2002, so the winter (djf) bar graph represents a discontinuous time period.

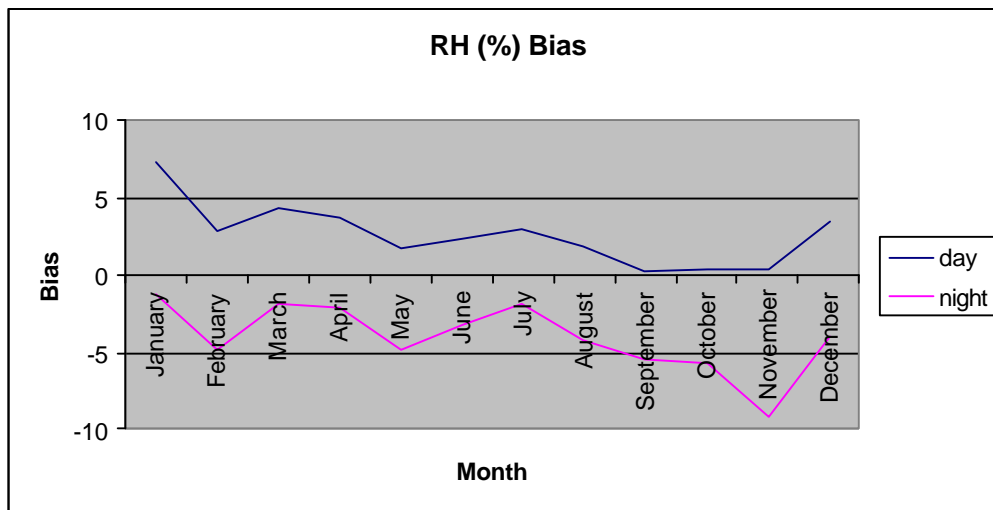


Figure 39. Monthly RH biases for the 12-km VISTAS region are plotted. The “day” period is defined to be 12Z-23Z, while “night” is defined to be 00Z-11Z.

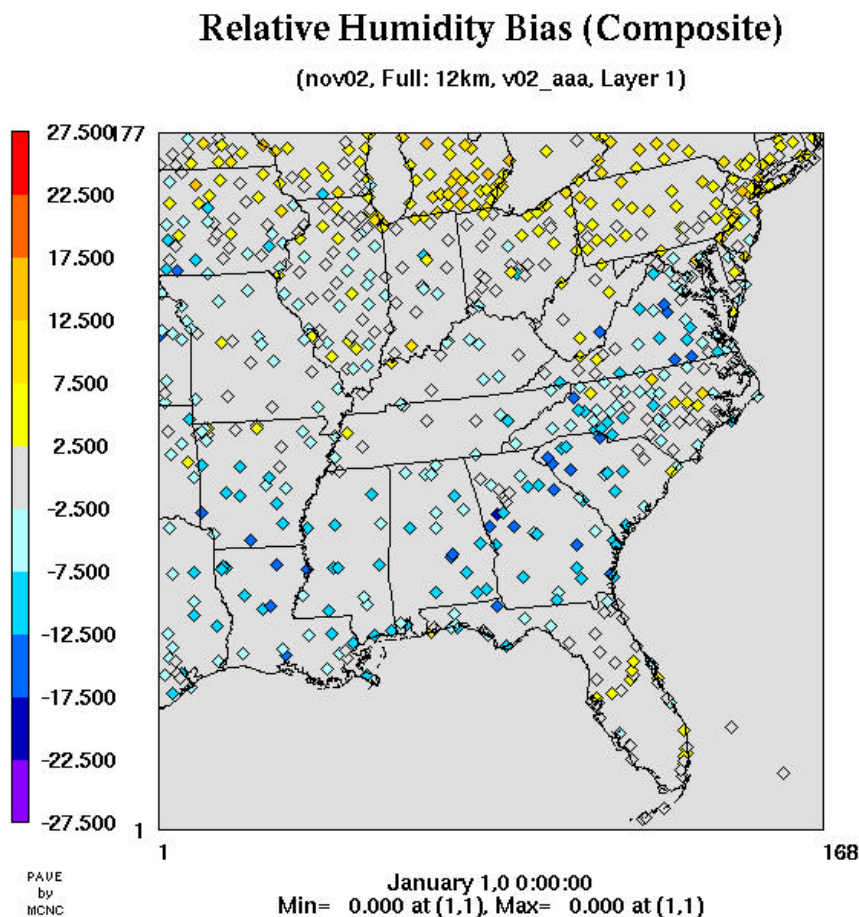


Figure 40. Site-specific RH biases (%) for November 2002 are displayed for each site in the 12-km grid. Note that the PAVE date label (January 1, 0) is nonsensical and should be ignored since it is only a placeholder.

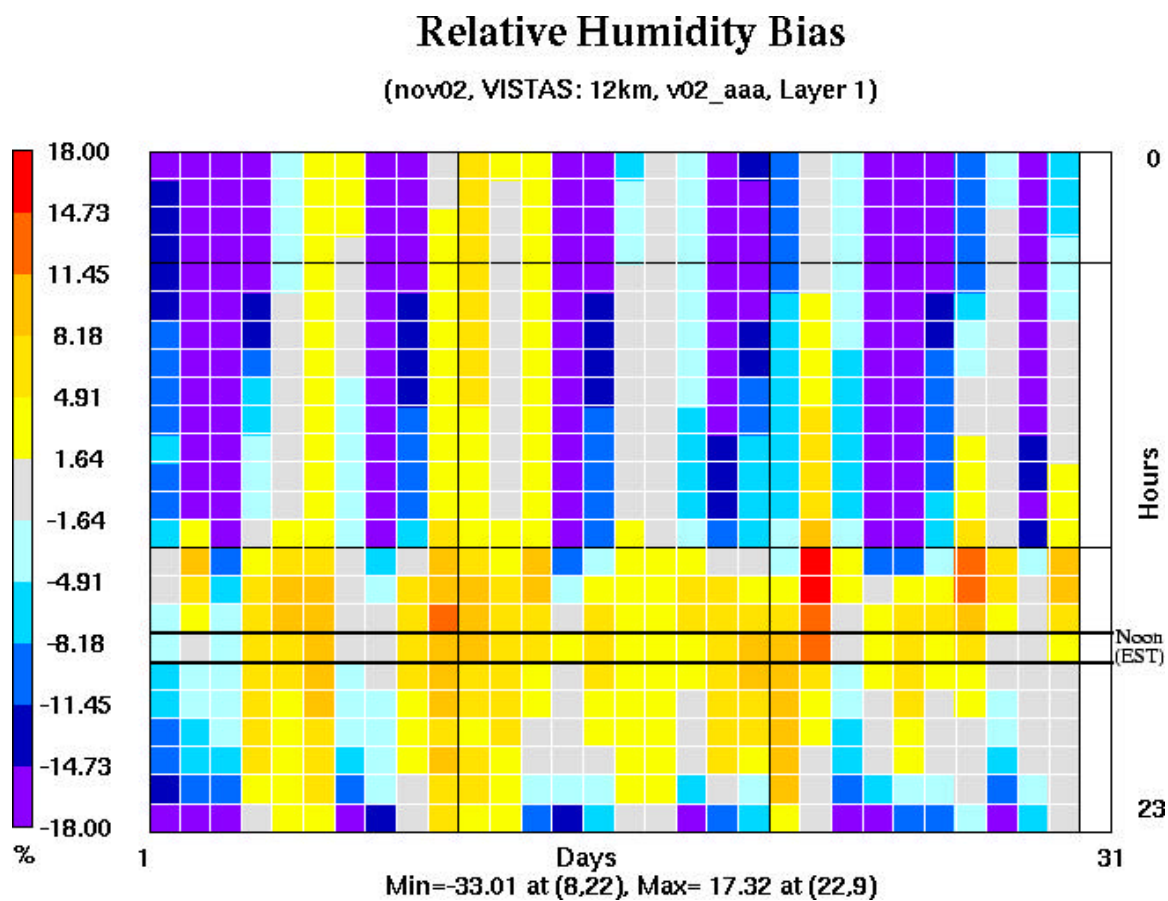


Figure 41. The November 2002 12-km VISTAS “Bakergram” for relative humidity biases (%) is plotted. The hourly biases are shown in a calendar-like layout so that the upper left cell represents the 00Z bias on the first day of the month.



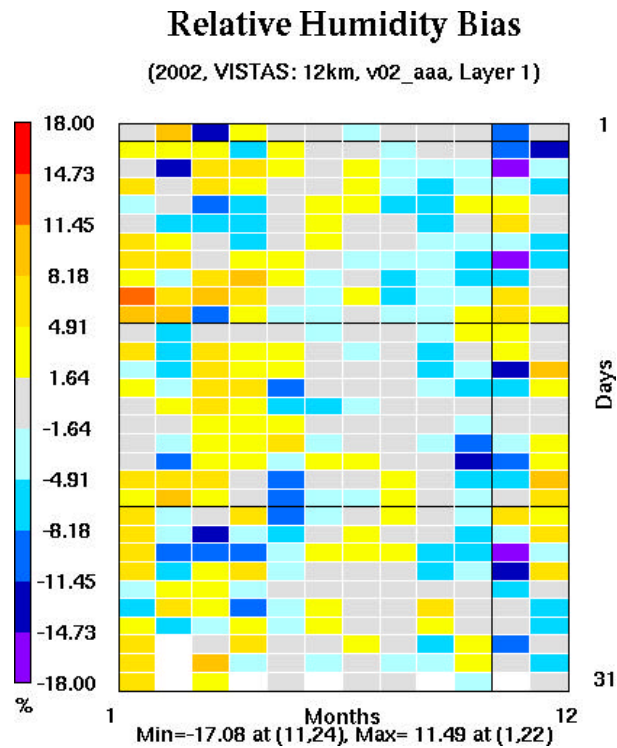


Figure 42. The 2002 12-km VISTAS “Bakergram” for relative humidity bias is plotted. The data are shown in a calendar-like layout so that the upper left cell represents the bias on the first day of January.

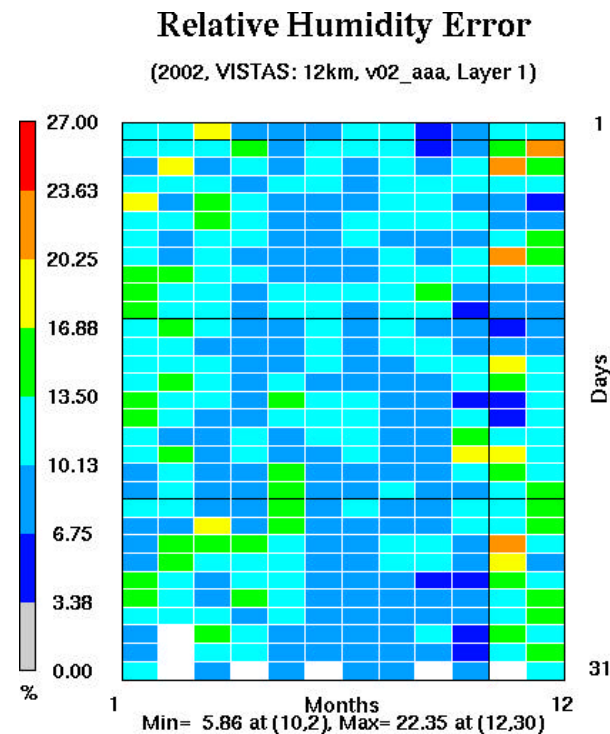


Figure 43. The 2002 12-km VISTAS “Bakergram” for relative humidity error is plotted. The data are shown in a calendar-like layout so that the upper left cell represents the bias on the first day of January.



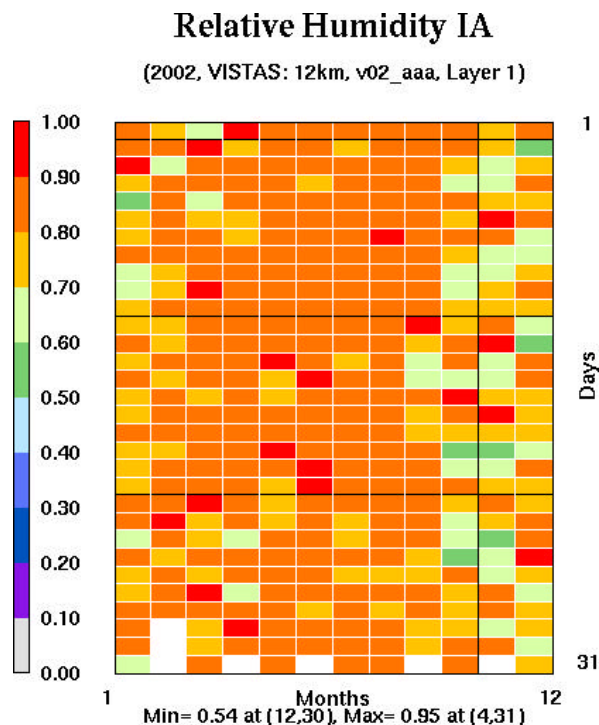


Figure 44. The 2002 12-km VISTAS “Bakergram” for relative humidity index of agreement is plotted. The data are shown in a calendar-like layout so that the upper left cell represents the bias on the first day of January.

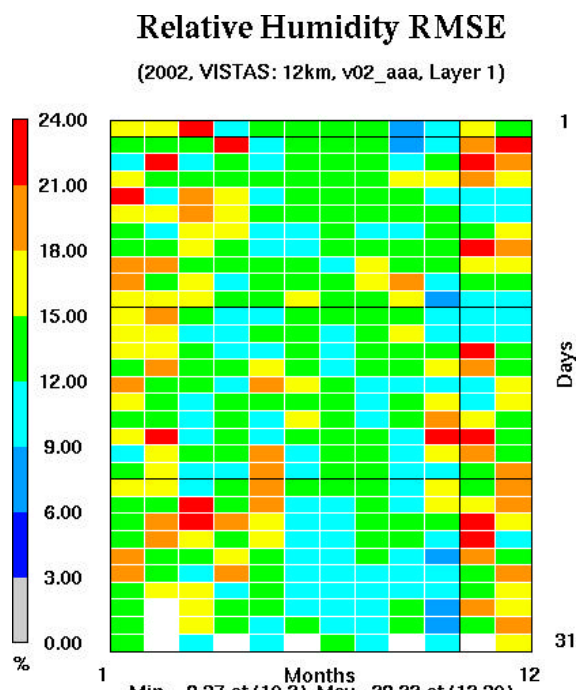


Figure 45. The 2002 12-km VISTAS “Bakergram” for relative humidity root mean square error is plotted. The data are shown in a calendar-like layout so that the upper left cell represents the bias on the first day of January.

## Wind Speed

Let us now focus on wind speed performance, starting with the standard include-all-calms-as-zero approach. Figure 46 shows that the model is positively biased with regard to wind speed for all months and for both grids. The bias is especially acute at 12-km resolution, presumably due to the weaker nudging applied to the winds at that scale. The greatest bias occurs in November, while the smallest bias occurs in March. Both are surprising results. The seasonal bar chart (figure 47) shows a general increase in speed bias from spring to autumn. Figures 48-49 reveal that the bulk of the speed bias occurs at night, quite likely in part to the presence of numerous calm observations. The site-specific spatial bias plot for this month is shown in figure 50. The northern third of the region is generally unbiased with regard to wind speed, while most of the VISTAS states exhibit a weak to moderate positive bias, peaking in North Carolina. Figure 51 shows that the speed biases are indeed primarily a nighttime phenomena, and figure 52 shows that weak wind speeds lasting almost the entire day is not uncommon in the southeast. Note that November 15 was chosen to be a representative day, not an extreme calm day. The annual wind speed Bakergrams are shown in figures 53-56.

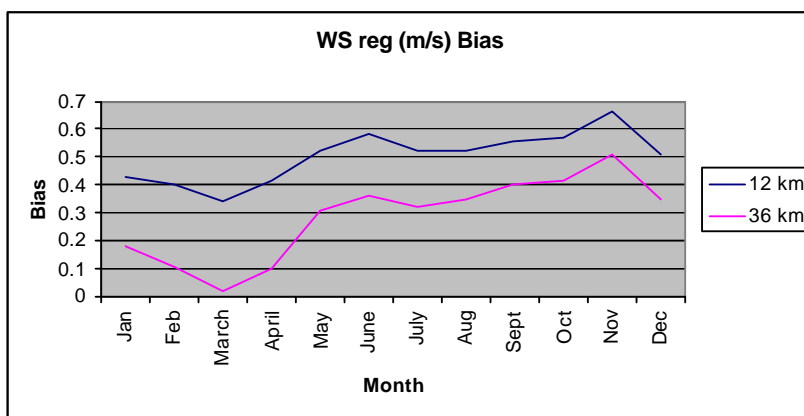


Figure 46. VISTAS region wind speed (regular) biases (m/s) are plotted for both 12-km and 36-km resolutions.

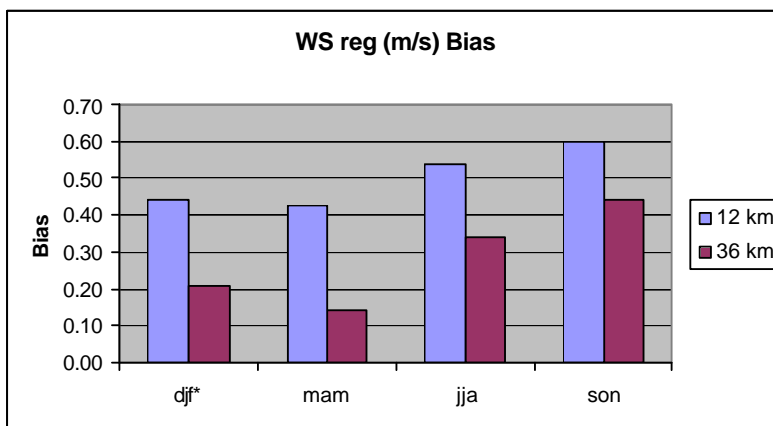


Figure 47. Seasonally aggregated VISTAS region wind speed (regular) biases are shown for both the 36-km and 12-km grids.

\*All months are in 2002, so the winter (djf) bar graph represents a discontinuous time period.

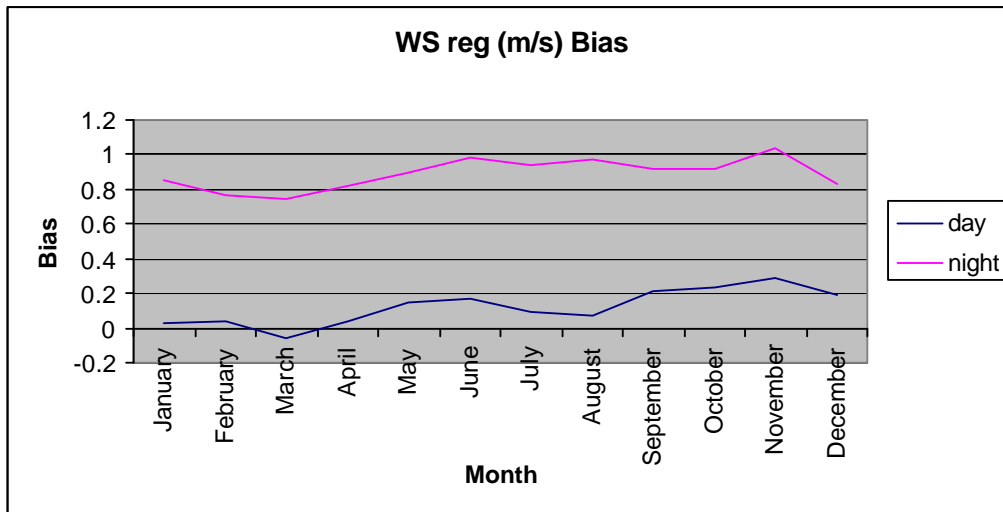


Figure 48. Monthly wind speed (regular) biases for the 12-km VISTAS region are plotted. The “day” period is defined to be 12Z-23Z, while “night” is defined to be 00Z-11Z.

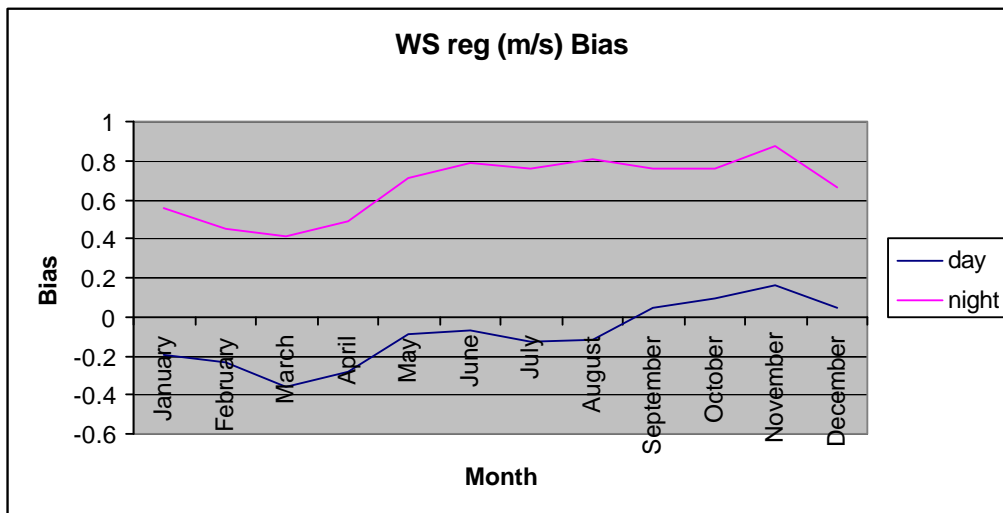


Figure 49. Monthly wind speed (regular) biases for the 36-km VISTAS region are plotted. The “day” period is defined to be 12Z-23Z, while “night” is defined to be 00Z-11Z.

## Wind Speed Bias (Composite)

(nov02, Full: 12km, v02\_aaa, 10m)

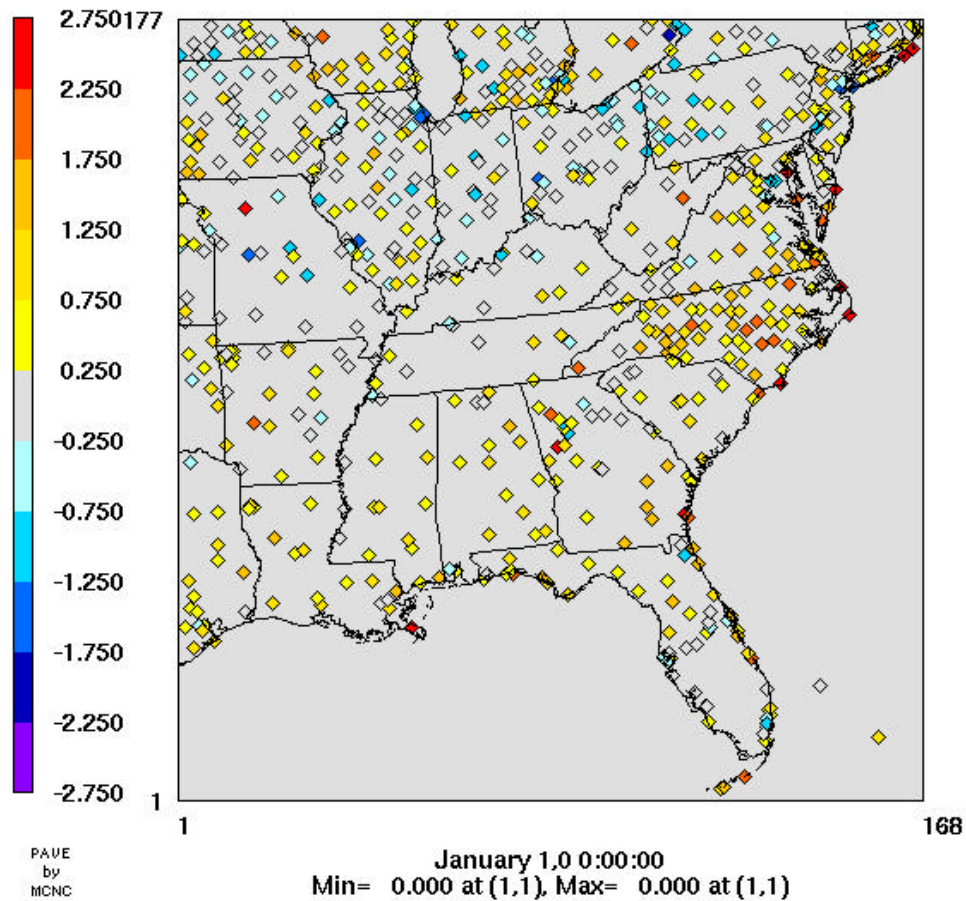


Figure 50. Site-specific wind speed (regular) biases (%) for November 2002 are displayed for each site in the 12-km grid. Note that the PAVE date label (January 1, 0) is nonsensical and should be ignored since it is only a placeholder.

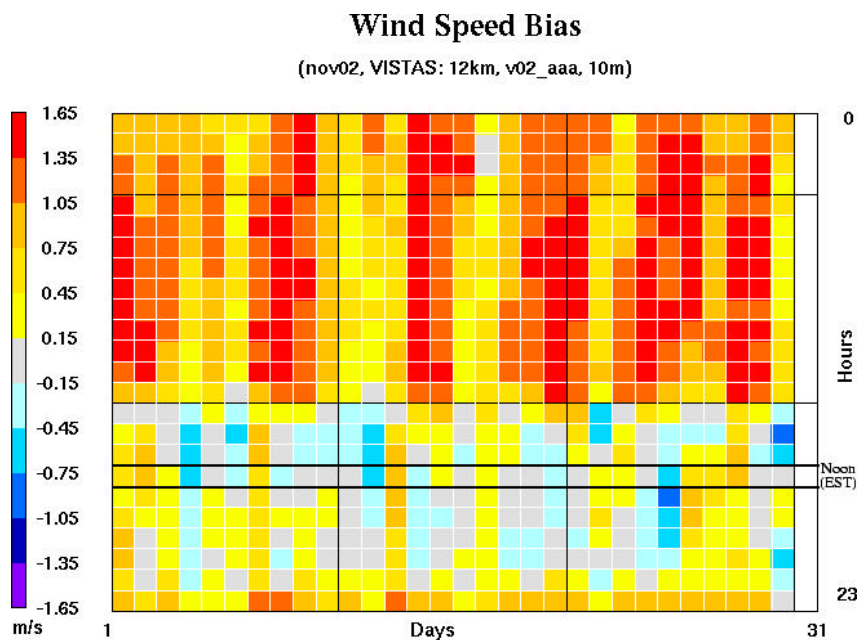


Figure 51. The November 2002 12-km VISTAS “Bakergram” for wind speed (regular) biases (%) is plotted. The hourly biases are shown in a calendar-like layout so that the upper left cell represents the 00Z bias on the first day of the month.

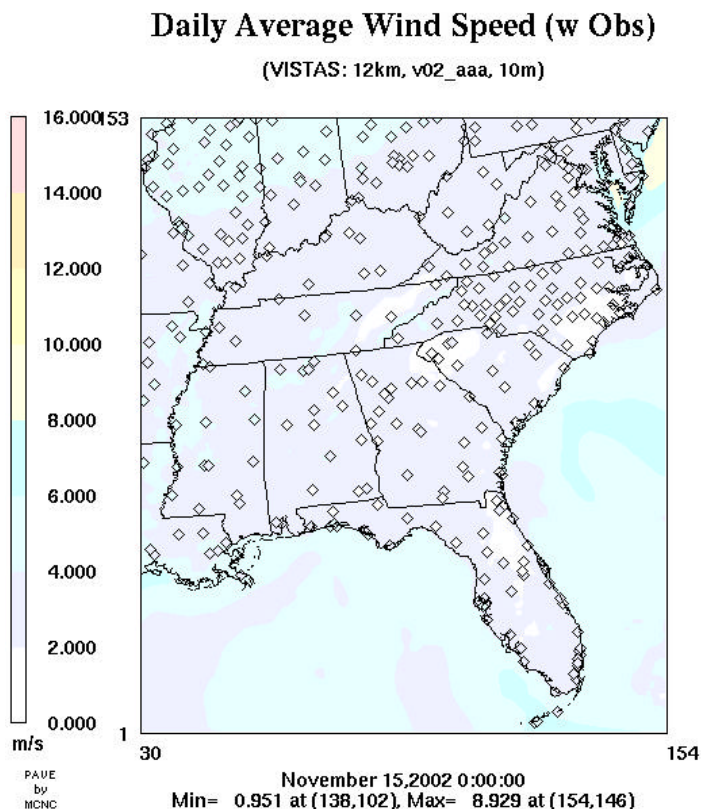


Figure 52. The November 15, 2002 12-km VISTAS daily averaged wind speed (with observations overlaid) is plotted.

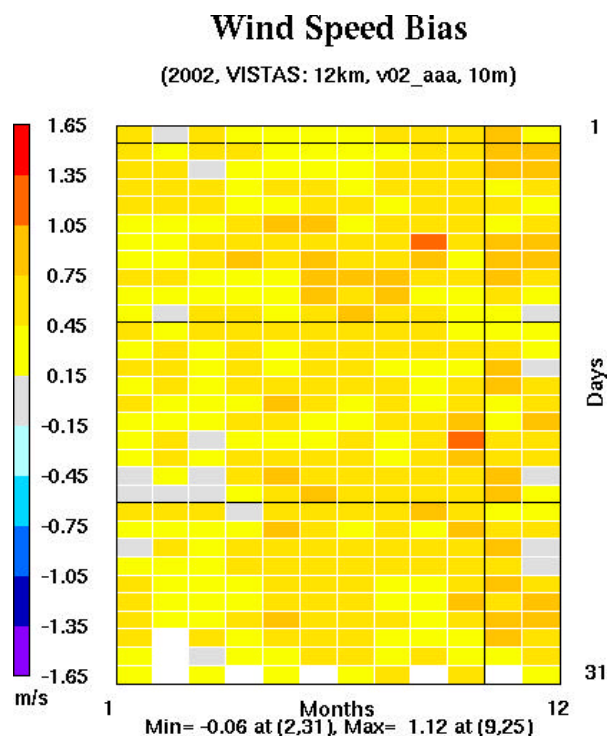


Figure 53. The 2002 12-km VISTAS “Bakergram” for wind speed (regular) bias is plotted. The data are shown in a calendar-like layout so that the upper left cell represents the bias on the first day of January.

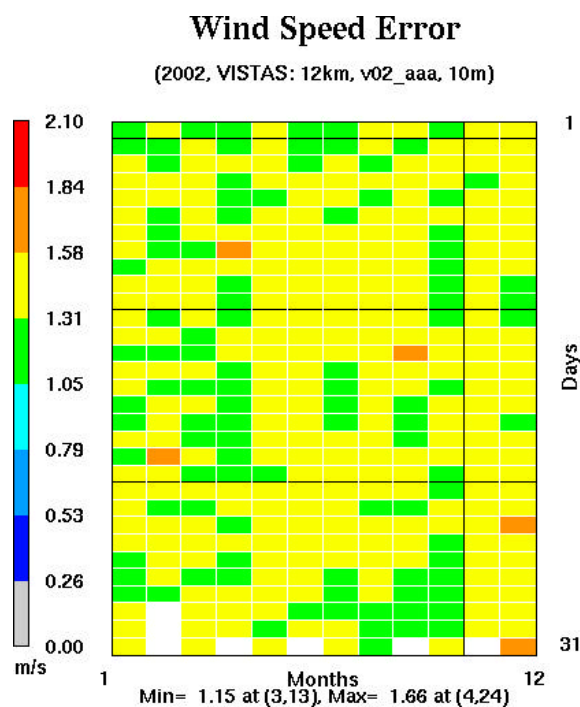


Figure 54. The 2002 12-km VISTAS “Bakergram” for wind speed (regular) error is plotted. The data are shown in a calendar-like layout so that the upper left cell represents the bias on the first day of January.

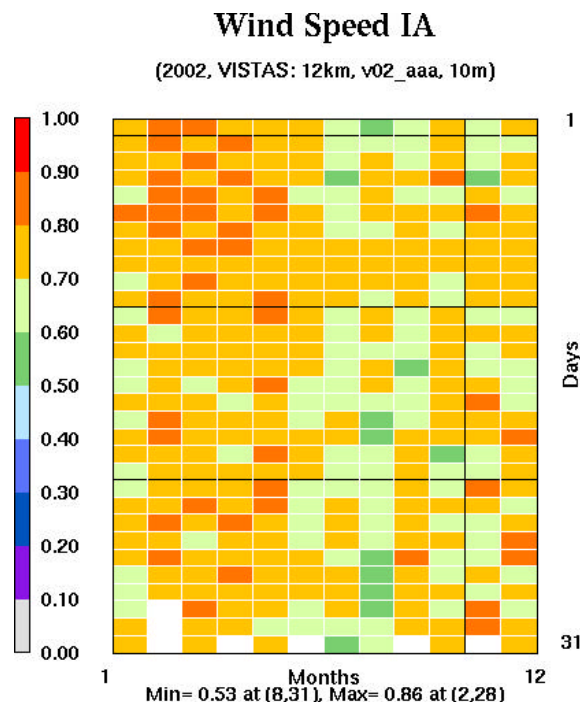


Figure 55. The 2002 12-km VISTAS “Bakergram” for wind speed (regular) index of agreement is plotted. The data are shown in a calendar-like layout so that the upper left cell represents the bias on the first day of January.

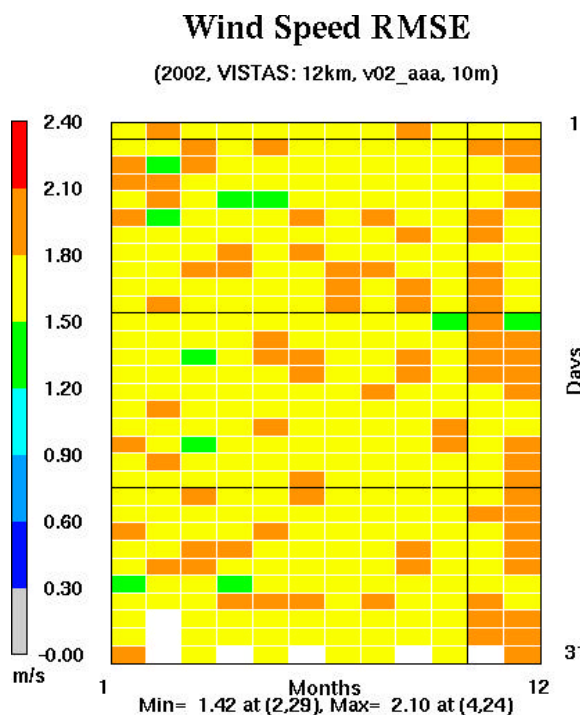


Figure 56. The 2002 12-km VISTAS “Bakergram” for wind speed (regular) root mean square error is plotted. The data are shown in a calendar-like layout so that the upper left cell represents the bias on the first day of January.



So what happens statistically if we consider only non-zero wind speed observations? Figure 57 shows that the resultant biases are practically non-existent at 12-km, while a slight low bias is evidenced at 36-km. Figure 58 consolidates the data into seasonal bins. So clearly the majority of the wind speed (regular) high biases stem from comparing model winds, which have no threshold issues, with observations, which obviously do. Figures 59-60 break the data into day/night periods.

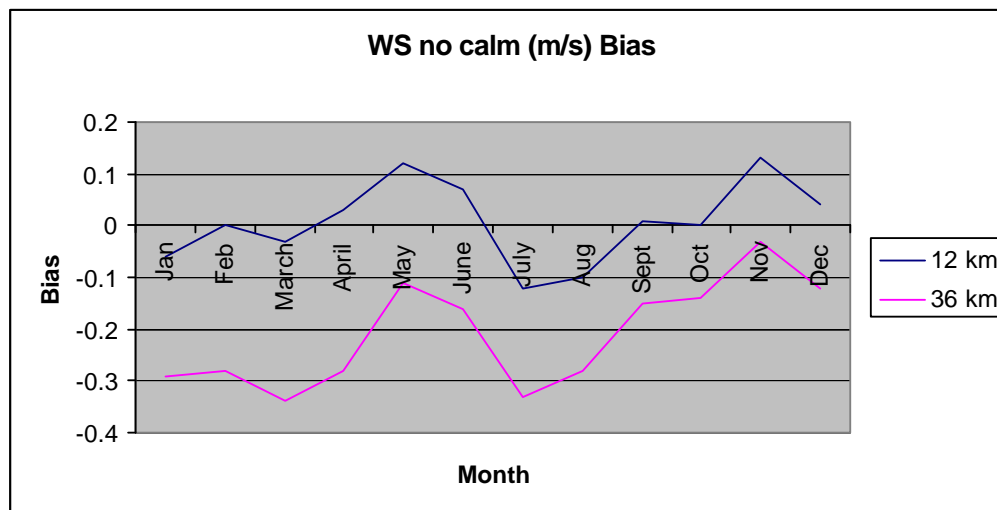


Figure 57. VISTAS region wind speed (no calms) biases (m/s) are plotted for both 12-km and 36-km resolutions.

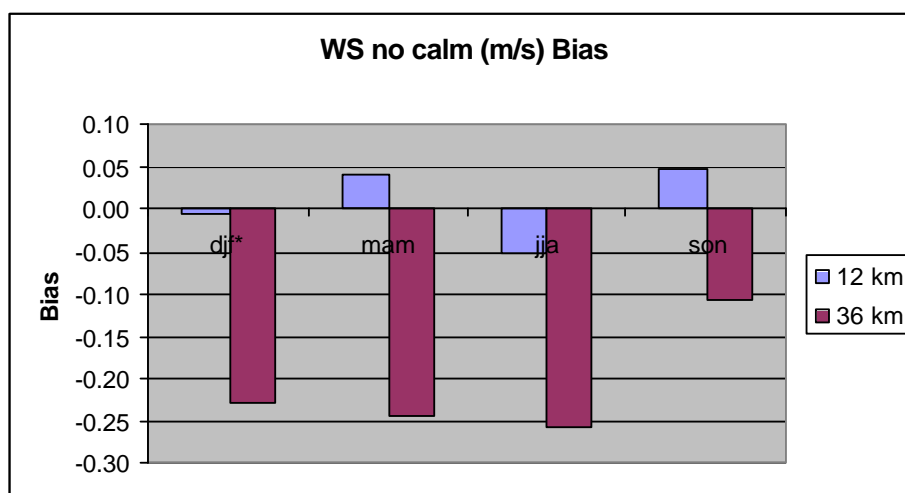


Figure 58. Seasonally aggregated VISTAS region wind speed (no calms) biases are shown for both the 36-km and 12-km grids.

\*All months are in 2002, so the winter (djf) bar graph represents a discontinuous time period.

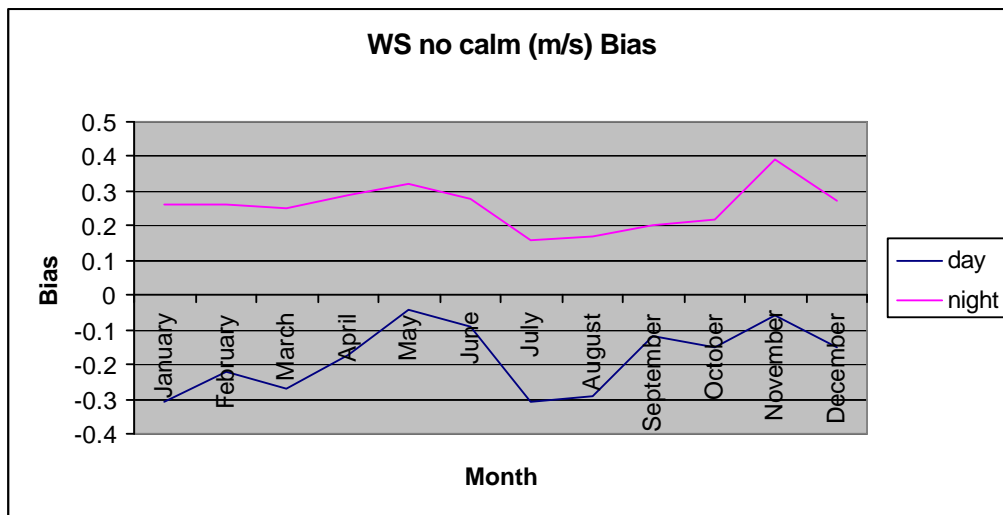


Figure 59. Monthly wind speed (no calms) biases for the 12-km VISTAS region are plotted. The “day” period is defined to be 12Z-23Z, while “night” is defined to be 00Z-11Z.

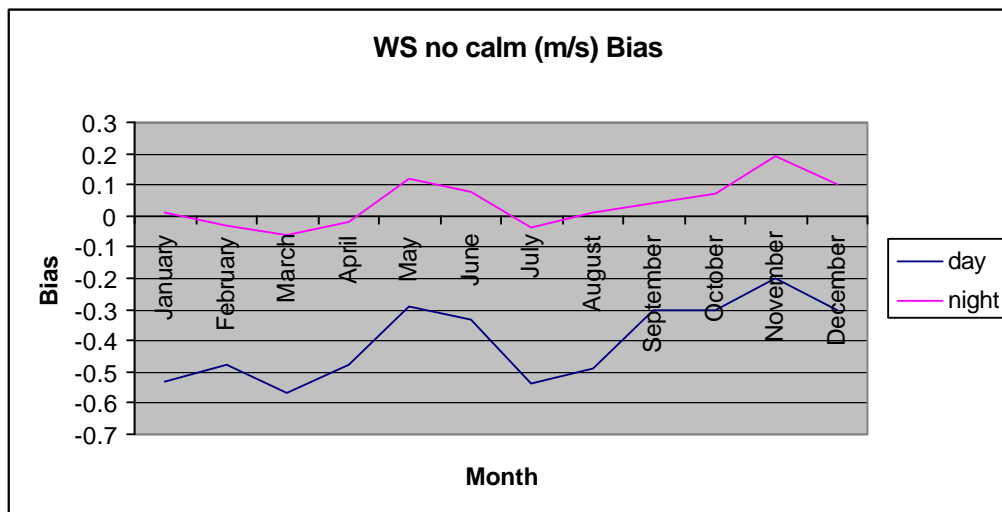


Figure 60. Monthly wind speed (no calms) biases for the 36-km VISTAS region are plotted. The “day” period is defined to be 12Z-23Z, while “night” is defined to be 00Z-11Z.

We have already discussed how not including calm reports probably introduces a low bias into the wind speed calculations. Figures 61-63 show the results we obtain by substituting a value of 1.5 knots (mid-point between 0.0 and lowest observed report of 3 knots) for each of the calm reports. A general positive bias is noted, especially at night and at 12-km resolution, but the magnitude of the biases are reduced by ~0.2 m/s.

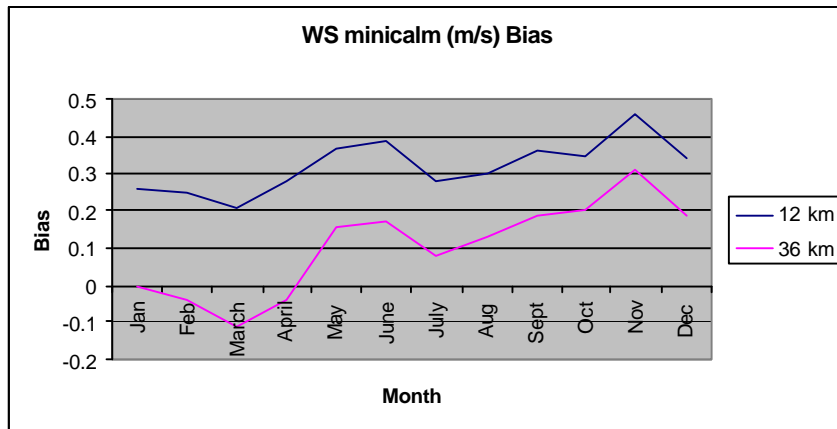


Figure 61. VISTAS region wind speed (minimum calms) biases (m/s) are plotted for both 12-km and 36-km resolutions.

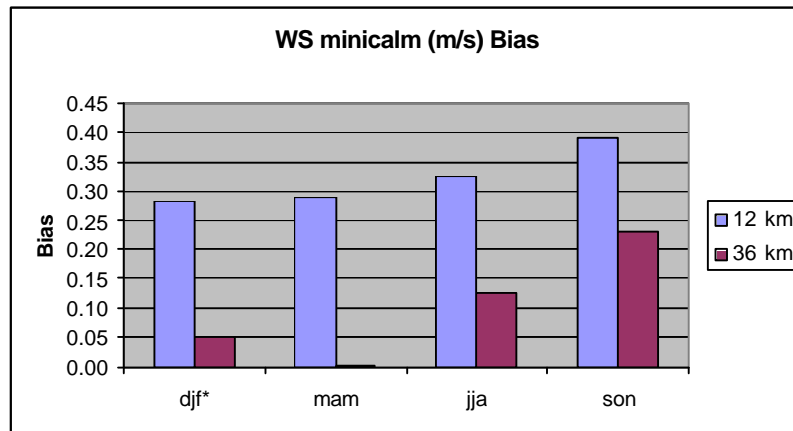


Figure 62. Seasonally aggregated VISTAS region wind speed (minimum calms) biases are shown for both the 36-km and 12-km grids.

\* All months are in 2002, so the winter (djf) bar graph represents a discontinuous time period.

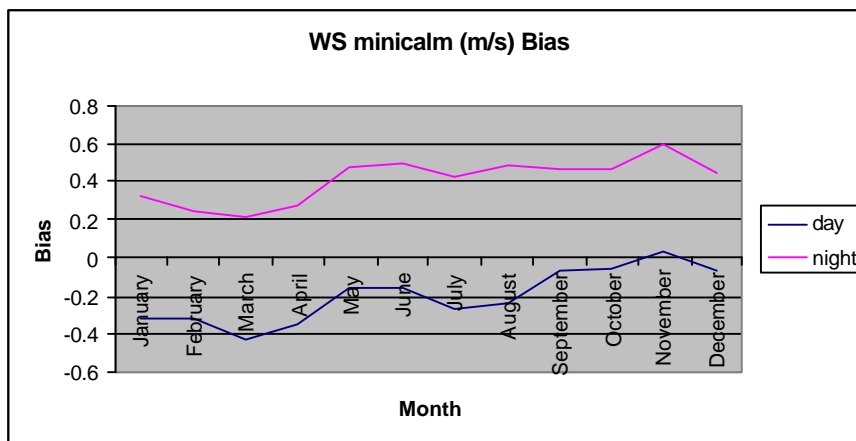


Figure 63. Monthly wind speed (minimum calms) biases for the 12-km VISTAS region are plotted. The “day” period is defined to be 12Z-23Z, while “night” is defined to be 00Z-11Z.

## Wind Direction

Let us now consider wind direction performance. Figure 64 shows the monthly wind direction errors over the VISTAS region for both model domains. The performance of the two grids is very similar, and surprisingly enough the 12-km grid has a slightly lower error. The increased nudging strength at 36-km might have been expected to yield a lower direction error. We know that all wind direction errors do not have the same effect of air quality modeling. A 90 degree direction error at light winds speeds might have a less deleterious effect than a 40 degree error at moderate wind speeds. A better way of treating wind direction discrepancies between the model and the observations is to calculate the magnitude of the error wind vector. This approach properly treats winds as vectors and allows us to quantify the combined effect of speed and direction errors. Figure 65 shows the resultant plot. As a rule the two grids track very similarly, with the 36-km domain yielding slightly superior results, undoubtedly due to the presence of stronger nudging. Also note how the result for November does not stick out as an outlier, even though wind speed performance exhibited its highest bias during that month. The wind direction bias and error annual Bakergram plots are displayed in figures 66-67, followed by the annual Bakergram for the magnitude of the error wind vector.

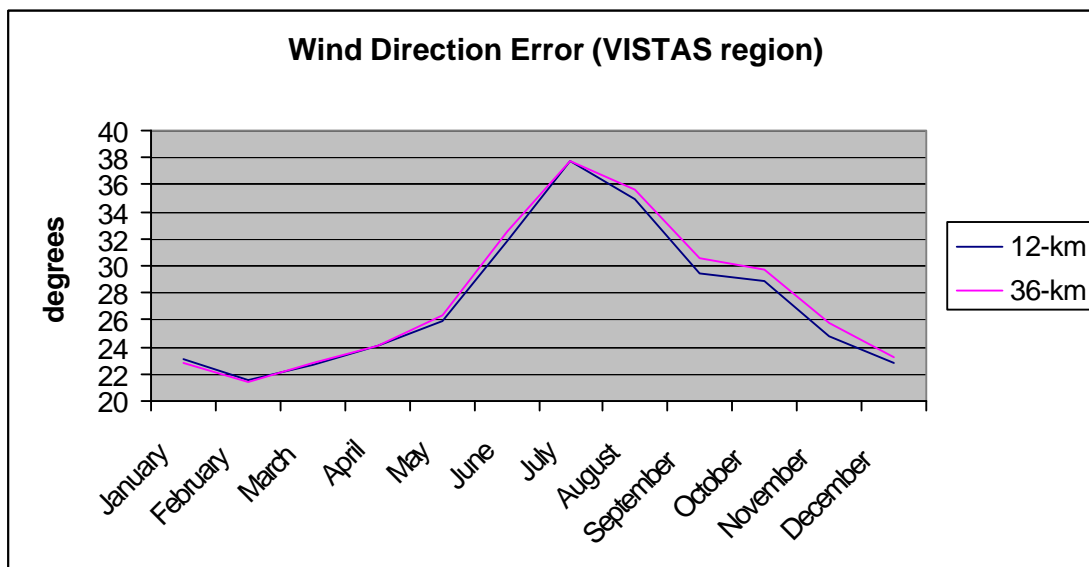


Figure 64. VISTAS region wind direction errors are plotted for both 12-km and 36-km resolutions.

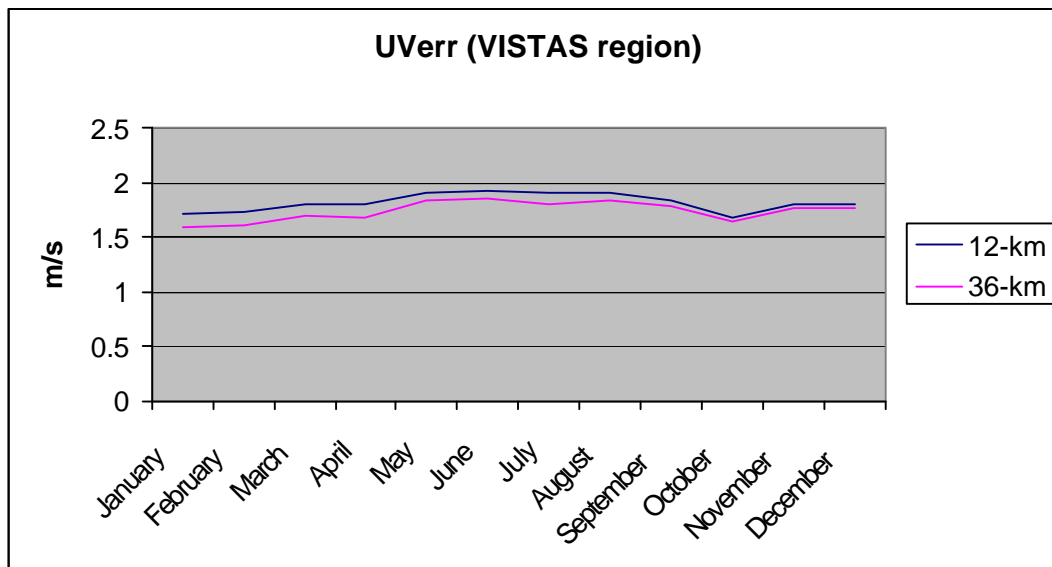


Figure 65. The magnitude of the error wind vector for the VISTAS region is plotted for both 12-km and 36-km resolutions.

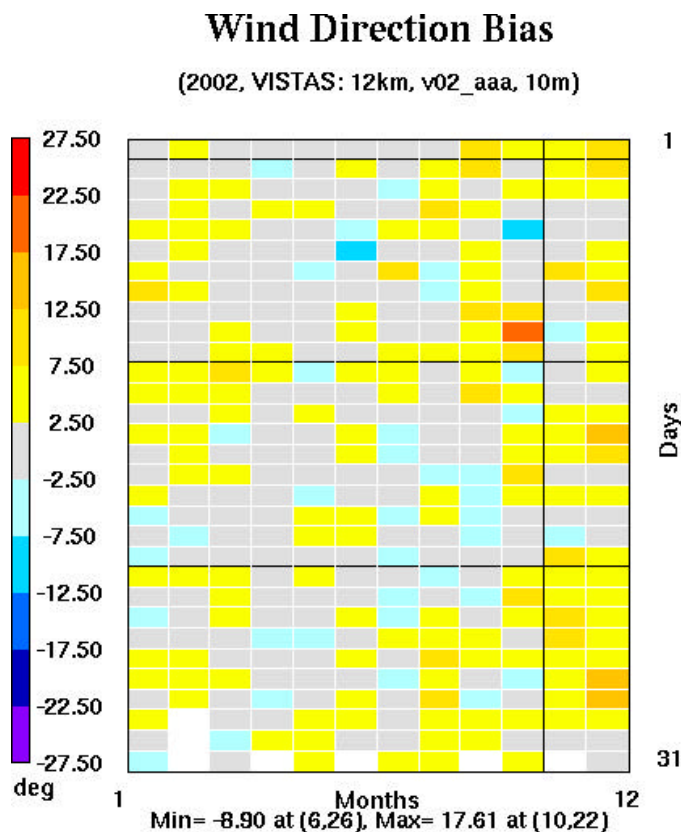


Figure 66. The 2002 12-km VISTAS “Bakergram” for wind direction bias is plotted. The data are shown in a calendar-like layout so that the upper left cell represents the bias on the first day of January.

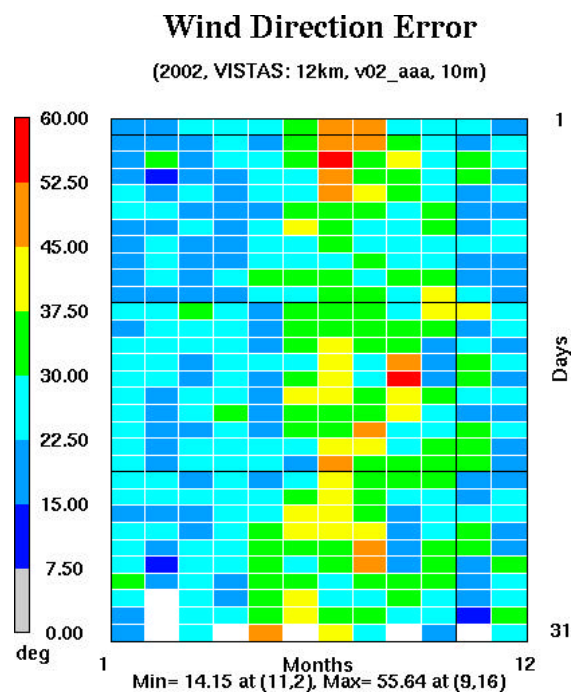


Figure 67. The 2002 12-km VISTAS “Bakergram” for wind direction error is plotted. The data are shown in a calendar-like layout so that the upper left cell represents the bias on the first day of January.

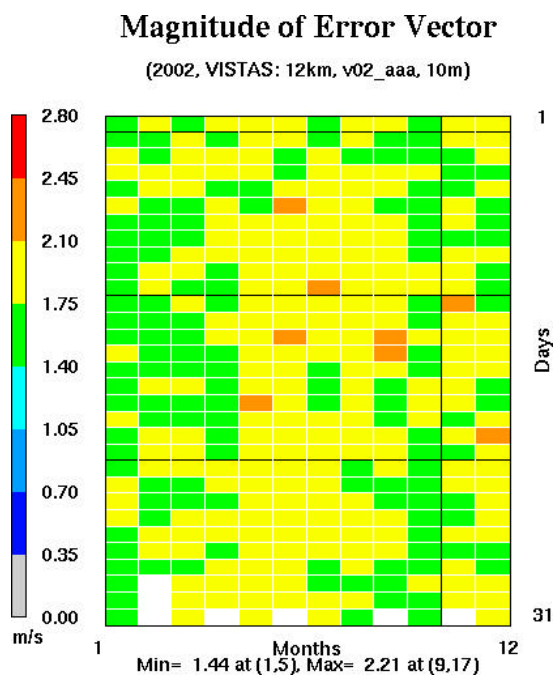


Figure 68. The 2002 12-km VISTAS “Bakergram” for magnitude of the error wind vector is plotted. The data are shown in a calendar-like layout so that the upper left cell represents the bias on the first day of January.

## Clouds

Since the alternative cloud fraction variable “CLD2” is deemed more meteorologically consistent with the cloud observations than is the MCIP-derived variable “CLD”, we will focus our attention there. Figures 69-70 show a strong seasonal variation to cloud bias. For most of the year clouds are relatively unbiased. However, through the summer months a noticeable positive bias appears, especially at 12-km. Figures 71-72 show that most of the bias occurs at night. It is difficult to know if this nighttime bias is indeed real, since cloud observations at night might not be as accurate as they are during the daytime. Figure 73 shows that the bias for July is widespread with little spatial variation. The Bakergram (figure 74) reveals that the nighttime bias is more or less a constant feature. If the observations are accurate, it appears that MM5 is lacking a key cloud disintegration process that occurs in the real world. Figures 75-76 show the average observed and modeled cloud coverage in a Bakergram format. Note that the observations show a distinct diurnal variation in that cloud coverage is greatest in the afternoon and smallest in the late overnight periods. Another evident cycle occurs at the synoptic scale and can be seen on an approximately 10-day time scale. The model does a nice job replicating the synoptic scale variations, but the diurnal variations are completely out of phase. Since the nocturnal bias is more significant at 12-km than it is at 36-km, one must consider the possibility that the internal cloud parameterizations need to be adjusted to run as successfully at finer scale resolutions. The full suite of annual Bakergram products for clouds is shown in figures 77-80.

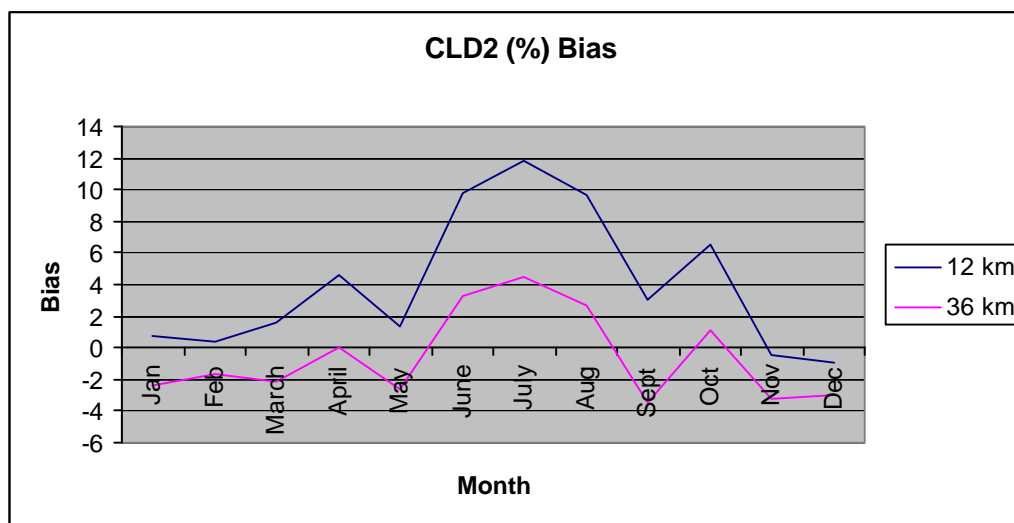


Figure 69. VISTAS region alternative cloud biases are plotted for both 12-km and 36-km resolutions.

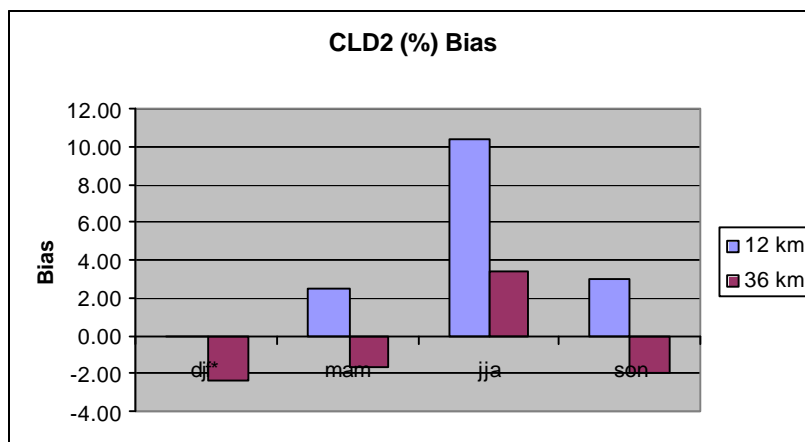


Figure 70. Seasonally aggregated VISTAS region alternative cloud biases are shown for both the 36-km and 12-km grids.  
 \*All months are in 2002, so the winter (djf) bar graph represents a discontinuous time period.

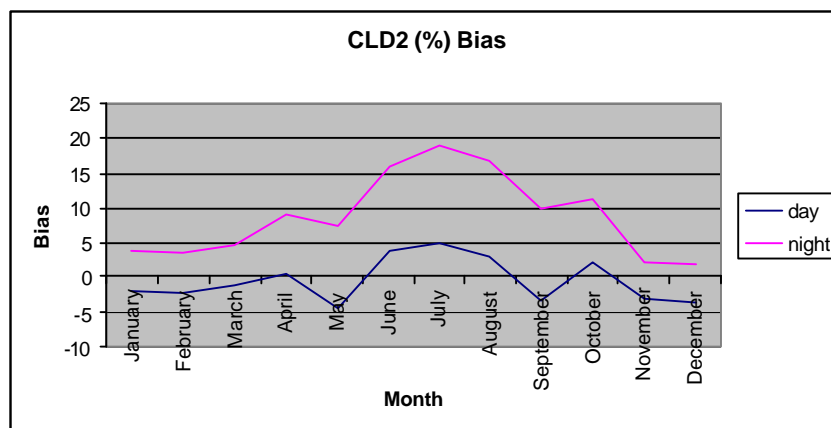


Figure 71. Monthly alternative cloud biases for the 12-km VISTAS region are plotted. The “day” period is defined to be 12Z-23Z, while “night” is defined to be 00Z-11Z.

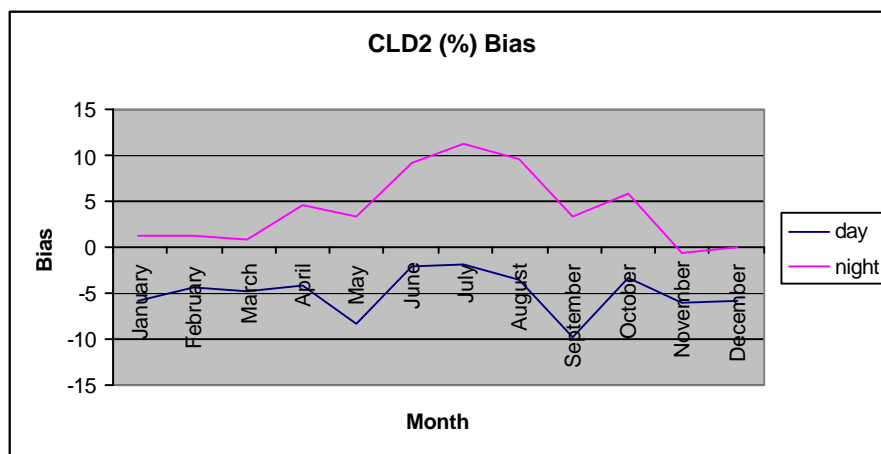


Figure 72. Monthly alternative cloud biases for the 36-km VISTAS region are plotted. The “day” period is defined to be 12Z-23Z, while “night” is defined to be 00Z-11Z.



## Alternate Clouds Bias (Composite)

(jul02, Full: 12km, v02\_aaa)

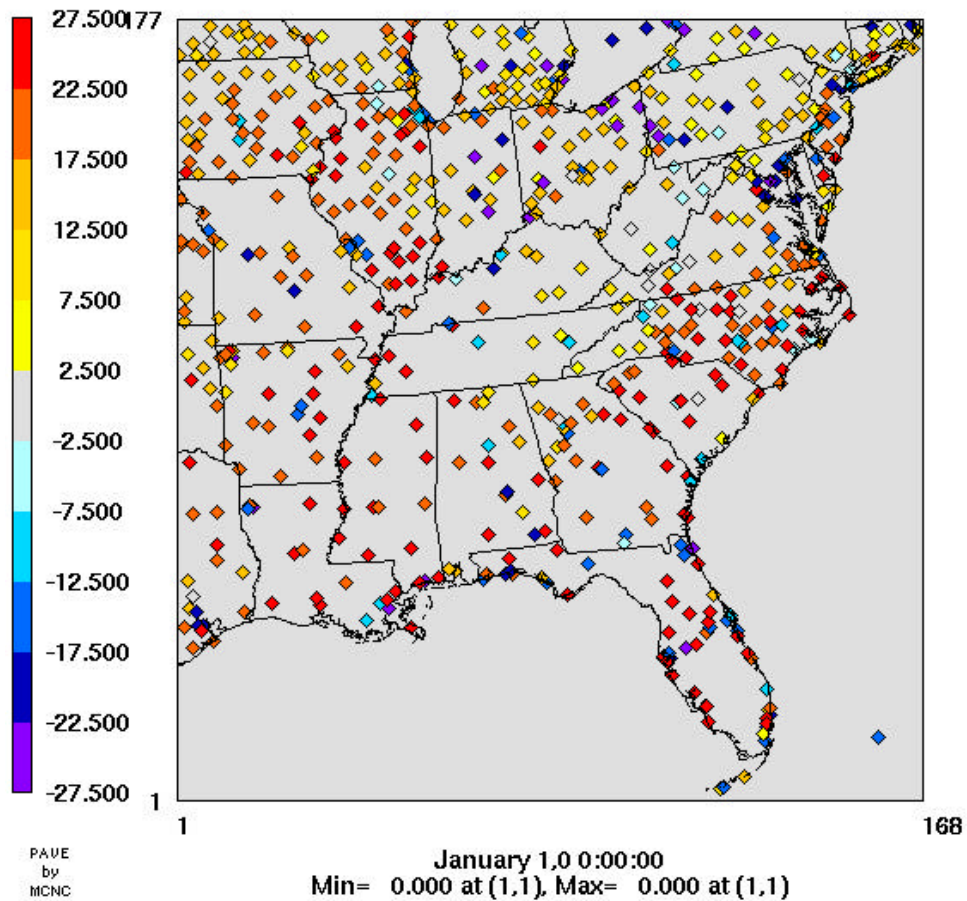


Figure 73. Site-specific cloud (alternative) biases (%) for July 2002 are displayed for each site in the 12-km grid. Note that the PAVE date label (January 1, 0) is nonsensical and should be ignored since it is only a placeholder.

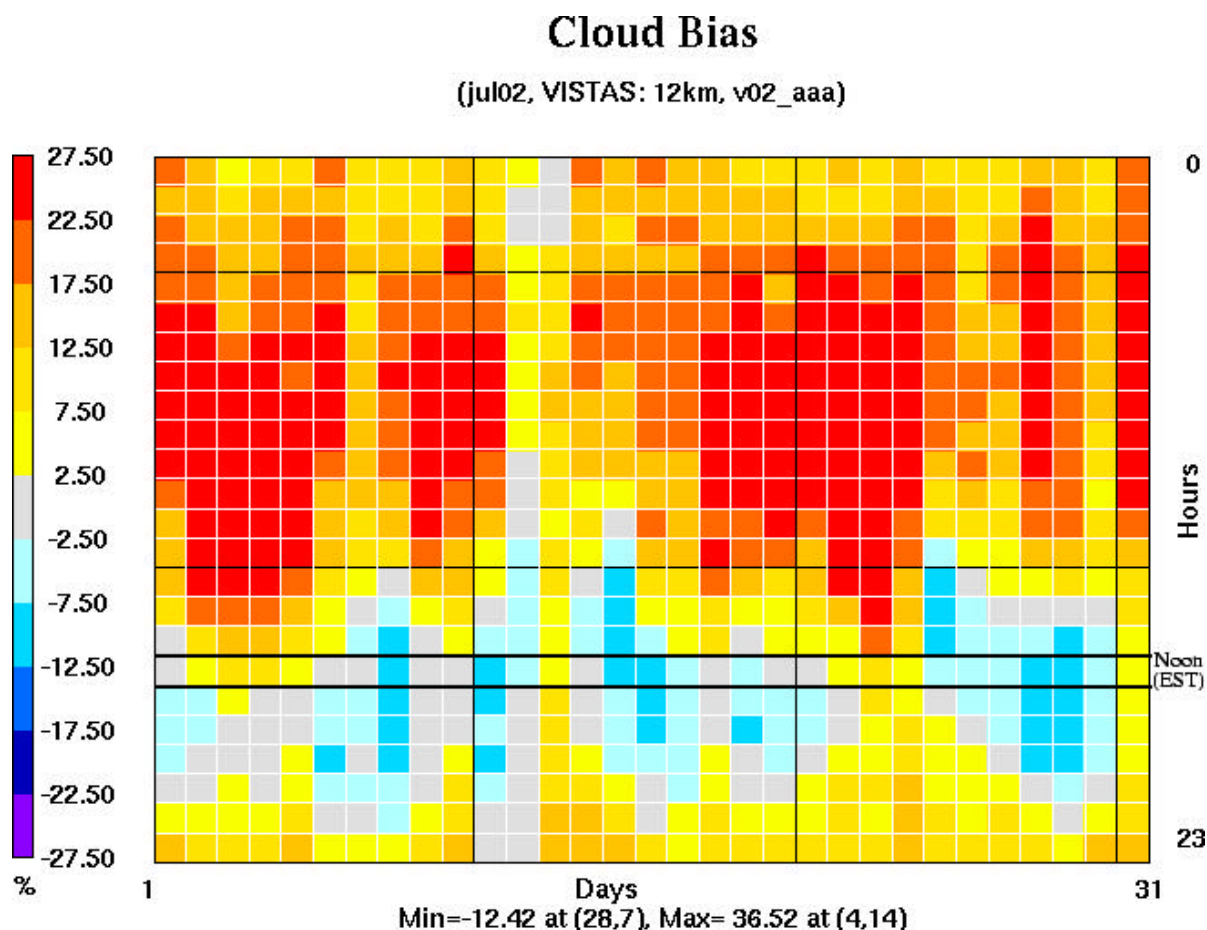


Figure 74. The July 2002 12-km VISTAS “Bakergram” for cloud (alternative) biases (%) is plotted. The hourly biases are shown in a calendar-like layout so that the upper left cell represents the 00Z bias on the first day of the month.

## Average Observed Clouds

(jul02, VISTAS: 12km, v02\_aaa)

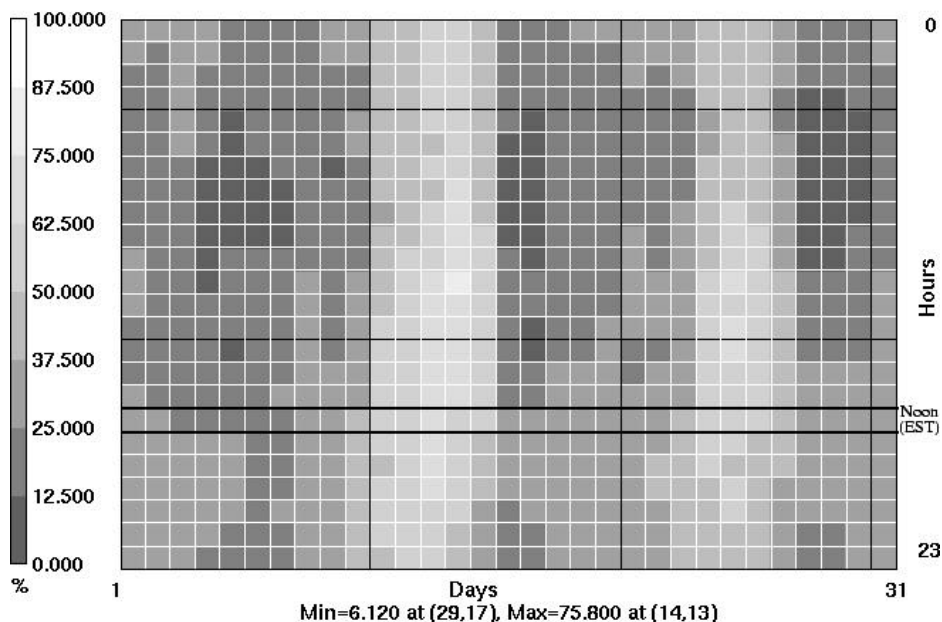


Figure 75. The July 2002 12-km VISTAS “Bakergram” for observed cloud coverage (%) is plotted. The hourly values are shown in a calendar-like layout so that the upper left cell represents the 00Z bias on the first day.

## Average Modeled Clouds

(jul02, VISTAS: 12km, v02\_aaa)

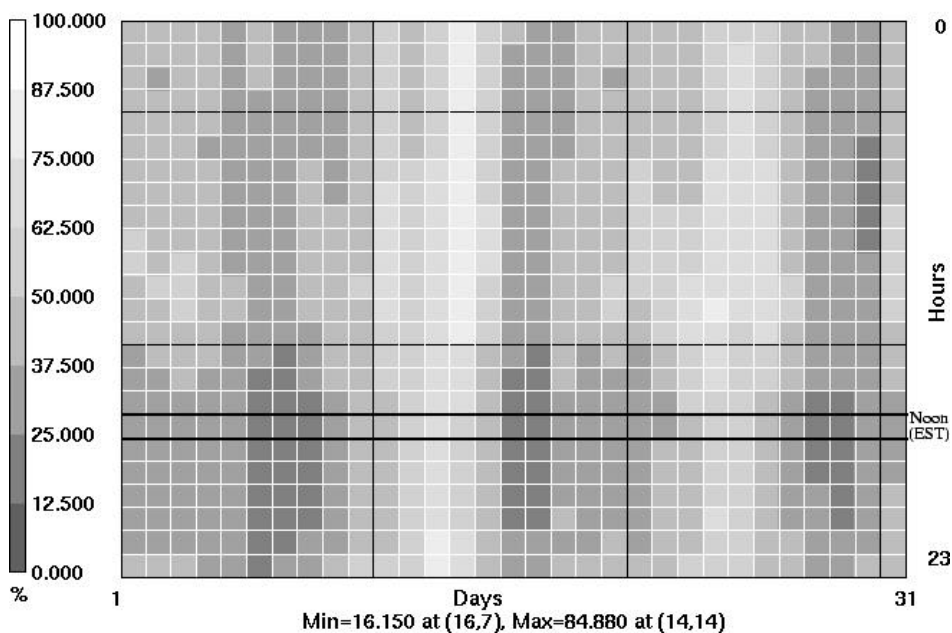


Figure 76. The July 2002 12-km VISTAS “Bakergram” for modeled cloud coverage (%) is plotted. The hourly values are shown in a calendar-like layout so that the upper left cell represents the 00Z bias on the first day.

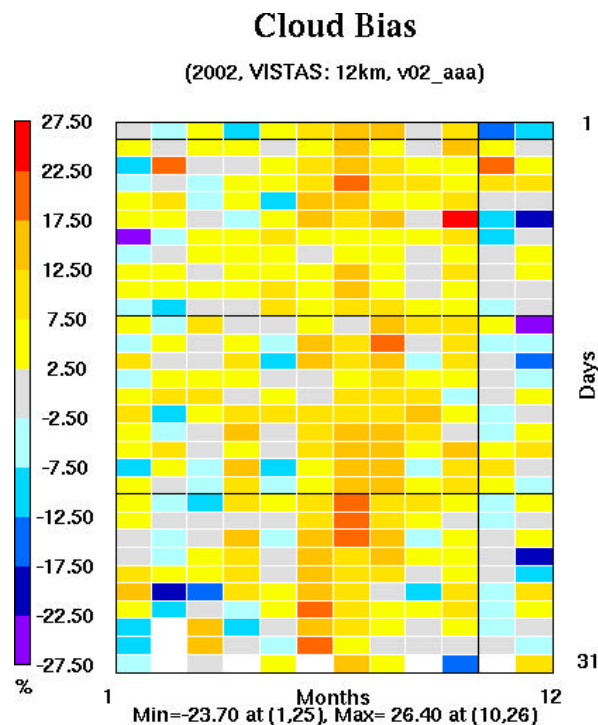


Figure 77. The 2002 12-km VISTAS “Bakergram” for cloud coverage (alternative) bias is plotted. The data are shown in a calendar-like layout so that the upper left cell represents the bias on the first day of January.

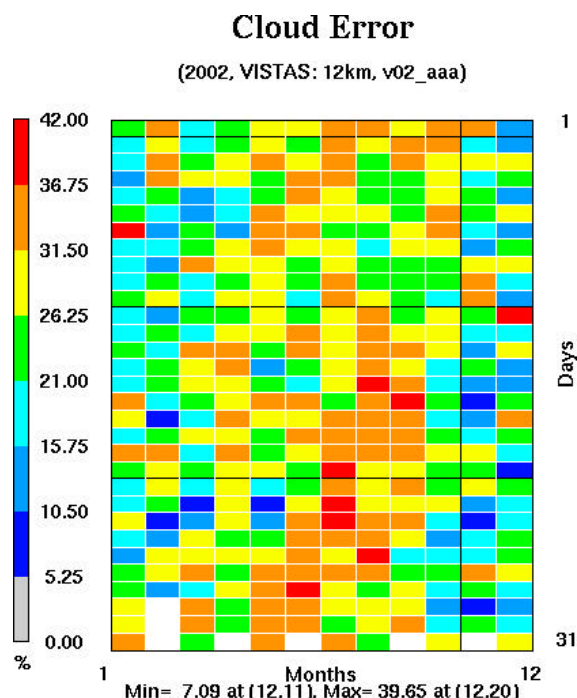


Figure 78. The 2002 12-km VISTAS “Bakergram” for cloud coverage (alternative) error is plotted. The data are shown in a calendar-like layout so that the upper left cell represents the bias on the first day of January.

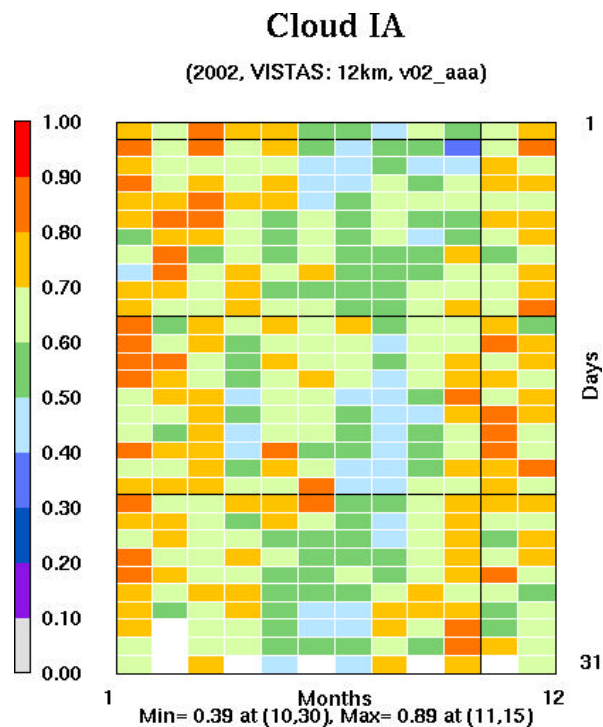


Figure 79. The 2002 12-km VISTAS “Bakergram” for cloud coverage (alternative) index of agreement is plotted. The data are shown in a calendar-like layout so that the upper left cell represents the bias on the first day of January.

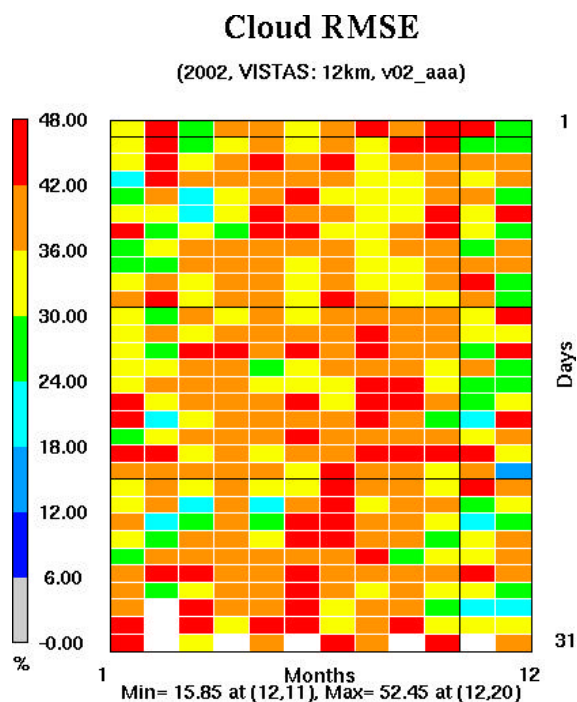


Figure 80. The 2002 12-km VISTAS “Bakergram” for cloud coverage (alternative) root mean square error is plotted. The data are shown in a calendar-like layout so that the upper left cell represents the bias on the first day of January.

## **Precipitation**

To begin our precipitation analysis, consider the monthly obs/model accumulated precipitation plots for the 12-km grid shown in figures 81-92. For most of the year the model does a nice job in replicating the observed precipitation field. However, the model appears to noticeably overestimate the amount of precipitation in the summer months, especially in June and July (figures 86-87). Interestingly enough in the fall the model underestimates precipitation amounts, coinciding with the dry bias noted in the mixing ratio statistics (figure 28).

The summertime accumulation bias could result from at least two model inadequacies. One is that the model could fire off convection (or just regular rain for that matter) too often, possibly most every afternoon. The second possibility is that the model triggers rainfall at approximately the correct frequency, but the model could overestimate the intensity of the rainfall. The first possibility is the more serious model flaw from an air quality perspective, since the presence/absence of rain affects pollution concentrations more than predicting 2 inches of rain when only 1 inch actually occurred. To address this issue, consider the statistical time series plots for precipitation shown in figures 93-98. Figure 93 shows the precipitation statistics for the 0.01-inch threshold level at 12-km resolution, and reveals that the model is slightly biased high for the first third of the year. During the summer the model is slightly low biased, reaching a yearlong minimum in September. By December the model has essentially become unbiased. When examining these statistical plots, remember that the process of gridding observed precipitation could cause the spatial extent of precipitation coverage – especially at lower thresholds - to be slightly larger than what it really is. This would introduce an artificial negative precipitation bias. At the same time, we are assuming that any precipitation that falls in a cell covers the entire cell, which may or may not be true. This effect could cause an artificial high precipitation bias. With those caveats out of the way, it is interesting that the precipitation bias trace is similar to the mixing ratio bias trace (figure 27). The threat score indicates that the model shows considerable skill in predicting measurable precipitation year-round, with the expected slight decline in skill over the summer months. The 36-km results (figure 94) show unbiased statistics for the first half of the year, followed by a slight negative bias that maintains itself the entire second half of the year.

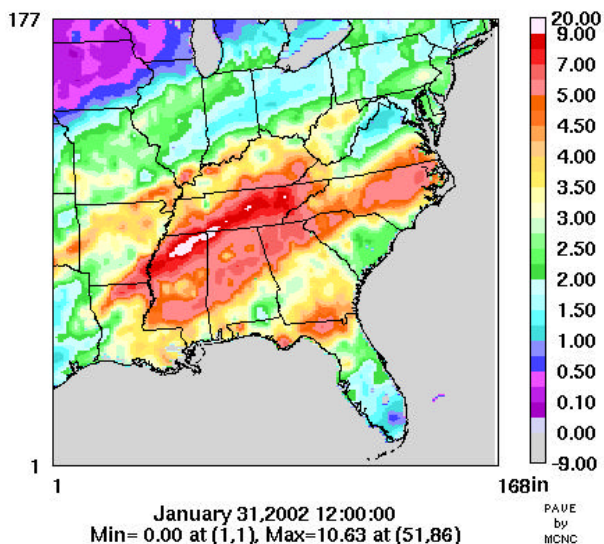
Figure 95 shows the 12-km precipitation statistics at the 0.05-inch threshold. The results are not all that different from the 0.01-inch threshold results, though the summertime threat scores are slightly lower. Figure 96 reveals that the 36-km precipitation (0.05-inch) is slightly biased high for the first eight months of the year, after which it becomes essentially unbiased. At the higher threshold level of 0.25-inch, figures 97-98 show that the model exhibits a significant summer increase in precipitation bias.

These statistics indicate that the model suffers from the more benign weakness mentioned above, namely overestimating the predicted amount of precipitation when it actually occurs. Perhaps the model precipitation efficiency is too great? More research needs to be made on this topic.



### Monthly Total Precipitation (Obs)

(jan02, Full: 12km, v02\_aaa)



### Monthly Total Precipitation (MM5)

(jan02, Full: 12km, v02\_aaa)

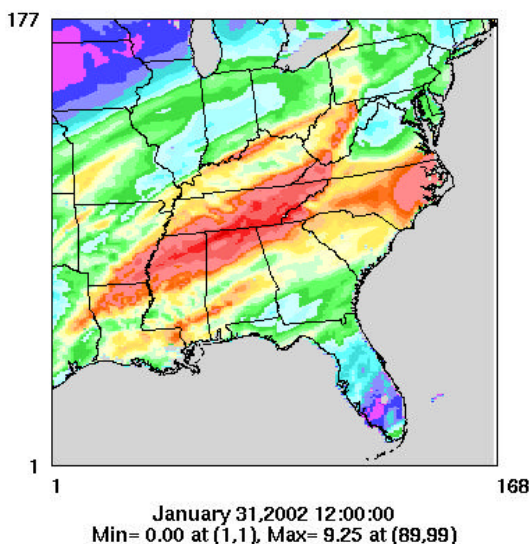
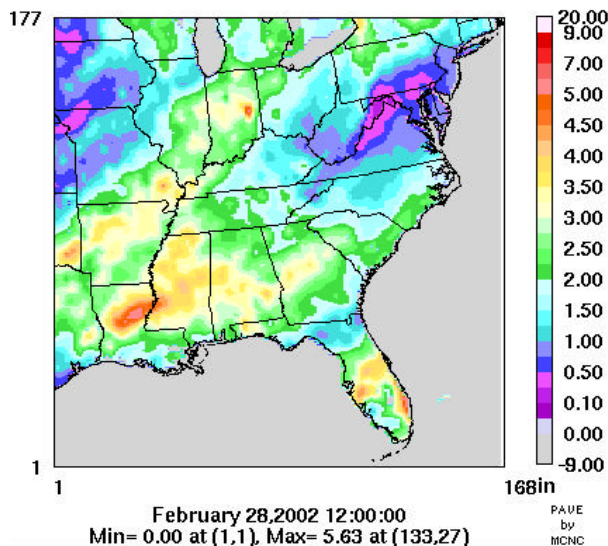


Figure 81. The January 2002 12-km accumulated precipitation from the Climate Prediction Center is juxtaposed with the MM5 accumulated precipitation.

### Monthly Total Precipitation (Obs)

(feb02, Full: 12km, v02\_aaa)



### Monthly Total Precipitation (MM5)

(feb02, Full: 12km, v02\_aaa)

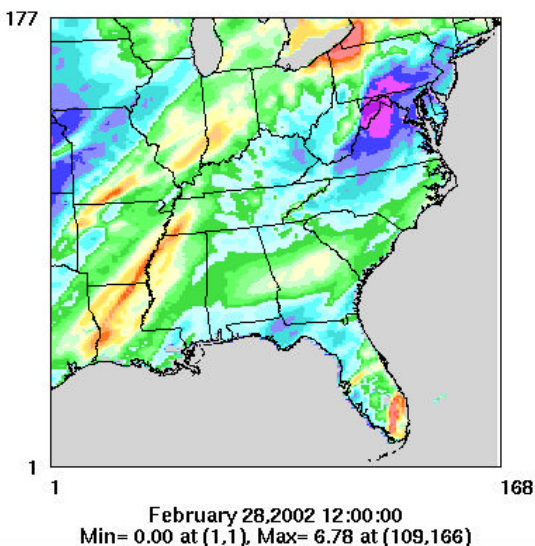
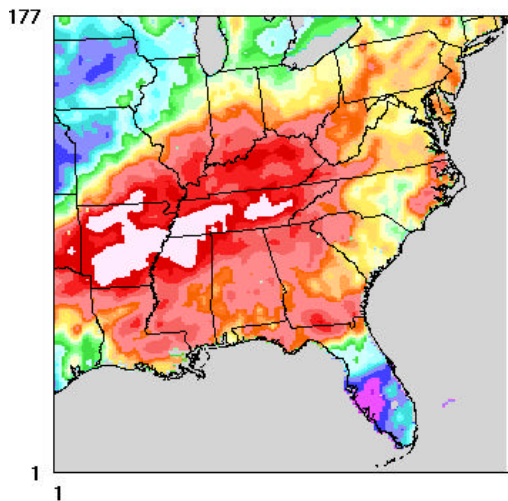


Figure 82. The February 2002 12-km accumulated precipitation from the Climate Prediction Center is juxtaposed with the MM5 accumulated precipitation.

### Monthly Total Precipitation (Obs)

(mar02, Full: 12km, v02\_aaa)



### Monthly Total Precipitation (MM5)

(mar02, Full: 12km, v02\_aaa)

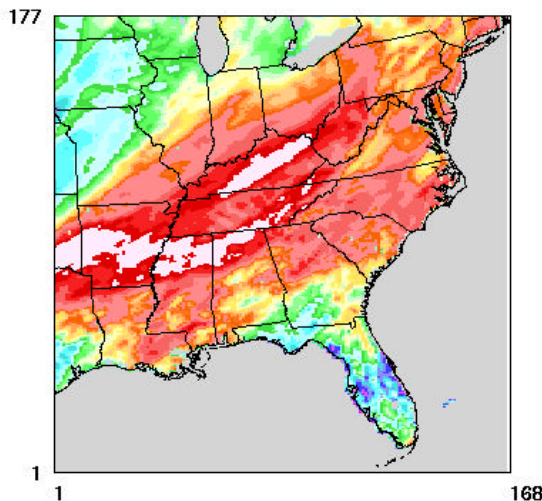
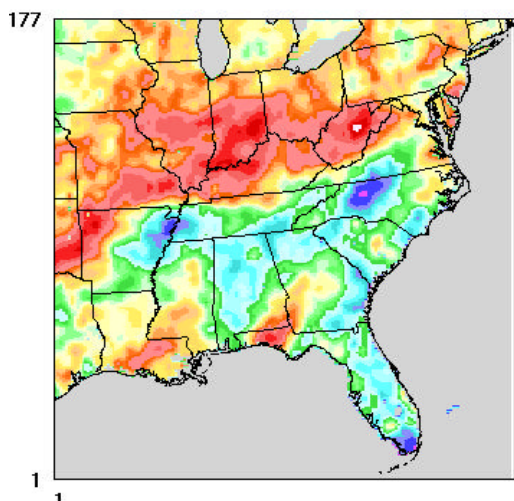


Figure 83. The March 2002 12-km accumulated precipitation from the Climate Prediction Center is juxtaposed with the MM5 accumulated precipitation.

### Monthly Total Precipitation (Obs)

(apr02, Full: 12km, v02\_aaa)



### Monthly Total Precipitation (MM5)

(apr02, Full: 12km, v02\_aaa)

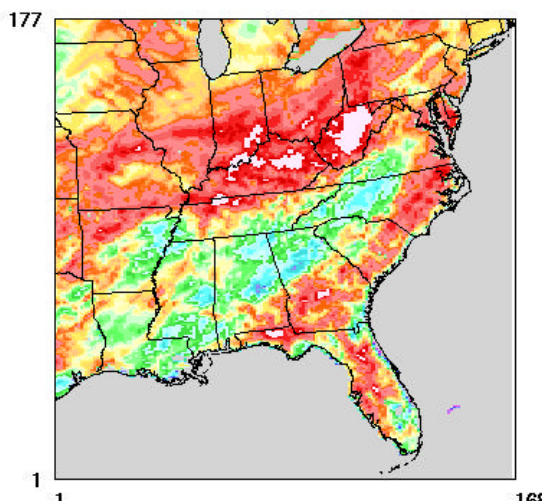
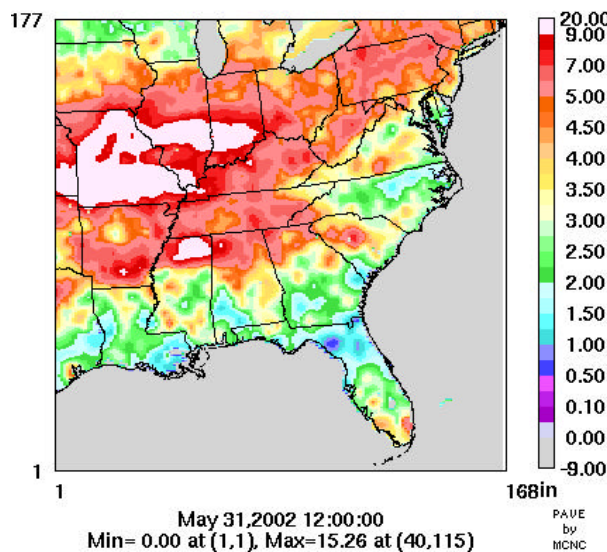


Figure 84. The April 2002 12-km accumulated precipitation from the Climate Prediction Center is juxtaposed with the MM5 accumulated precipitation.



### Monthly Total Precipitation (Obs)

(may02, Full: 12km, v02\_aaa)



### Monthly Total Precipitation (MM5)

(may02, Full: 12km, v02\_aaa)

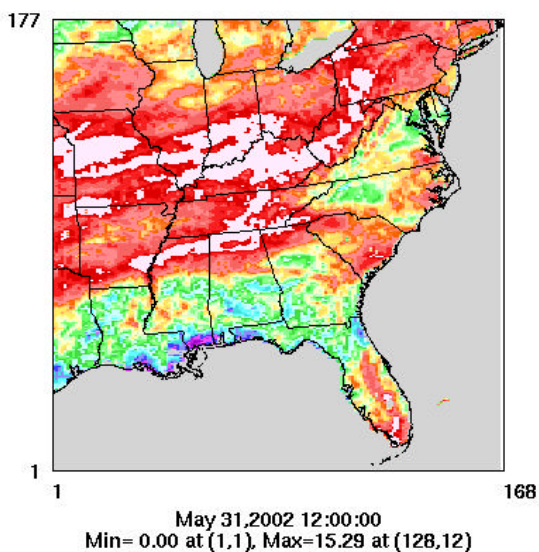
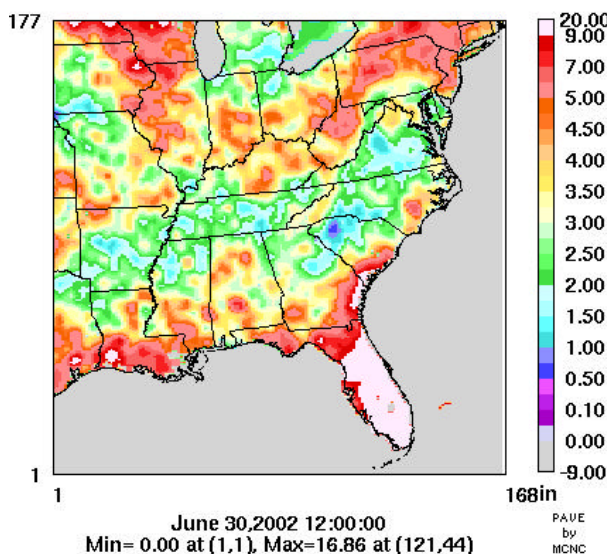


Figure 85. The May 2002 12-km accumulated precipitation from the Climate Prediction Center is juxtaposed with the MM5 accumulated precipitation.

### Monthly Total Precipitation (Obs)

(jun02, Full: 12km, v02\_aaa)



### Monthly Total Precipitation (MM5)

(jun02, Full: 12km, v02\_aaa)

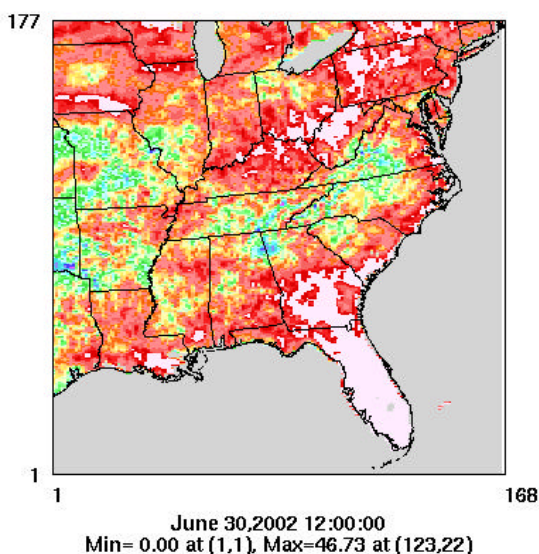
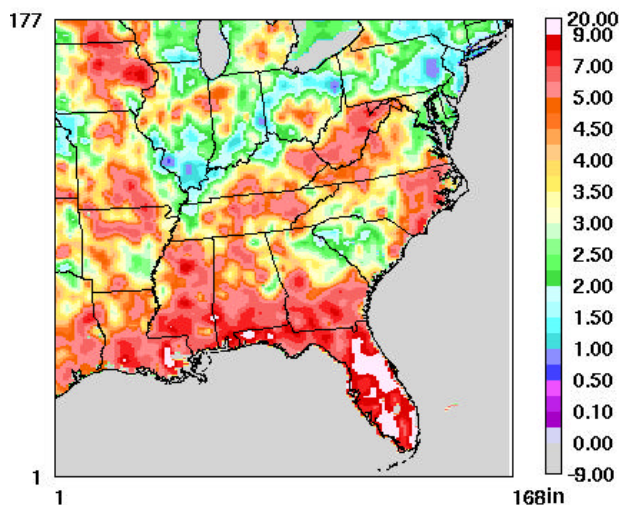


Figure 86. The June 2002 12-km accumulated precipitation from the Climate Prediction Center is juxtaposed with the MM5 accumulated precipitation.

## Monthly Total Precipitation (Obs)

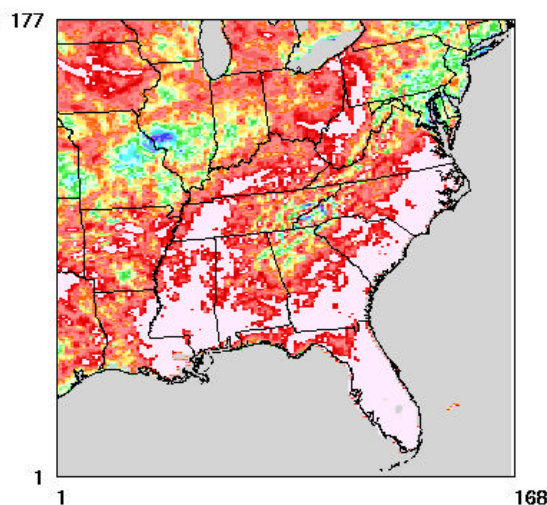
(jul02, Full: 12km, v02\_aaa)



July 31,2002 12:00:00  
Min= 0.00 at (1,1), Max=11.65 at (125,18)

## Monthly Total Precipitation (MM5)

(jul02, Full: 12km, v02\_aaa)

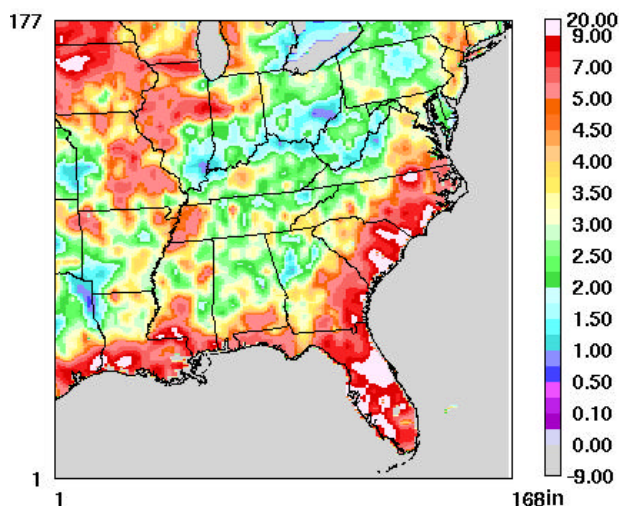


July 31,2002 12:00:00  
Min= 0.00 at (1,1), Max=42.48 at (123,23)

Figure 87. The July 2002 12-km accumulated precipitation from the Climate Prediction Center is juxtaposed with the MM5 accumulated precipitation.

## Monthly Total Precipitation (Obs)

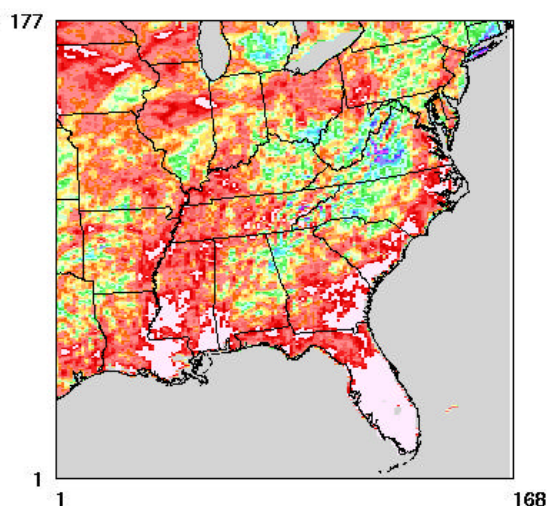
(aug02, Full: 12km, v02\_aaa)



August 31,2002 12:00:00  
Min= 0.00 at (1,1), Max=11.89 at (120,44)

## Monthly Total Precipitation (MM5)

(aug02, Full: 12km, v02\_aaa)



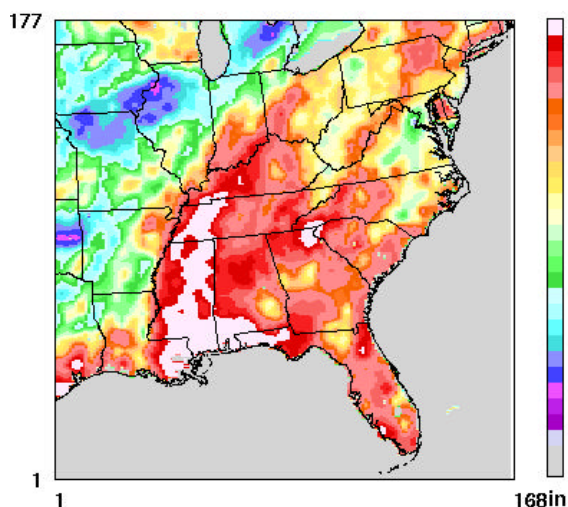
August 31,2002 12:00:00  
Min= 0.00 at (1,1), Max=39.03 at (128,15)

Figure 88. The August 2002 12-km accumulated precipitation from the Climate Prediction Center is juxtaposed with the MM5 accumulated precipitation.



### Monthly Total Precipitation (Obs)

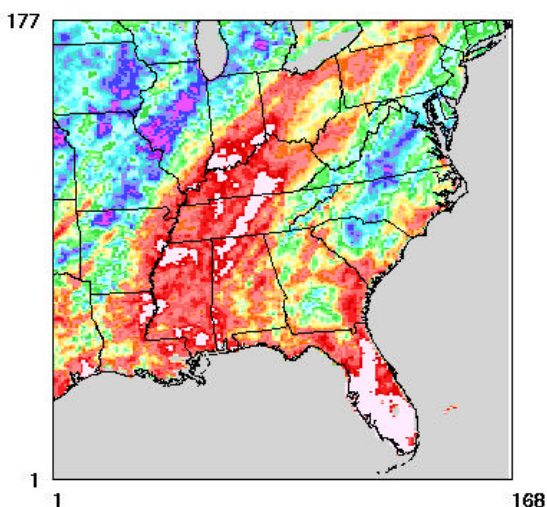
(sep02, Full: 12km, v02\_aaa)



September 30,2002 12:00:00  
Min= 0.00 at (1,1), Max=18.05 at (49,46)

### Monthly Total Precipitation (MM5)

(sep02, Full: 12km, v02\_aaa)

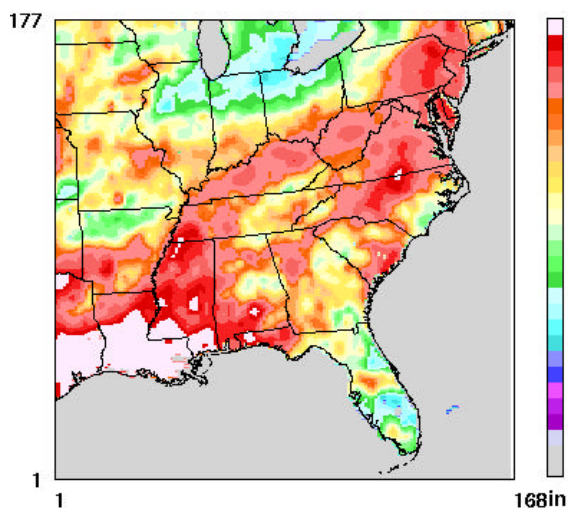


September 30,2002 12:00:00  
Min= 0.00 at (1,1), Max=32.56 at (122,20)

Figure 89. The September 2002 12-km accumulated precipitation from the Climate Prediction Center is juxtaposed with the MM5 accumulated precipitation.

### Monthly Total Precipitation (Obs)

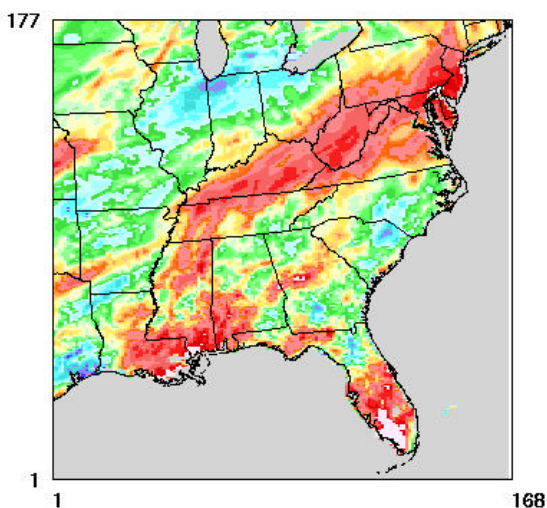
(oct02, Full: 12km, v02\_aaa)



October 31,2002 12:00:00  
Min= 0.00 at (1,1), Max=20.87 at (25,45)

### Monthly Total Precipitation (MM5)

(oct02, Full: 12km, v02\_aaa)

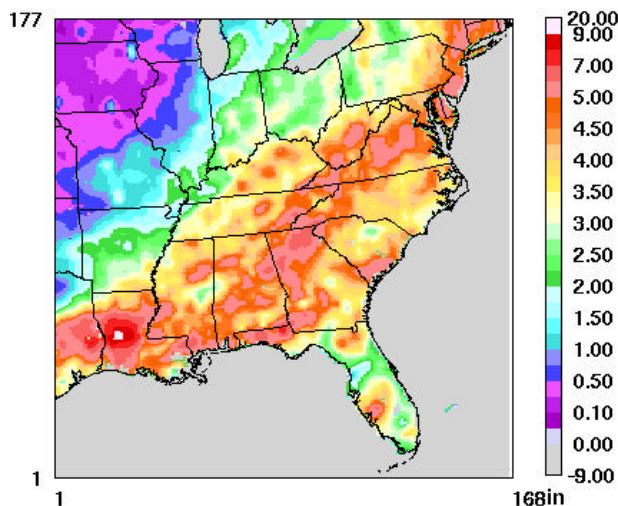


October 31,2002 12:00:00  
Min= 0.00 at (1,1), Max=23.23 at (122,17)

Figure 90. The October 2002 12-km accumulated precipitation from the Climate Prediction Center is juxtaposed with the MM5 accumulated precipitation.

## Monthly Total Precipitation (Obs)

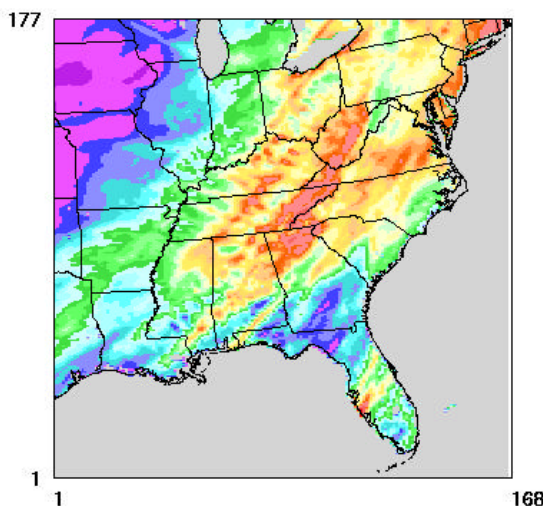
(nov02, Full: 12km, v02\_aaa)



November 30,2002 12:00:00  
Min= 0.00 at (1,1), Max= 9.26 at (25,55)

## Monthly Total Precipitation (MM5)

(nov02, Full: 12km, v02\_aaa)

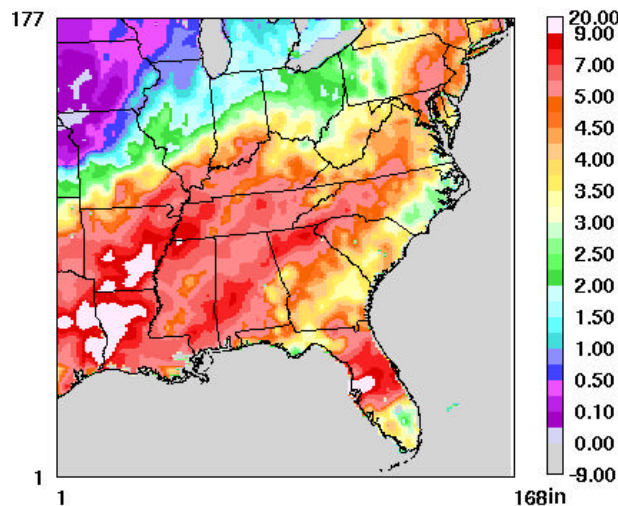


November 30,2002 12:00:00  
Min= 0.00 at (1,1), Max= 9.12 at (114,25)

Figure 91. The November 2002 12-km accumulated precipitation from the Climate Prediction Center is juxtaposed with the MM5 accumulated precipitation.

## Monthly Total Precipitation (Obs)

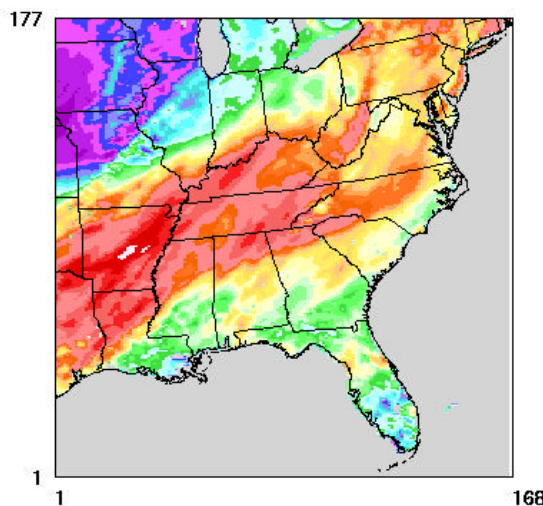
(dec02, Full: 12km, v02\_aaa)



December 31,2002 12:00:00  
Min= 0.00 at (1,1), Max= 11.88 at (110,35)

## Monthly Total Precipitation (MM5)

(dec02, Full: 12km, v02\_aaa)



December 31,2002 12:00:00  
Min= 0.00 at (1,1), Max= 9.27 at (35,88)

Figure 92. The December 2002 12-km accumulated precipitation from the Climate Prediction Center is juxtaposed with the MM5 accumulated precipitation.

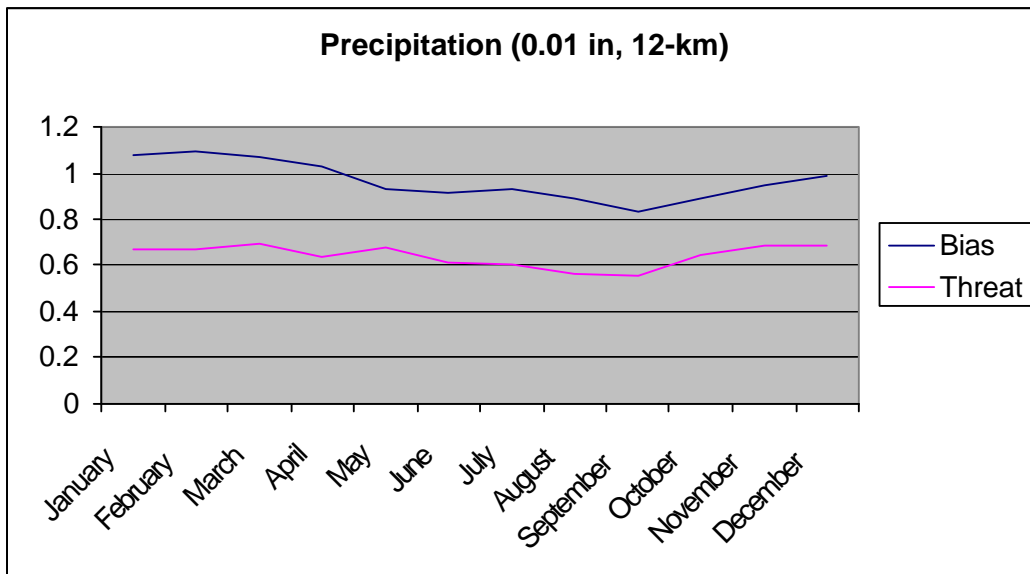


Figure 93. The 0.01 in threshold precipitation bias and threat score for the 12-km domain is shown for modeling year 2002.

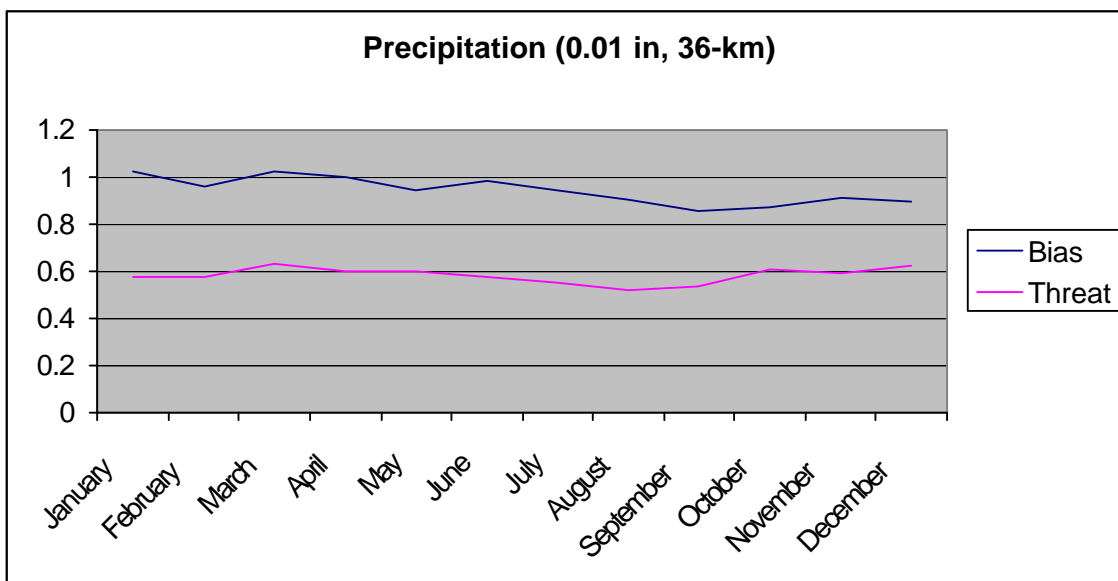


Figure 94. The 0.01 in threshold precipitation bias and threat score for the 36-km US region is shown for modeling year 2002.

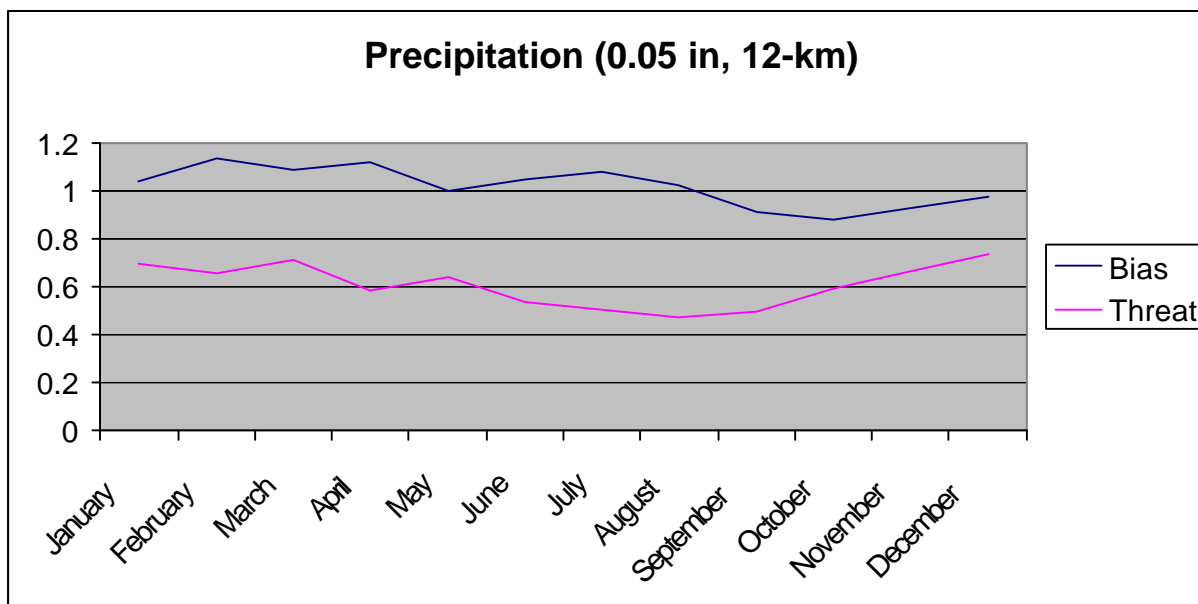


Figure 95. The 0.05 in threshold precipitation bias and threat score for the 12-km domain is shown for modeling year 2002.

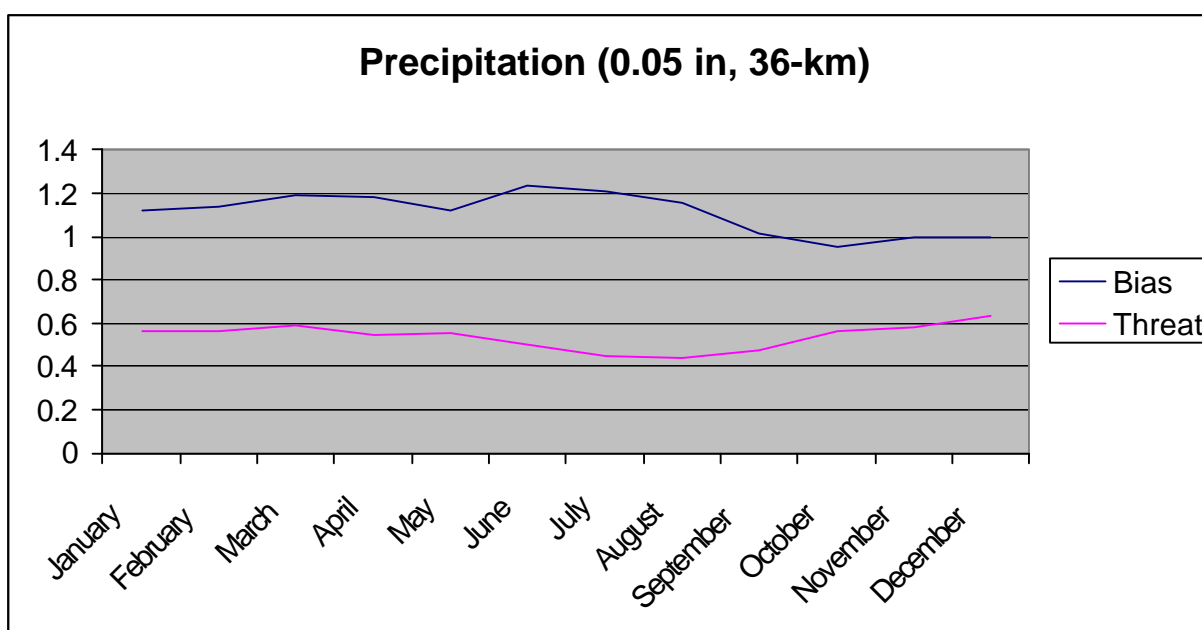


Figure 96. The 0.05 in threshold precipitation bias and threat score for the 36-km US region is shown for modeling year 2002.

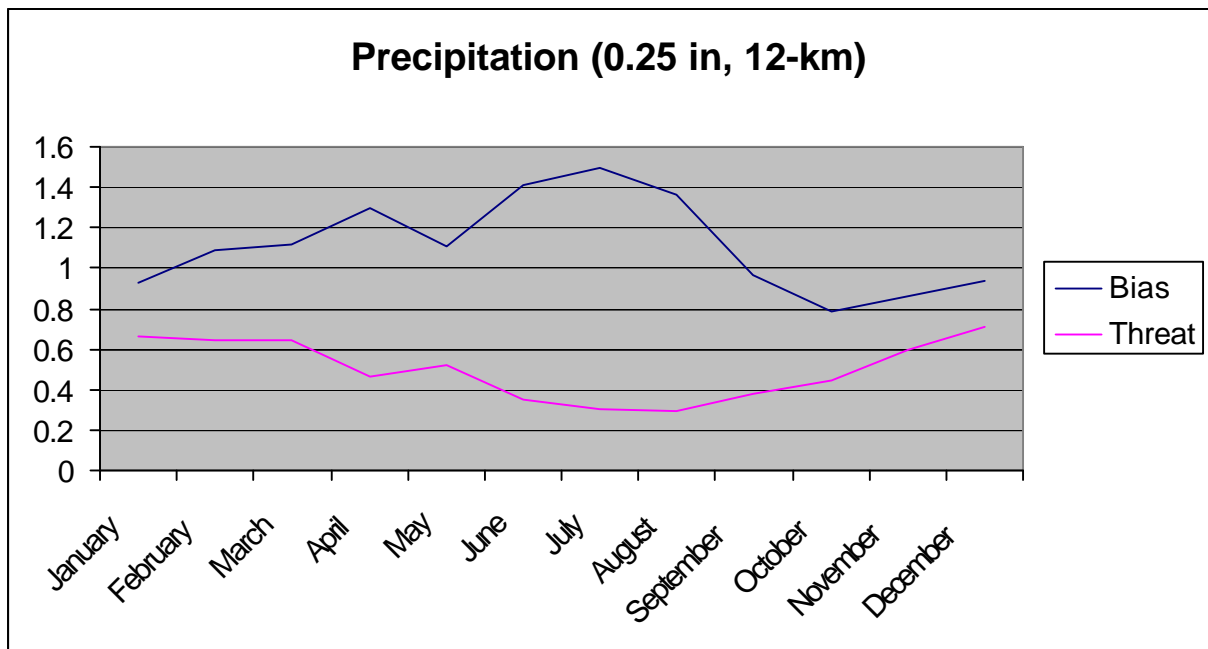


Figure 97. The 0.25 in threshold precipitation bias and threat score for the 12-km domain is shown for modeling year 2002.

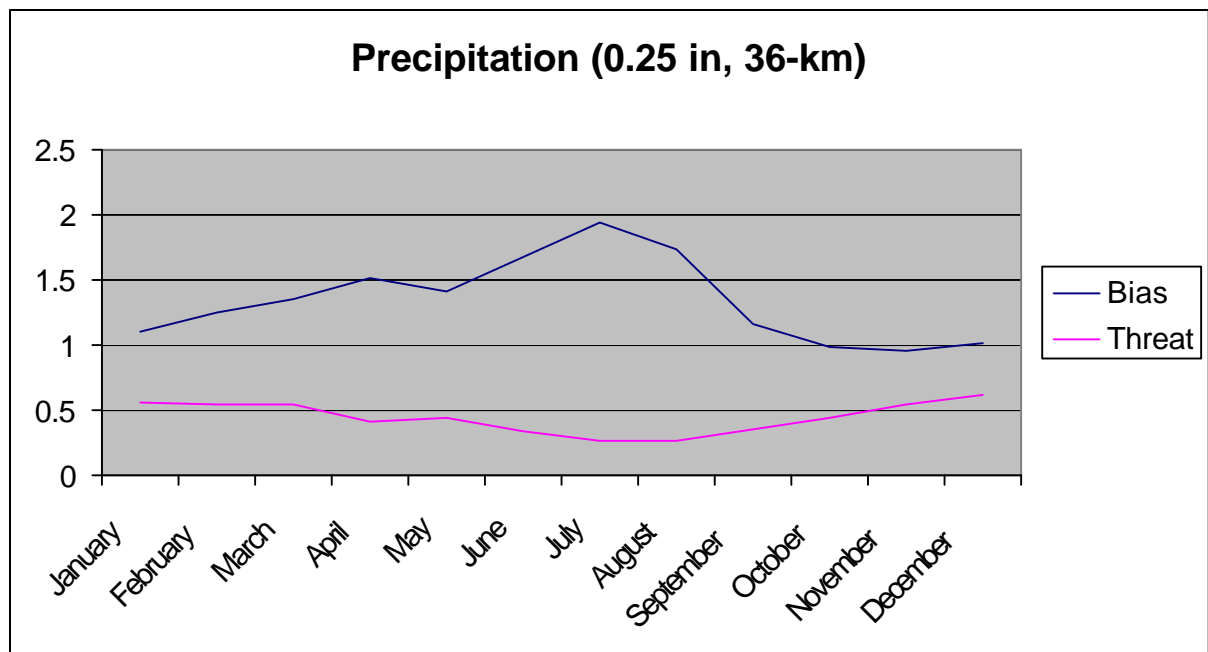


Figure 98. The 0.25 in threshold precipitation bias and threat score for the 36-km US region is shown for modeling year 2002.

## 4 Summary and Conclusions

- Generally speaking, MM5 performed quite well at both 36-km and 12-km resolutions. Synoptic features were routinely accurately predicted, and the model showed considerable skill in replicating the state variables. Most of the time the model statistics easily fell within the expected “benchmarks”.
- The model shows evidence of being adversely affected by poor soil initialization at times. This is particularly evident for September and November, and it might cause the autumnal dry bias evidenced both in the mixing ratio statistics and also in the precipitation statistics. At the time of our modeling, the P-X LSM only allowed three soil initialization options: 1) Table look-up, 2) EDAS, and 3) interppx. Sensitivity testing showed that interppx can produce more severe cold biases, so we chose the EDAS option. Unfortunately that option initializes soil moisture from a layer 100-200 cm deep, whereas the P-X LSM extends downward only 100 cm. In the future improved model performance might be attained by more wisely initializing soil moisture.
- The model is noticeably cold biased in the winter months. This was expected based on our sensitivity modeling, and it appears to be related to the manner in which soil temperatures are initialized.
- The summertime diurnal cloud cycle appears to be out of phase with the observed cycle. The model maximizes cloud coverage at night and minimizes cloud coverage in the afternoon, while the observations indicate that the exact opposite should occur.
- The model noticeably overestimates the amount of summertime precipitation, but not the spatial coverage of measurable precipitation.
- While no modeling is perfect, the results of this effort should produce credible inputs for subsequent air quality modeling.



## 5 Acknowledgements

Atmospheric data were provided by the Data Support Section of the Scientific Computing Division at the National Center for Atmospheric Research. NCAR is supported by grants from the National Science Foundation. Original sources of the datasets ds353.4, ds464.0, and ds609.2 were provided to NCAR by the National Center for Environmental Prediction. The original source of dataset ds472.0 was provided to NCAR by the Techniques Development Laboratory.

Profiler data obtained from the NOAA Profiler Network were provided by Forecast Systems Lab. Daily US .25x.25 gridded precipitation observations were provided by the Climate Prediction Center. Visible and Infrared satellite imagery were obtained from the National Climatic Data Center's historical GOES browse server. Surface analysis maps were obtained from Unisys website, [weather.unisys.com](http://weather.unisys.com); the data on this site are provided from the National Weather Service via the NOAAPORT satellite data service.

Specific sites of surface station data for time-series plots were obtained from the National Park Service courtesy of NPS Air. These data are part of the Interagency Monitoring of Protected Visual Environments (IMPROVE) monitoring sites. Additional surface data from the SouthEastern Aerosol Research and Characterization Study experiment (SEARCH) were obtained from Atmospheric Research and Analysis, Inc. Other surface data were provided courtesy of Mike Abraczinskas of NCDAQ.

The authors would like to acknowledge MCNC Enterprise Grid Services for the use of their computation resources. We would like to thank Kirk Baker of LADCO for his initial development of the Mosaic summary plots (Bakergrams). We also would like to acknowledge Mike Abraczinskas and Nick Witcraft of NCDAQ for the generation and use of most of the excel plots.

## 6 References

- Emery, C., E. Tai, and G. Yarwood, 2001. "Enhanced Meteorological Modeling and Performance Evaluation for Two Texas Episodes", report to the Texas Natural Resources Conservation Commission, prepared by ENVIRON, International Corp, Novato, CA.
- Grell, G. A., J. Dudhia, and D. R. Stauffer, 1994: A description of the fifth-generation Penn State/NCAR Mesoscale Model (MM5). NCAR Tech. Note, NCAR/TN-398+STR, 122 pp.
- Olerud, D. K. Alapaty, and N. Wheeler, 2000: Meteorological Modeling of 1996 for the United States with MM5. MCNC – Environmental Programs, Research Triangle Park, NC. Final report submitted to OAPQS, US EPA.
- Olerud, D. T., 2003: Evaluation Methodologies for Meteorological Modeling in Support of VISTAS (Visibility Improvement - State and Tribal Association), VISTAS task 1 deliverable. Available from Mike Abraczinskas, Meteorologist, NC Division of Air Quality, 1641 Mail Service Center, Raleigh, NC 27699-1641
- Olerud, D. T., 2003: Summation of Relevant MM5 Sensitivity Modeling in Support of VISTAS (Visibility Improvement - State and Tribal Association), VISTAS task 2a deliverable. Available from Mike Abraczinskas, Meteorologist, NC Division of Air Quality, 1641 Mail Service Center, Raleigh, NC 27699-1641
- Olerud, D. T., 2003: Recommended MM5 Sensitivity Modeling in Support of VISTAS (Visibility Improvement - State and Tribal Association)] VISTAS Task 2b deliverable. Available from Mike Abraczinskas, Meteorologist, NC Division of Air Quality, 1641 Mail Service Center, Raleigh, NC 27699-1641
- Olerud, D. T., 2004: Protocol for Annual MM5 Sensitivity Modeling in Support of VISTAS (Visibility Improvement - State and Tribal Association)] VISTAS Task 3a deliverable. Available from Mike Abraczinskas, Meteorologist, NC Division of Air Quality, 1641 Mail Service Center, Raleigh, NC 27699-1641